Revisiting the Tamoxifen Scaffold to Create Therapeutics to Treat Amphetamine Abuse

by

Colleen Antonette Carpenter

A dissertation submitted in partial fulfillment
of the requirements for the degree of
Doctor of Philosophy
(Pharmacology)
in the University of Michigan
2017

Doctoral committee:

Professor Margaret E. Gnegy, Chair
Assistant Professor Emily Jutkiewicz
Professor Robert T. Kennedy
Professor John R. Traynor

"Our deepest fear is not that we are inadequate. Our deepest fear is that we are powerful beyond measure. It is our light, not our darkness that most frightens us. We ask ourselves, Who am I to be brilliant, gorgeous, talented, fabulous? Actually, who are you not to be? You are a child of God. Your playing small does not serve the world. There is nothing enlightened about shrinking so that other people won't feel insecure around you. We are all meant to shine, as children do. We were born to make manifest the glory of God that is within us. It's not just in some of us; it's in everyone. And as we let our own light shine, we unconsciously give other people permission to do the same. As we are liberated from our own fear, our presence automatically liberates others."

Marianne Williamson

"We pass through this world but once. Few tragedies can be more extensive than the stunting of life, few injustices deeper than the denial of an opportunity to strive or even to hope, by a limit imposed from without, but falsely identified as lying within."

Stephen Jay Gould

"May love swell everywhere today. May it invite you. May it comfort you. May it surprise you. May it overwhelm you. May it unmoor you. May it ignite you. May it surround you. May it incite you. May it empower you. May it envelope you. May it soothe you. May it consume you. May you face it. Boldly. Humbly. Desperately."

Jason Harris

Colleen Antonette Carpenter

ccarpen@umich.edu

ORCID iD: 0000-0003-1981-2108

Dedication

I would like to firstly dedicate my thesis to my mother, Lorna Whyte, whose sacrifices, encouragement, love and support helped me to get to where I am today. To my sisters, you mean the world to me, and this success is your success. This is also for all the little brown girls, especially from my hometown of Port Antonio, who feel overwhelmed by and unworthy of their dreams; you are worthy and it's time to see the world as your stage.

Acknowledgement

To my current mentor, Margaret Gnegy, thank you for granting me the opportunity to be in your lab. Through your guidance, I learnt how to think more critically and creatively as a scientist, and also how to more effectively communicate my science. You went above and beyond my expectations for a graduate school mentor and I will forever be grateful for your unwavering support. To the rest of my thesis committee, Emily Jutkiewicz, John Traynor, Robert Kennedy and Sivaraj Sivarmakrishnan (now at University of Minnesota), I appreciated all your insightful comments and guidance as I tackled the ups and downs of my project. I would also like to thank Hollis Showalter and Roderick Sorenson for creating the compound that was the foundation for the majority of my thesis work and for all the other intellectual contributions you offered over the years.

Of course, to my labmates; Alex, Bipasha, Kadee, Rachel, Sarah, Simar and Tracelyn, thank you for helping me survive graduate school and for making the lab fun to work in. I am also super grateful for the scientific contributions Alex and Rachel made to my thesis project. I really loved being in the Pharmacology Department and thankful that I was able to call it my department home for the past few years. Special shout-outs to Lori Isom, Lisa Fletcher-Garber and Eileen Ferguson for being my sounding-boards on many occasions! Many thanks to my previous mentors, Erika Taylor (Wesleyan University) and Betsy Herold (Albert Einstein College of Medicine), for supporting my early scientific years.

It takes a village to raise a child and my village is pretty great. My family is filled with strong, hardworking, genuine people and I am here largely because of their unconditional love and support. A thousand thank you's to my mom, Lorna, my sisters, Nadia and Nicole, and my brother, Duran. Also much thanks and respect to my aunts; Annette, Doreen, Maxine, my uncles; Everton and Ecknol, and my cousins (who I can easily call my siblings); Jennelle, Everton and Danicia. To my amazing friends (i.e. sisters from other misters), Carolyn, Julliana, Kara, Kayla, Marie-eve, Rachelle, Sabah and Stacianne, you all are such incredible women and thank you for helping me live life to the fullest. To my fiancé, Carter, I cannot find the words to succinctly describe how much you mean to me and how much I respect you as a person, a friend and a scientist. I honestly cannot, do not, want to imagine graduate school without you. Thank you for believing in me and loving me. I am also super grateful for the friends I have made during my time at Michigan. I especially have to thank Chanrith, Kristin, Elizabeth, Nancy and Nayiri for all the adventures and for helping me stay sane during graduate school.

This last year was a total rollercoaster for me medically. Thank you to the University of Michigan Health System, especially to the cancer center, for taking such great care of me and providing life-saving resources. Most importantly, thank you God for making all this possible. Ok, I think I am done acknowledging for now!

Table of Contents

List of figures

List of abbreviations

Aldehyde dehydrogenase: ALDH
Amphetamine: AMPH
Analysis of variants: ANOVA
Attention-deficit/hyperactivity disorder: ADHD
$Ca^{2+/}$calmodulin-dependent protein kinase II: CAMKII
Cyclic AMP: cAMP
3,4-Dihydroxy-L-phenylalanine: L-DOPA
Diacyglycerol: DAG
Dopamine transporter: DAT
D2 receptor: D2R
D2 receptor, short variant: $D2R_S$
D2 receptor, long variant: $D2R_L$
Estrogen receptor α: ERα
Fluorescence resonance energy transfer: FRET
Food and drug administration: FDA
Glyceraldehyde 3-phosphate dehydrogenase: GAPDH
G protein-coupled receptor: GPCR
Growth associated protein-43: GAP-43
Human embryonic kidney cell: HEK cell
Leucine transporter: LeuT
Monoamine oxidase: MAO
Myristoylated alanine-rich C- kinase substrate: MARCKS
Norepinephrine transporter: NET
4-β-phorbol-12,13-dibutyrate: PDBu
Phorbol 12-myristate 13-acetate: PMA
Protein kinase B: AKT
Protein kinase C: PKC
Selective estrogen receptor modulator: SERM
Serotonin transporter: SERT
Structure-activity relationship: SAR
Thin-layer chromatography: TLC
Time-of-Flight mass spectrometer in a positive ESI mode: TOFES+
Topological polar surface area: tPSA
Transmembrane: TM
Vesicular monoamine transporter: VMAT

Abstract

Amphetamine (AMPH) and its congeners are the second most widely abused drugs globally and their continued overuse comes with a high economic, health and social cost. Yet after decades of research, an effective treatment for AMPH abuse and addiction remains elusive. To tackle this unmet need, we have taken a step back to re-examine and further elucidate the mediators of AMPH reinforcement in hopes of finding novel targets for drug development. The reinforcing properties of AMPH are believed to stem from its reversal of the dopamine transporter (DAT), which greatly increases extracellular dopamine levels in the brain. Protein kinase C (PKC) is a major mediator of DAT localization and activity, and PKC activation facilitates AMPH-stimulated dopamine release. Inhibiting PKC attenuates the neurochemical and behavioral effects of AMPH. Therefore PKC inhibitors could be an appropriate pharmacological treatment for AMPH abuse and addiction.

In pursuit of a blood-brain barrier permeant PKC inhibitor, we identified tamoxifen, a drug commonly used to prevent the recurrence of breast cancer, as a promising candidate. In fact, tamoxifen stands as the only validated CNS-permeant PKC inhibitor to date. Tamoxifen does act on other molecular targets, including the estrogen receptor (ER), and its promiscuity makes it an unattractive contender for AMPH abuse treatment. Nonetheless, tamoxifen has been the object of many structure-activity relationship studies and we have used the information from these investigations to make a

new generation of selective CNS permeant PKC inhibitors based on the tamoxifen scaffold.

I evaluated the actions of these tamoxifen analogues at PKC and ER, in hopes of finding compounds with increased selectivity for PKC inhibition and reduced ER affinity compared to tamoxifen. This led me to our lead compound, **6c**, which asymmetrically modulates DAT functioning in *in vitro* rat models. Specifically, **6c** more potently blocks dopamine efflux compared to uptake. I demonstrated that **6c** does not elicit these effects on dopamine transport by altering DAT levels or binding near the dopamine substrate site. Significantly, as predicted, **6c** crosses the blood-brain barrier and potently inhibits striatal PKC activity *in vivo*. I also illustrate that **6c** has a direct effect on PKC and can disrupt PKC conformational changes without having effects on PKC translocation. Peripheral administration of the compound leads to significant decreases in AMPH-induced dopamine release, hyperlocomotion and reinforcement *in vivo*, predicting therapeutic effectiveness of **6c**. Finally, I demonstrate that the *in vivo* effects of **6c** are not due to its action on other closely related kinases that regulate DAT function. Together, the results from my thesis work highlight the potential of repurposing the tamoxifen scaffold to create new CNS-permeant PKC inhibitors and provide a foundation for developing therapeutics to treat AMPH addiction.

Chapter 1. Introduction

Drug addiction is a chronic relapsing disorder, characterized by uncontrolled, compulsive, and harm-inducing drug consumption (Herman and Roberto, 2015; Nestler, 2004). It represents a significant global burden due to the loss of productivity, health care costs and criminal justice expenses linked to the disorder. In the US alone, addiction to illicit drugs is estimated to cost more than $600 billion annually (Herman *et al*, 2015). My thesis focuses on the abused stimulant amphetamine (AMPH), the prototype for a group of structurally and pharmacologically similar compounds called "AMPH-like stimulants" or "AMPHs". AMPHs are the second most widely abused drug in the world, falling right behind cannabis (UNODC, 2012).

Behavioral therapies serve as the primary intervention mechanism to help individuals battling AMPH abuse and addiction. Unfortunately, these therapies provide limited benefits and to date, there are no therapeutics available to treat these patients (Vocci and Montoya, 2009). It is therefore imperative that more research be done to further understand the mechanism of action of AMPHs in an effort to unveil druggable targets that contribute to AMPH-type stimulant abuse. My thesis work aims to address this unmet need and although centered on AMPH, I believe the results from this project will also apply to its congeners.

History of AMPH

AMPH is a well-known stimulant and some of its physiological effects include increased activity, euphoria and stereotypic behaviors such as rocking and pacing. Many historical accounts of AMPH begin in 1887, when the drug was first synthesized by the Romanian chemist, Lazar Edelman, in Germany. However, the clinical beginnings of AMPH are tied to the history of the structurally similar compound, ephedrine. Traditional Chinese medicine has employed the plant-derived stimulant ephedra (ma huang) for the treatment of asthma and the common cold for over 5000 years (Greene *et al*, 2008). The pharmacological effects of the preparation are mainly credited to the alkaloids ephedrine and pseudoephedrine. By the 1920s the sympathomimetic actions of ephedrine were well known in medicine and it was successfully marketed in the United States and Europe as a decongestant and asthma-relieving therapeutic. In a systematic search for novel sympathomimetics that were more efficacious and more cheaply synthesized than ephedrine, the American chemist, Gordon Alles, independently resynthesized AMPH. AMPH finally entered the Western market in the form of an inhaler to treat nasal congestion in 1932 (Greene *et al*, 2008; Heal *et al*, 2013).

By World War II, the drug gained much popularity as a means to promote wakefulness and boost performance of pilots and other servicemen. As the therapeutic uses for AMPH increased, there was a growing awareness of its misuse and abuse among consumers. By 1959, AMPH inhalers were banned by the Food and Drug administration (FDA) as AMPH abuse became rampant. There was also an explosion in the production of AMPH congeners, namely methamphetamine and methylenedioxymeth-amphetamine (MDMA), for recreational purposes, and the illicit use of AMPH continued through the

decades (Berman *et al*, 2008; Greene *et al*, 2008; Maxwell and Rutkowski, 2008). At low doses, AMPH remains FDA approved for the treatment of attention-deficit/hyperactivity disorder (ADHD) and narcolepsy. However, as a Schedule II drug, it is recommended that the medical use of AMPH be tightly controlled due to its abuse potential (Berman *et al*, 2008).

The abuse of AMPH and its congeners has placed an enormous weight on our psychiatric and medical resources (Brackins *et al*, 2011). AMPH overuse is known to precipitate psychosis or mood disorders. Early studies in which healthy patients were given AMPH in consecutively higher doses showed that AMPH could elicit acute psychosis in these patients and the effects were blocked using antipsychotic drugs (Espelin and Done, 1968; Klawans, 1968). The hyperactivity resulting from AMPH is used to model mania in animal studies. Other detrimental side effects of AMPH include hyperthermia, nephrotoxicity, cardiotoxicity and hepatotoxicity (Bramness *et al*, 2012; Carvalho *et al*, 2012). Strikingly, emergency department visits related to ADHD stimulant medications increased by over 200% between 2005 and 2010 (Substance Abuse and Mental Health Services Administration, 2013).

Mechanism of action of AMPH

AMPHs are all β-phenyl-ethylamine derivatives that structurally resemble catecholamine neurotransmitters, see Figure 1.1 for comparison to dopamine (Heal *et al*, 2013). Their close resemblance to these monoamines led to the idea that AMPHs act as a substrate for plasmalemmal monoamine re-uptake transporters (norepinephrine transporter; NET, serotonin transporter; SERT or dopamine transporter; DAT) that can provide an entry for the drugs into the presynaptic neuronal cytosol. The primary role of

these transporters is to clear their respective monoamines from the synapse after exocytotic release. Therefore by acting as a substrate at the transporters, AMPH competitively blocks monoamine reuptake, and consequently increases synaptic monoamine levels.

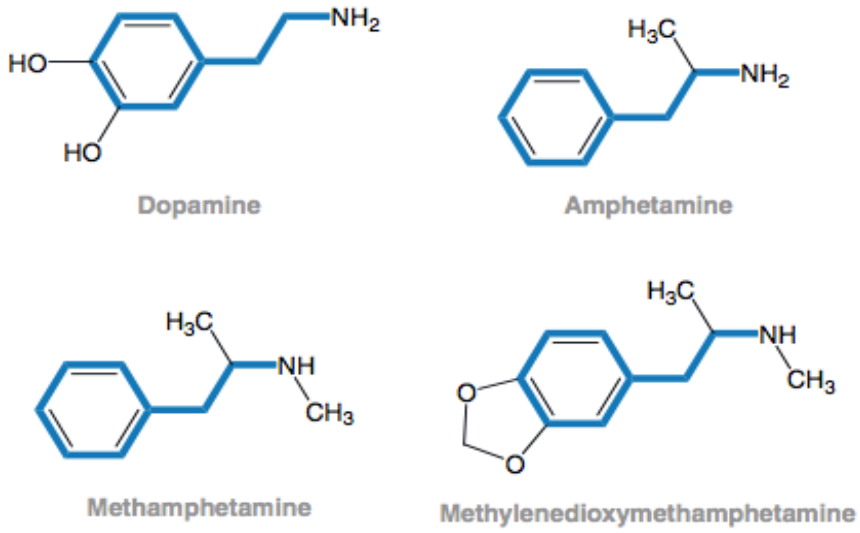

Figure 1.1. The structure of the catecholamine dopamine and some of its congeners.
The common structural motif is emphasized by the bold blue outline (Fleckenstein et al, 2007).

In the presence of a newly synthesized pool of substrates at the cytoplasmic face of monoamine transporters, AMPH also elicits the reverse transport or efflux of catecholamines from the cytosol into the synapse (Chiueh and Moore, 1975; Parker and Cubeddu, 1986). Specifically, once bound to the outward-facing conformation of the transporters, AMPH is co-transported with sodium and chloride into the cytosol. The resulting rise in intracellular sodium promotes the reverse transport of endogenous substrates. This change in the intracellular sodium levels is crucial for substrate efflux and this is exemplified by the fact that Na^+/K^+-ATPase blockers, such as ouabain or monensin (dissipates the sodium gradient), can lead to monoamine efflux in the absence of AMPH (Liang and Rutledge, 1982; Raiteri *et al*, 1978; Scholze *et al*, 2000; Sitte *et al*,

2000). Some of the early evidence pointing to the importance of plasmalemmal transporters to this process came from Raiteri and colleagues, where the group showed that AMPH-induced dopamine release was blocked by the dopamine reuptake inhibitor, nomifensine (Raiteri *et al*, 1979). Relatedly, it was later shown that AMPH-induced increases in extracellular dopamine was absent in striatal slices from mice lacking the dopamine transporter (Jones *et al*, 1998).

There are also other mechanisms that are believed to contribute to AMPH-stimulated monoamine efflux. If not degraded, cytosolic monoamines are taken up into vesicles by the vesicular monoamine transporter (VMAT) for storage until an action potential prompts their release. AMPH binds to VMAT with tighter affinity than the monoamines (excluding serotonin) and hence blocks the monoamine transport into the vesicles (Gonzalez *et al*, 1994). Additionally, according to the weak base hypothesis, AMPH (pKa 9.9) alkalinizes the vesicles once taken up and disrupts the proton gradient required for monoamine storage (Sulzer and Rayport, 1990). Recent work employing optical methods in *Drosophila* brain further proves AMPH disrupts the vesicular pH gradient and vesicular contents important for monoamine storage (Freyberg *et al*, 2016). Specifically, fluorescent sensors showed that AMPH redistributes vesicular contents in addition to reducing H^+ levels in the vesicles (Freyberg *et al*, 2016). However, the need for VMAT in AMPH action has been debated, with many conflicting results. Additionally, using cellular models lacking VMAT, our group and others have shown that this transporter is not required for AMPH-stimulated dopamine release (Fon *et al*, 1997; Kantor *et al*, 2001; Pifl *et al*, 1995).

There is also a less recognized notion that AMPHs may also serve as competitive inhibitors of catecholamine metabolizing enzyme monoamine oxidase (MAO), leading to lower rates of amine metabolism. It is considered at most a weak MAO inhibitor *in vitro* and at high doses it may act as a competitive MAO type A inhibitor *in vivo* (Mantle et al, 1976). The presence of an α-methyl group on the AMPH molecule prevents its oxidation by the enzyme (Carvalho *et al*, 2012). The blockade of VMAT and inhibition of MAO are both believed to lead to increases in cytosolic dopamine and ultimately monoamine efflux.

In summary, through these various mechanisms (however large or small each contribution), AMPHs lead to a significant, action potential-independent, increase in the extracellular concentration of dopamine, norepinephrine and serotonin when administered. This is depicted in Figure 1.2, using the dopamine transporter as an example.

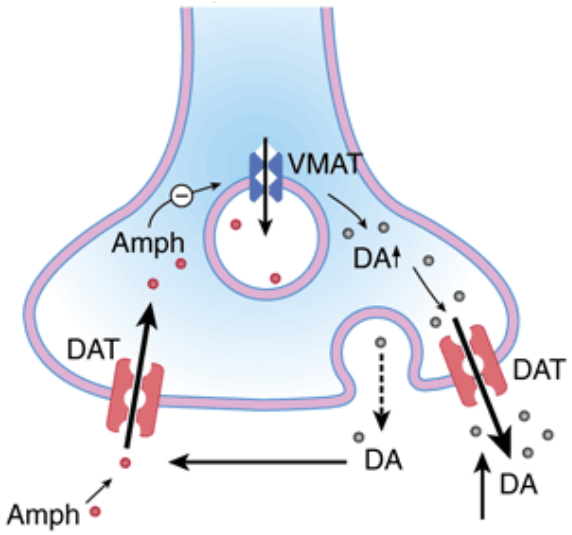

Figure 1.2. Actions of AMPH at the dopaminergic terminal.
As a substrate of the catecholamine transporter (in this case DAT), AMPH is transported into the cytosol. Through various mechanisms, including competitively blocking dopamine uptake at the vesicle, AMPH increases cytosolic dopamine. The cytosolic dopamine is then transported out of the terminal via the AMPH-induced reversal in transporter direction (Lüscher, 2012).

Addictive liability

As mentioned, the actions of AMPHs on the monoamine transporters are generally non-specific and the elevation of norepinephrine, serotonin and dopamine all have various effects on the mood and alertness of the consumer. However, the reinforcing effects of AMPHs have been directly linked to its elevation of extracellular dopamine concentrations and subsequently, the lengthening of DA receptor signaling along the reward circuit. This is also a trait of other drugs of abuse such as opiates, ethanol, nicotine and cocaine. In 1988, Di Chiara and Imperato demonstrated in freely moving Sprague-Dawley rats, that drugs abused by humans increased synaptic dopamine levels in the mesolimbic system (Di Chiara and Imperato, 1988). Drugs that do not carry an abuse liability such as imipramine and diphenhydramine failed to alter the extracellular dopamine levels in the same experimental setup.

Therefore to create effective treatments for AMPH abuse, we must consider the life cycle of dopamine and the various regulators of extracellular dopamine levels for clues of novel druggable targets that can prevent AMPH abuse.

Dopamine

Having major central and peripheral actions, dopamine has gained much attention since the 1950s when Arvid Carlsson demonstrated it was a *bona fide* neurotransmitter and not just a precursor to norepinephrine (Carlsson, 1993). Peripherally, the catecholamine has roles in hormone regulation and renal functioning. In the CNS, dopaminergic transmission is critical for proper execution of various functions, such as learning, sleep, working memory, voluntary movement, reward and reinforcement. Mid-brain dopaminergic neurons are especially important for the latter two processes. These

neurons are divided into subgroups (A8, A9, A10) based on anatomical and functional differences. The A9 cell bodies are found in the substantia nigra and terminate in the dorsal striatum (nigrostriatal pathway). Meanwhile, the dopaminergic neurons originating in the ventral tegmental area (A10) innervate the ventral striatum (mesolimbic pathway) and the prefrontal cortex (mesocortical pathway), Figure 1.3 (Andén *et al*, 1964; Dahlström and Fuxe, 1963). Although there is mounting evidence for nigral modulation of reward and reinforcement (Kimura and Matsumoto, 1997; Ramayya *et al*, 2014; Routtenberg and Malsbury, 1969; Wise, 2009), the mesolimbic and mesocortical pathways, sometimes referred to as the mesocorticolimbic pathways, are generally thought to be the most important regulators of these processes.

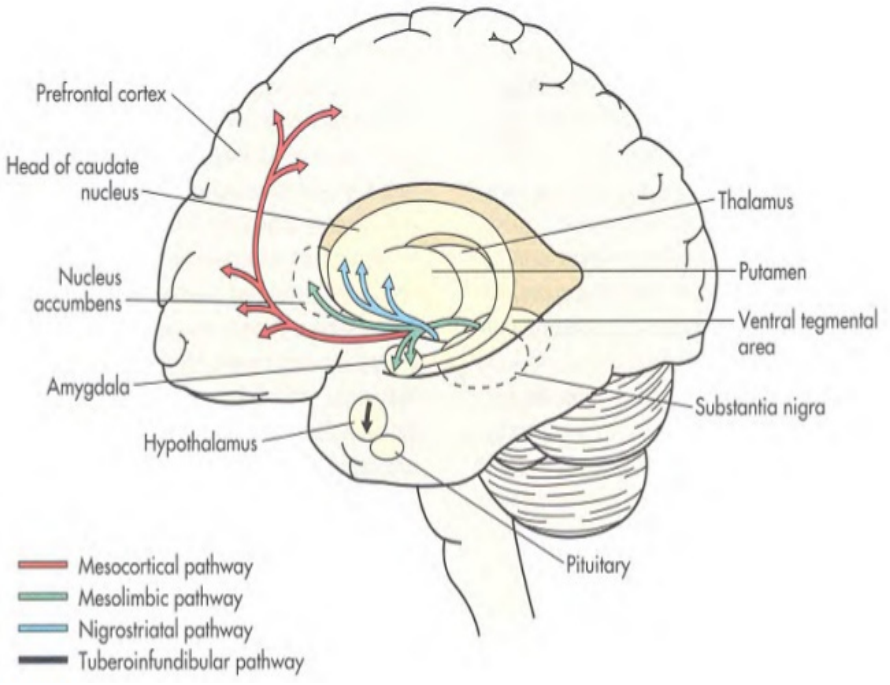

Figure 1.3. Major dopaminergic pathways.
(Brody *et al*, 1998)

In neurons, dopamine is synthesized from the amino acid tyrosine. Specifically, tyrosine is converted to L-DOPA (3,4-Dihydroxy-L-phenylalanine) by the cytosolic enzyme tyrosine hydroxylase and then L-DOPA is converted to dopamine via aromatic amino acid decarboxylase. The synthesis of L-DOPA is the rate-limiting step in the pathway. Once synthesized, dopamine is packaged in specialized vesicles where it remains until an action potential initiates the exocytotic release of the vesicular contents into the synapse (Elsworth and Roth, 1997). The synaptic dopamine can now bind to its postsynaptic receptors to propagate neuronal signaling. Dopamine exerts its actions by relatively slow modulation of glutamatergic- and GABAergic- mediated fast neurotransmission (Beaulieu and Gainetdinov, 2011).

Regulation of extracellular dopamine levels

DAT

Once dopamine is released, it must be cleared quickly to prevent overstimulation of post-synaptic receptors and downstream neuronal circuits. This is done partially through enzymatic degradation or simple diffusion of dopamine. However, the primary mechanism of removing dopamine from the synaptic cleft, particularly in the nigrostriatal and mesolimbic pathways, is *via* DAT. DAT is a part of the SLC6 Na^+/Cl^--dependent transporter family (also includes NET and SERT) and is only found on dopaminergic neurons. DAT couples the potential energy generated by the movement of sodium and chloride down their electrochemical gradient to move dopamine into the neuron. Once in the cytosol, dopamine can be repackaged into vesicles for release upon a new action potential.

In 1991, DAT from rat was first cloned and sequenced, closely followed by the cloning of human DAT in 1992 (Giros *et al*, 1991; Giros *et al*, 1992; Kilty *et al*, 1991; Shimada and Kitayama, 1991). Mammalian DAT cDNA sequences display a high degree of homology; for example, human DAT shares roughly 90% homology with rat, bovine and mouse (Sotnikova *et al*, 2006). In addition to mammalian DAT, the protein has also been identified in *Caenorhabditis elegans* and *Drosophila melanogaster*. Much of our current knowledge of the structure and function of DAT has been gained through its close relatives, the bacterial leucine transporter (LeuT) and recently crystallized *Drosophila melanogaster* DAT (Beuming *et al*, 2008; Penmatsa *et al*, 2013; Zhou *et al*, 2007).

DAT possesses twelve transmembrane (TM) spanning helices with a cytoplasmic N- and a C- terminal tail. TMs 1, 3, 6 and 8 provide the pathway for substrate translocation, with TM 1 and 6 forming the core of the active site (Vaughan and Foster, 2013). Based on the alternating access model (first proposed by Oleg Jardetzky in 1966), it was believed that DAT cycles through an inward and an outward facing conformation. This would mean the substrate cavity alternates between the synaptic and the cytoplasmic face of the transporter. LeuT studies further expanded this model to include an additional low-energy state, the occluded conformation. One theory purports that binding of one molecule of dopamine to the substrate site in the outward facing conformation initiates transport, followed by the binding of two sodium ions and a chloride. Binding of the ions triggers the conformational changes needed for dopamine to be released on the cytosolic face. Studies with LeuT demonstrate that a second substrate molecule can bind to an allosteric site (the S2 site, versus the primary substrate site, S1) and this event may facilitate the conformational change from the occluded to inward-facing conformation

and the release of the substrate and sodium into the cytosol (German *et al*, 2015; Schmitt *et al*, 2013; Shan *et al*, 2011; Shi *et al*, 2008).

Several important components on the cytosolic side of the presynaptic dopamine terminal ensure efficient repackaging of the dopamine and prevent the accumulation of cytosolic dopamine. Firstly, the turnover number of VMAT, which transports dopamine into the vesicles, is 2 to 3 times higher than that of the monoamine transporters, and this creates a gradient for dopamine to be taken up into the vesicles versus diffusing in the cytosol (Erreger *et al*, 2008; Peter *et al*, 1994; Sucic *et al*, 2010).

Secondly, the terminal also contains a class of degrading enzymes referred to as the mitochondrial monoamine oxidases (MAO-A and B). MAOs can be found in the mitochondrial outer membrane, although is it important to note MAO-B is predominantly expressed in non-neuronal cells. Through oxidative deamination, they convert dopamine to 3,4-dihydroxyphenyl-acetaldehyde, which is further oxidized by aldehyde dehydrogenase (ALDH) to 3,4-dihydroxyphenylacetic acid (DOPAC). Another major dopamine metabolizing enzyme localized to glial and postsynaptic cells is catechol-*O*-methyl transferase (COMT). COMT catalyzes the methylation of dopamine to 3-methoxytyramine and this is later metabolized to homovanillic acid by MAO and ALDH. COMT also facilitates the conversion of DOPAC to homovanillic acid (Meiser *et al*, 2013).

Post-translational modification is one of the most important regulators of DAT functioning. This generally occurs through the phosphorylation, palmitoylation, ubiquitination or glycosylation of the transporter (German *et al*, 2015; Vaughan *et al*, 2013). These mechanisms can affect DAT transport kinetics in addition to distribution.

Phosphorylation of DAT is postulated to occur through a battery of kinases, including the ubiquitously expressed protein kinase C (PKC). A string of serines on the N-terminal tail form the putative PKC sites of DAT (see Figure 1.4). Studies in both heterologous cells and synaptosomes found that acute activation of PKC by phorbol esters, such as phorbol 12-myristate 13-acetate (PMA), led to impaired dopamine uptake functioning and reduced DAT expression levels (Copeland *et al*, 1996; Vaughan *et al*, 1997; Zhu *et al*, 1997). Mechanistically, these down-regulating effects were thought to stem from phosphorylation-dependent DAT internalization. However, elimination of the putative PKC substrate phosphorylation sites, either through mutation or truncation, terminated PKC induced DAT phosphorylation but surprisingly did not affect DAT trafficking.

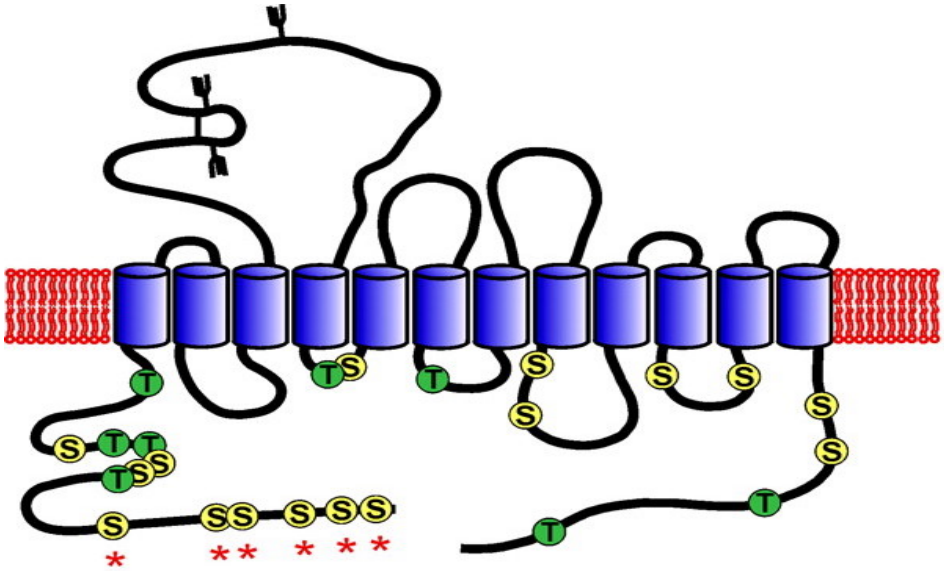

Figure 1.4. Depiction of DAT with putative PKC phosphorylation sites.
(Vaughan, 2004)

PKC also modulates the reversal transport at DAT, that is, dopamine efflux. PMA-triggered PKC activity promotes dopamine efflux in rat striatal slices and

synaptosomes, an effect independent of extracellular calcium. Treatment with the selective PKC inhibitor, Ro31-8220, blocks this effect (Cowell *et al*, 2000). Correspondingly, PKC activation either *via* Gq-coupled glutamate receptors or directly with PMA promotes dopamine efflux in nigral slices (Opazo *et al*, 2010). Interestingly, AMPH increases PKC activity, which facilitates its ability to induce dopamine efflux (Cowell *et al*, 2000; Giambalvo, 1992, 2004; Kantor and Gnegy, 1998). There is still much to learn about the exact mechanism by which AMPH activates PKC. One proposed mechanism is through the trace amine associated receptor 1, which binds trace amines, monoamines and AMPH-like psychostimulants (Miller, 2011). A more direct mechanism may be the increase in intracellular calcium that follows AMPH treatment. The increased intracellular calcium could then activate PKC (Gnegy *et al*, 2004; Kantor *et al*, 2004).

Some of the post-translational mechanisms that regulate DAT have apparent reciprocal roles. For instance, it was recently reported that surface DATs that exhibited high levels of phosphorylation but low levels of palmitoylation have reduced maximal velocity (V_{max}) for dopamine uptake and increased transporter downregulation. Conversely, DAT populations with low levels of phosphorylation but high levels of palmitoylation have increased V_{max} and show no significant PKC-induced DAT downregulation (Moritz *et al*, 2015). Although less discussed, ubiquitination and glycosylation are very important in modulating DAT localization. PKC-triggered ubiquitination of DAT on the N-terminus governs whether internalized DAT will be directed towards recycling or will be degraded. (Miranda *et al*, 2005). On the other hand, the extent of transporter glycosylation dictates both its kinetics and its propensity for endocytosis. As shown in human embryonic kidney (HEK) cells expressing human DAT,

preventing or reducing transporter glycosylation, reduces DAT uptake functioning and promotes its endocytosis (Li *et al*, 2004).

Although mentioned already, the interaction of DAT with proteins such as palmitoylating enzymes and protein kinases is an important mode of DAT regulation. DAT also interacts with non-enzymatic proteins, for example adaptor proteins such as PDZ domain protein interacting with C-kinase 1 (PICK1) or the dopamine D2 autoreceptor (discussed in the next section). There is evidence that SLC6 transporters can form homodimers and other higher order oligomeric complexes (Schmid *et al*, 2001; Sitte *et al*, 2004). A study using both fluorescence resonance energy transfer microscopy and coimmunoprecipitation, demonstrated that DAT can oligomerize and this complex was found in the endoplasmic reticulum and at the cell surface (Sorkina *et al*, 2003). DAT uptake and efflux functions can be differentially regulated and it is plausible that differences in DAT oligomeric states during these processes could account for this.

D2 autoreceptor

In the synaptic cleft, dopamine can activate five G protein-coupled receptors (GPCRs); D1, D2, D3, D4 and D5. Based on their pharmacological, structural, and biochemical properties, the receptors are further subdivided into two classes, the D1-like (D1 and D5) and D2-like (D2, D3, D4) receptors. In 1978, Spano and colleagues carried out one of the pioneering studies that demonstrated that the difference in the two classes lies in their ability to modulate adenylyl cyclase activity and therefore cyclic AMP (cAMP) production (Spano *et al*, 1978). Specifically, the D1-like class of receptors activates the $G\alpha_{s/olf}$ pathway which increases intracellular cAMP via adenylyl cyclase activation. On the other hand, the D2-like family of receptors stimulates the $G\alpha_{i/o}$

pathway that decreases cAMP concentrations by inhibiting adenylyl cyclase. There is also a geographical difference in the groupings. D1 and D5 receptors are found exclusively post-synaptically while D2 and D3 can be found both on the pre- and post-synaptic membrane (Beaulieu *et al*, 2011).

The D2-like family of receptors, mainly the D2 receptors (D2Rs), serve a critical function in the regulation of extracellular dopamine and dopaminergic signaling. These D2Rs can be found on the soma and dendrites of dopamine neurons in the ventral tegmental area and substantia nigra *pars compacta*, in addition to being on the dopaminergic terminals. The presynaptic localization of D2Rs allows them to serve as an autoreceptor. Through a negative-feedback mechanism, activation of the receptors modulates neuronal firing rate and the release and synthesis of dopamine. As previously mentioned, D2R activation decreases cAMP levels but its coupling to the $G_{i/o}$ pathway also causes an increase in potassium currents via G-protein activated inwardly rectifying potassium channels and inhibition of calcium channels. Their activation also indirectly inhibits tyrosine hydroxylase and decreases dopamine transporter expression. This results in a reduction in the excitability of dopamine neurons and halts further synthesis and release of dopamine (Ford, 2014; Neve *et al*, 2004).

Alternative splicing results in two variants of D2 receptors, D2 short ($D2R_S$) and D2 long ($D2R_L$) that differ by 29 amino acids. Initial insights into the physiological roles of the isoforms were gained from the creation of selective $D2R_L$ knockout mice, which had a compensatory overexpression of $D2R_S$ (Usiello *et al*, 2000; Wang *et al*, 2000). These mice had reduced biochemical and behavioral responses linked to post-synaptic striatal D2Rs while maintaining classic autoinhibitory effects. Therefore it was postulated

that $D2R_S$ was the isoform responsible for D2 autoreceptor functioning. However, results from later experiments challenged this notion. For instance, both $D2R_S$ and $D2R_L$ mRNA are expressed in individually isolated dopaminergic substantia nigra pars compacta neurons. In fact, more cells showed $D2R_L$ expression than $D2R_S$. Also dopaminergic substantia nigra *pars compacta* neurons from D2 receptor null mutant mice can generate large inhibitory potassium currents when treated with a D2 agonist after viral restoration of either $D2R_S$ or $D2R_L$. This demonstrates that either isoform can display auto-inhibitory actions (Jang *et al*, 2011; Neve *et al*, 2013).

Although not as profusely studied as DAT, we now have insight into some of the components of D2R regulation. In 1991, it was shown that sodium levels and pH could affect D2R function. More specifically, the concentrations of Na^+ and H^+ ions can significantly change the affinity of the receptor for dopamine and other ligands, hinting that the ionic environment of the receptor can modulate the conformational state of the protein (Neve, 1991). D2R function is also modulated by kinases including protein kinase A (PKA), G protein-coupled receptor kinase (GRK) and PKC; the consensus sequences on the receptor for these three enzymes have been successfully identified. D2R phosphorylation initiated by PKA affects the binding affinity of the receptor for ligands (Elazar and Fuchs, 1991). Meanwhile, GRK phosphorylation seems to play a role in D2R receptor recycling after agonist stimulation (Namkung *et al*, 2009). PKC activation via 4-β-phorbol-12,13-dibutyrate (PDBu) reduces the autoinhibitory actions of D2R on stimulation-evoked dopamine overflow (Cubeddu *et al*, 1989) and silencing ($PKC\beta^{-/-}$ or chemical inhibitors) of the PKCβ isoform potentiates D2R inhibition of chemically and electrically stimulated dopamine release (Luderman *et al*, 2015). PKC-induced

phosphorylation of D2R also leads to the desensitization and β-arrestin- and dynamin-dependent internalization of the receptor (Namkung and Sibley, 2004).

In the previous section, it was briefly mentioned that D2R and DAT directly interact. Several lines of evidence support this contention. DAT, D2R and tyrosine hydroxylase coexist in striatal axon and axonal terminals (Hersch *et al*, 1997). A direct interaction between DAT-D2R was identified between the N-terminus of DAT and the third intracellular loop of D2R (Lee *et al*, 2007). Further evidence of functional interdependence between the two proteins is provided by genetic deletions of the proteins. The ability of DAT to clear dopamine is significantly blunted in $D2R^{-/-}$ mice and $DAT^{-/-}$ mice have reduced D2R expression and activity (Dickinson *et al*, 1999; Jones *et al*, 1999). Dissecting the communication between these two major regulators of extracellular dopamine may be key in creating a therapeutic against AMPH abuse. Chen and colleagues, showed that inhibiting PKC, specifically PKCβ, lowers D2R-induced DAT trafficking in neuroblastoma cells and striatal preparations (Chen *et al*, 2013). PKC sits as a common denominator in the regulation of DAT-D2R functioning and could serve as a druggable target to reduce AMPH-stimulated dopamine release, and ultimately reduce the reinforcing effects of the drug. PKC inhibition is particularly of interest, since PKC activation mediates AMPH-induced dopamine efflux and also suppresses D2R autoinhibitory function. Before delving into whether PKC is a viable target, a better understanding of the enzyme is necessary.

PKC and PKC inhibitors

As alluded to previously, PKC is a major mediator of the cross-talk between DAT and D2R. PKC consists of a family of serine/threonine kinases that have been linked to a

vast and diverse collection of GPCR and growth factor-dependent cellular pathways such as proliferation, migration, inflammation and neurotransmission (Dempsey *et al*, 2000; Mochly-Rosen *et al*, 2012). It is therefore not surprising that dysregulation of PKC contributes to many known diseases such as cancer, heart disease, psoriasis and bipolar disorder (Mochly-Rosen *et al*, 2012).

There are ten homologous isoforms of PKC and in addition to being widely expressed, many of the PKC isoforms are co-expressed in the same cells. PKC is a single polypeptide that has two major structural domains: the C-terminal catalytic domain and the N-terminal regulatory domain (Newton, 1995). The C-terminus is highly conserved among the PKC isoforms but also among other kinases in the AGC (Protein Kinase A, G & C) superfamily of enzymes to which PKC also belongs. The catalytic domain is the site of substrate phosphorylation and possesses a conserved ATP and magnesium-binding site, along with a binding site for the substrate phosphoacceptor sequence (Mochly-Rosen *et al*, 2012). Conversely, the regulatory domain is poorly conserved. It is preceded by an autoinhibitory pseudosubstrate region and can contain a PKC homology 1 (C1), PKC homology 2 (C2) and the Phox and Bem1 (PB1) domains (Figure 1.5). Phorbol esters and lipid second messengers (eg. diacyglycerol (DAG) and arachidonic acid) bind to the C1 domain while the C2 domain is responsible for calcium and phosphatidylserine binding. The PB1 domain is a key structure for protein interactions and can bind scaffold, adaptor and other kinases such as mitogen-activated protein/extracellular-signal-regulated kinase kinase (Kazi, 2011; Moscat *et al*, 2006). Overall the regulatory domain is responsible for locking the enzyme in its inactive state and hence restricts the enzyme activity.

The PKC isoforms are divided into their subfamilies based on structural differences in the N-terminal regulatory domain that mediates the activation of the enzyme. The two major groups are the conventional PKCs (α, βI, βII, γ), which are activated by the phospholipid, DAG and Ca^{2+}, and the novel PKCs (δ, ε, θ, η) that only require DAG for activation. The final group is the atypical PKCs (ζ, λ/ι) that do not respond to the same second messengers as the other subfamilies and have a significantly different homology when compared to the other isoforms (Wu-Zhang and Newton, 2013). Three-dimensional crystallographic structures of PKC exist for the following catalytic domains: PKCβII (Moscat *et al*, 2006), PKCθ ((Xu *et al*, 2004) and PKCι

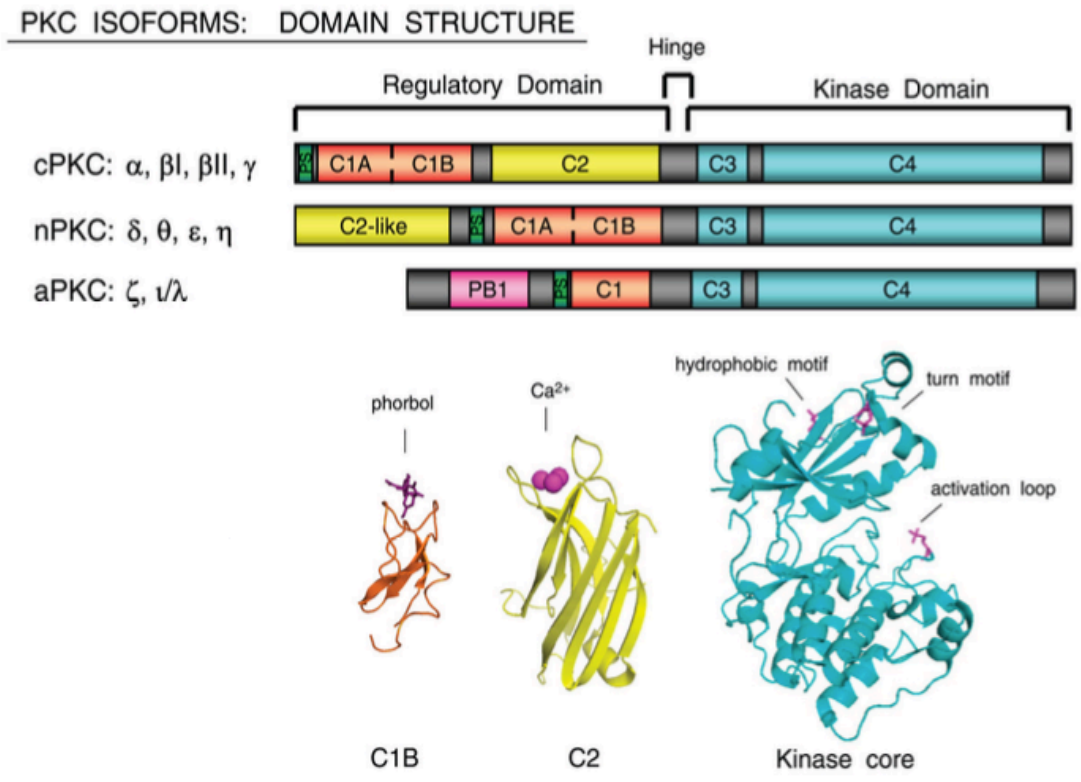

Figure 1.5. Domain structures of PKC subfamilies.
(Steinberg, 2008)

(Messerschmidt *et al*, 2005). There are still no resolved three-dimensional structures of PKC regulatory domains; nonetheless, the function of these domains have been comprehensively validated in various biochemical analyses. Figure 1.5 highlights our current knowledge of the structural differences in PKC isoform structure.

To gain insight into the *in vivo* contributions of specific PKC isoforms to disease initiation and progression, selective PKC inhibitors were created. Some of the challenges faced in this pursuit arise from the fact that PKC isoforms share at least 70% homology at the ATP binding site and there are no crystallographic data of full- length PKC isoforms that would help with *in silico* high throughput screening. In some cases, compounds that were initially classified as selective were later found to have multiple off-target effects. One of the most popular of these cases was Rottlerin, which was initially marketed as a selective PKCδ inhibitor but was later shown to inhibit multiple kinases (including checkpoint kinase 2) and non-kinase proteins (Soltoff, 2007). Even more unfortunate, cellular results gained from siRNA silencing of PKCδ or utilizing kinase dead enzyme did not align with events observed with Rottlerin treatments (Kang *et al*, 2004; Sarkis *et al*, 2006; Woo *et al*, 2004).

Yet, there has been some success in creating a collection of relatively selective PKC inhibitors. Many of these inhibitors bind to the active site and directly block catalysis, such as the bisindolylmaleimide compounds ruboxistaurin and enzastaurin, developed by Eli Lilly. Others interact with the regulatory domain. For instance, bryostatin binds to the C1 domain and has two-fold selectivity for PKCε compared to PKCα and PKCδ (Mochly-Rosen *et al*, 2012). For the purposes of treating brain disorders such as AMPH abuse, we would need the compound to cross the blood brain barrier and

be centrally active. Currently, there is only one known CNS permeant PKC inhibitor, tamoxifen, which inhibits all classical PKC isoforms (α, βI, βII, γ).

(*Trans*)-Tamoxifen (ICI 46,474)

In an interesting turn of events, tamoxifen was discovered in the 1960s from a research program geared at finding non-steroidal estrogen receptor (ER) antagonists that would serve as contraceptive agents. This logic was grounded in early studies done with the first non-steroidal anti-estrogen, MER-25, which produced antifertility effects in rats (Wiseman, 1994). It was soon determined that MER-25 was too toxic for clinical applications but in the meantime, other less toxic, non-steroidal antiestrogens were being made. Once this work was translated to humans, it was quite a surprise that non-steroidal antiestrogens either had no effect or in the case of the drugs tamoxifen and clomiphene, did the opposite as expected and induced fertility in sub-fertile women (Wiseman, 1994). Nonetheless, the initial clinical failures of tamoxifen would soon give way to its claim to fame.

In a sequence of serendipitous events, tamoxifen was found to be effective in treating breast cancer and was marketed in the UK by ICI Pharmaceuticals (now known as AstraZeneca) for this indication in 1973 (Jordan, 2003). In 1977, tamoxifen was approved by the US FDA for the treatment of metastatic breast cancer in post-menopausal women. It was later found to suppress ER-positive breast cancer in premenopausal women, lower contralateral breast cancer in breast cancer patients, lower the risk of breast cancer incidence in high risk women and also prevent the recurrence of breast cancer in previously diagnosed patients (Mourits *et al*, 2001; Peto and Group, 1993). Each year, approximately 1.6 million cases of ER-positive breast cancer are

diagnosed and tamoxifen remains one of the front line-treatment for these individuals. It has been estimated that tamoxifen has spared the lives of 400,000 women alive today, which is quite an impressive statistic (Jordan, 2003).

Tamoxifen is classified as a selective estrogen receptor modulator (SERM) since its actions are dependent on the target tissue and species being studied. More specifically, the compound may act as a pure ER agonist, a partial agonist or an antagonist in different contexts. For instance, tamoxifen is an ER antagonist in breast and mammary tissue but is estrogenic in bones. It has also been found that although tamoxifen is a partial ER agonist in rat uterine tissue, it exhibits estrogenic activity in mouse uterine tissue (Jordan, 2003; Wiseman, 1994)

While tamoxifen itself is biologically active, it is considered a prodrug as its metabolites, 4-hydroxytamoxifen and endoxifen (via N-desmethyltamoxifen), act more potently at the ER (Figure 1.6). The cytochrome P450 enzymes CYP2D6 and CYP3A4/5 catalyze the production of these metabolites. CYP2D6 is a highly polymorphic enzyme, which translates into significantly varied activity in humans (Jordan, 2007). Therefore the presence of CYP2D6 polymorphisms can affect the levels of the active metabolites generated upon tamoxifen administration and contribute to the variability in therapeutic benefits of the SERM in patients.

Although marketed as a SERM, tamoxifen has proven to be a promiscuous compound. In the early- to mid- 1980s, it was demonstrated that tamoxifen had two distinct effects on cell growth proliferation in ER-positive cell lines such as the Michigan Cancer Foundation-7 (MCF-7) cell line. At concentrations near its affinity for ER

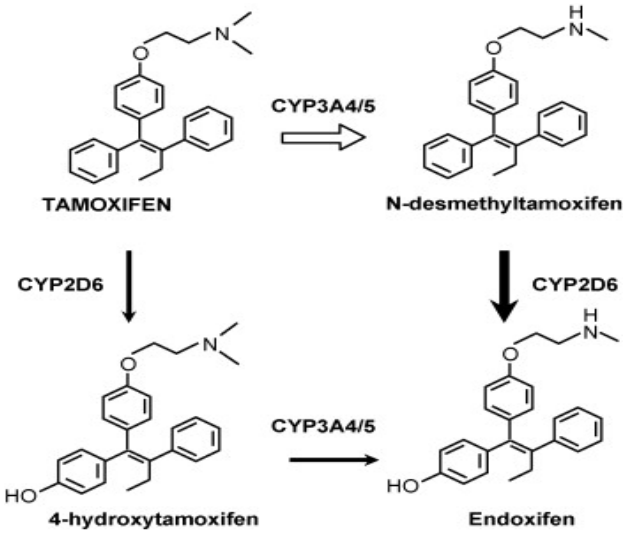

Figure 1.6. Tamoxifen and its metabolites.
(Jordan, 2007)

($K_d \approx 1$nM), tamoxifen was cytostatic and adding the naturally occurring ER agonist, 17β-estradiol, reversed this effect. At higher concentrations of 1-10 μM (levels achieved in patients) tamoxifen exhibited 17β-estradiol irreversible cytotoxic effects in ER-positive cell lines. Therefore, scientists began postulating that the *in vivo* anticancer effects of tamoxifen were only partially due to its action at ER and there were possibly other factors at play. In search of mediators that contributed to these cytotoxic effects, tamoxifen was later found to bind to other targets, such as PKC, calmodulin-dependent enzymes, acyl coenzyme A:cholesterol acyl transferase and the microsomal antiestrogen binding site (de Medina *et al*, 2004; Wiseman, 1994).

The jump from investigating the effects of tamoxifen on ER to its effect on PKC will not seem so unorthodox if one recalls that PKC was well-known to be a high affinity site for the tumor-promoting phorbol esters and that its activation played an important role in carcinogenesis and malignant transformation (de Medina *et al*, 2004; Griner and

Kazanietz, 2007). Therefore, the initial findings that tamoxifen inhibited PKC seemed a reasonable mechanism for the non-ER mediated antitumor effects of the compound.

Tamoxifen as a PKC inhibitor: *In vitro*

A series of studies done between the mid 1980s and the early 1990s uncovered tamoxifen's action as a PKC inhibitor. In 1985, O'Brian and colleagues were the first to report that tamoxifen inhibited the Ca^{2+} and phospholipid dependent PKC phosphotransferase activity with an IC_{50} of 100 μM in a partially purified enzyme system. Tamoxifen did not inhibit the PKC-induced phosphorylation of protamine sulfate, a Ca^{2+} and phospholipid independent process, and therefore implied tamoxifen acts at the regulatory domain of the enzyme. This study also showed that tamoxifen inhibited the binding of the PKC ligand [^{3}H]PDBu (O'Brian *et al*, 1985).

Huai-De and colleagues furthered these findings by revealing PKC inhibition by tamoxifen was competitive with phosphatidylserine but non-competitive with Ca^{2+} (Huai-De *et al*, 1985). The tamoxifen metabolites, 4-hydroxytamoxifen and N-desmethyltamoxifen, also exhibited more potent Ca^{2+} and phospholipid dependent PKC inhibitory activity (IC_{50}s of 25 μM and 8 μM respectively) in the same enzyme preparation used by O'Brian *et al*, 1985 (O'Brian *et al*, 1986). There are later reports, including data from O'Brian and colleagues, indicating that tamoxifen and its metabolites may also be able to directly bind and reduce the activity of the catalytic site of PKC (Nakadate *et al*, 1988; O'Brian *et al*, 1988).

Tamoxifen exhibits more potent inhibitory action on PKC-mediated effects in experiments conducted with cells compared to those using purified enzymes (Gundimeda *et al*, 1996; Horgan *et al*, 1986). Adding complexity to the picture of how tamoxifen

inhibits PKC activity, Gundimeda *et al*, showed that tamoxifen can partition in cell membranes, cause an initial translocation of PKC to the membrane, followed by inhibition and down-regulation of the enzyme. These effects of tamoxifen coincided with a release in arachidonic acid and are blocked with anti-oxidants, such as vitamin C, E and β-carotene, implying that the modulation of PKC by tamoxifen in cells is dependent on oxidative stress.

Tamoxifen as a PKC inhibitor: *In vivo*

Studies in patients with bipolar disorder have given us a clue as to whether PKC inhibition by tamoxifen can be useful in a clinical setting. Bipolar disorder is an affective or mood disorder in which patients swing between states of mania and depression. Symptoms include, but are not limited to, hyperactivity, impulsivity and anhedonia (Abrial *et al*, 2013). Enhanced PKC activity has been linked to the pathology of bipolar disorder. Post-mortem frontal cortex tissue from patients with bipolar disorder show elevated PKC-induced phosphorylation and sub-cellular distribution compared to healthy, matched controls (Wang and Friedman, 1996). The standard treatments for bipolar disorder, lithium and valproate, affect multiple signaling pathways but it has been proposed that their ability to block PKC activity contributes to their therapeutic benefits for bipolar disorder (Einat *et al*, 2007).

With this in mind, studies were conducted to see whether the PKC inhibitory effects of tamoxifen could relieve symptoms in patients with bipolar disorder. In 2000, Bebchuk and colleagues conducted the first study to answer this question. The results were that bipolar disorder patients given tamoxifen had a significant decrease in manic symptoms as evaluated on the Young Mania Rating Scale or YMRS (Bebchuk *et al*,

2000). In line with this, it was later reported that tamoxifen significantly reduced symptoms of mania in bipolar disorder patients in a double blind, placebo controlled study. However, there was no significant change in depression score (Zarate *et al*, 2007). These initial investigations were all conducted in adults but recently the effect of tamoxifen was explored in an adolescent bipolar disorder population. In this study, adolescents given tamoxifen plus lithium had an improvement in both manic and depressive symptoms compared with participants given lithium alone. It is noteworthy that there were no serious adverse effects of tamoxifen in any of these short trials (Fallah *et al*, 2016).

Modeling bipolar disorder in animals is difficult. The closest we have come to achieving this is by using AMPH to induce 'manic' effects or hyperactivity. In rats tamoxifen reduces AMPH-stimulated hyperlocomotion and reduces the phosphorylation of growth-associated protein at a site specific for PKC phosphorylation (Einat *et al*, 2007). Abrial, *et al*, reproduced these behavioral effects of tamoxifen in 2013. In addition to showing that tamoxifen reduces AMPH-induced hyperactivity, they also reported that tamoxifen reduces risk-taking behaviors, modeled using an open field test (Abrial *et al*, 2013). Contrary to the clinical trials, tamoxifen did induce depressive-like symptoms as inferred from the rats displaying increased immobility in forced-swim tests (Abrial *et al*, 2013).

With these promising results, tamoxifen could prove useful in PKC activation-related brain disorders like bipolar disorder and AMPH abuse. However, although patients generally tolerate the drug, reducing the target promiscuity of the tamoxifen could lead to increased therapeutic outcomes. If we knew more about how different

substructures on the tamoxifen scaffold facilitated its interaction with its known targets, we may be able to engineer a more selective brain-penetrant PKC inhibitor. Fortuitously, some of this knowledge is available.

Tamoxifen structure-activity studies

The increased curiosity in the antitumor mechanism of tamoxifen fostered an interest in the structure-activity relationship (SAR) of the tamoxifen at its known targets, namely the ER and PKC. The hope was that with a better understanding of the SAR, researchers could possibly make safer, more efficacious antitumor agents. Tamoxifen is a member of series of compounds called triphenylethylenes, to which the SERM clomiphene also belongs. One of the first studies that began to untangle the SAR of tamoxifen at PKC investigated the effects of side-chain substitutions on a closely related chemical class of compounds, the triphenylacrylonitriles. It was reported that diethylaminoethoxy side-chain substitutions, *i.e.* introducing basic residues, changed the manner by which the compounds inhibited the classical PKC isoforms. More specifically, phenyl substitutions with one or two diethylaminoethoxy groups flipped the mode of PKC inhibition from acting directly at the catalytic site to engaging the regulatory domain in a phospholipid-dependent manner (Bignon *et al*, 1989).

This was later expanded into more thorough SAR investigations dissecting the impact of both the di- and tri-phenylethylene structure on the activation and inhibition of classical PKC isoforms, which are well outlined in the 2004 review by DeMedina *et al*. These studies demonstrate that the PKC inhibitory properties of tamoxifen are facilitated by the presence of a) a basic side chain b) a phenylpropene moiety within the aromatic backbone c) a side chain with a protonable and H-bond donatable amino group.

Furthermore, replacing the ethyl group with a cyano group, adding another basic linker on the α-ring and adding substituents to the α-ring 4-position can all improve the scaffold's PKC inhibitory potential. Loss of the aminoethoxy side chain and the β-ring leads to tamoxifen analogues that can activate PKC. On the other hand, the triphenyethylene backbone and side chain on tamoxifen are essential for its ability to bind to the ER (de Medina *et al*, 2004).

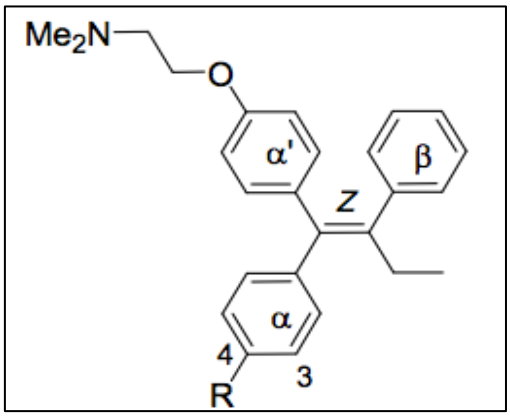

Figure 1.7. Substructures of tamoxifen.
adapted from (de Medina *et al*, 2004).

Thesis hypothesis and summary

By mediating the communication between D2R and DAT, PKC stands as a novel target for the modulation of extracellular dopamine. My central hypothesis is that PKC activation is a fundamental mediator of the action of AMPH at the dopaminergic synapse and ultimately AMPH reinforcement. Therefore I propose that brain-permeant PKC inhibitors will reduce the reinforcing effects of AMPH, hence providing a suitable pharmacological treatment for AMPH abuse.

There are *in vitro and in vivo* experiments that support this hypothesis. Our group has shown PKC inhibitors Gö6976, LY379196 and Ro31822 blocked AMPH-mediated

dopamine release in striatal slices (Johnson *et al*, 2005; Kantor *et al*, 1998). *In vivo*, accumbal administration of the PKC inhibitor Ro31822 reduced AMPH-stimulated dopamine overflow (Loweth *et al*, 2009). Recently we showed that accumbal administration of the PKCβ selective inhibitors, ruboxistaurin and enzastaurin, significantly decreased AMPH-induced dopamine overflow and hyperactivity in freely-moving rats (Zestos *et al*, 2016). A study conducted by Aujla and Beninger, showed that accumbal administration of the PKC inhibitor, NPC 15437, blocked AMPH-induced condition place-preference (Aujla and Beninger, 2003). These studies support the idea that PKC inhibition can block the rewarding and reinforcing effects of AMPH.

Since there are no selective brain-barrier permeant PKC inhibitors available, all the previously mentioned *in vivo* studies required direct CNS administration of the PKC inhibitors under investigation. If our endpoint is to use PKC inhibitors clinically for AMPH abuse, we must create compounds that are brain permeant. With the extent of SAR available on the non-selective PKC inhibitor and SERM tamoxifen, the goal of my thesis work was to create a new generation of brain-permeant tamoxifen analogues with improved selectivity for PKC inhibition. In Chapter 2, I present a collection of novel tamoxifen analogues generated through collaboration with the Vahlteich Medicinal Core at the University of Michigan. In addition to showing the novel routes and compound characterization methods used to make and identify the compounds, I also present the *in vitro* methodologies I employed to characterize the ER binding properties and PKC inhibitory activity of the compounds. Through these studies, I was able to identify a promising compound, **6c**, which was 250 times more potent than tamoxifen in inhibiting PKC *in vitro*, while not having appreciable affinity at ER.

In Chapter 3, I elucidate the effect of **6c** at the dopaminergic terminal. I begin by showing that the **6c** maintains PKC inhibitory activity in synaptosomes, a popularly used model for the dopaminergic terminal. Interestingly, **6c** shows PKC-substrate selectivity, which may be a clue of its action at PKC. I found that **6c** dose-dependently blocks AMPH-stimulated dopamine efflux and less potently blocks dopamine uptake. We found no binding site for the compound at the dopamine transporter and **6c** did not alter DAT levels at concentrations up to 3 μM. Finally, **6c** crosses the blood-brain barrier and was able to block *in vivo* AMPH neurochemical effects and reinforcement.

In Chapter 4, I present results that paint a more mechanistic picture of the direct action of **6c** on PKC. Using FRET (fluorescence resonance energy transfer)- based studies, my preliminary findings demonstrate that **6c** does not block PKC translocation but instead alters its conformational states. Next, I evaluated whether **6c** alters the activity of other feasible targets, such as protein kinase B (AKT) and Ca^{2+}/calmodulin-dependent protein kinase II (CAMKII), that also affect dopamine transporter function. I found that **6c** does not affect AKT or CAMKII activity. In an effort to bolster our hypothesis that PKC is the likely culprit mediating the ability of **6c** to block AMPH effects *in vivo*, I show that **6c** inhibits PKC activity *in vivo*. To cap off this chapter, I present my findings assessing whether cells are the best systems for deciphering the action of compounds at the dopaminergic terminal. This small investigation demonstrates that DAT-modulating effects of **6c** observed *in vivo* are better modeled in synaptosomes versus cells.

In the final chapter, I discuss the utility of repurposing the tamoxifen scaffold for novel therapeutics. There are still many unanswered questions regarding the mechanism of action of **6c**. For instance, is there still a possibility that the compound could be

allosterically modulating DAT? Is **6c** working through one or multiple PKC isoforms? I address questions regarding the effects of **6c** on the uptake functioning of the transporter and postulate why **6c** is not likely a primary reinforcer. I also present future studies we hope will address these ruminations.

References

Abrial E, Etievant A, Bétry C, Scarna H, Lucas G, Haddjeri N, Lambás-Señas L (2013). Protein kinase C regulates mood-related behaviors and adult hippocampal cell proliferation in rats. *Progress in neuro-psychopharmacology and biological psychiatry* **43**: 40-48.

Andén N-E, Carlsson A, Dahlström A, Fuxe K, Hillarp N-Å, Larsson K (1964). Demonstration and mapping out of nigro-neostriatal dopamine neurons. *Life sciences* **3**(6): 523-530.

Aujla H, Beninger RJ (2003). Intra-accumbens protein kinase C inhibitor NPC 15437 blocks amphetamine-produced conditioned place preference in rats. *Behavioural Brain Research* **147**(1–2): 41-48.

Beaulieu JM, Gainetdinov RR (2011). The physiology, signaling, and pharmacology of dopamine receptors. *Pharmacological reviews* **63**(1): 182-217.

Bebchuk JM, Arfken CL, Dolan-Manji S, Murphy J, Hasanat K, Manji HK (2000). A preliminary investigation of a protein kinase C inhibitor in the treatment of acute mania. *Archives of general psychiatry* **57**(1): 95-97.

Berman S, O'Neill J, Fears S, Bartzokis G, London ED (2008). Abuse of amphetamines and structural abnormalities in the brain. *Annals of the New York Academy of Sciences* **1141**: 195-220.

Beuming T, Kniazeff J, Bergmann ML, Shi L, Gracia L, Raniszewska K, Newman AH, Javitch JA, Weinstein H, Gether U, Loland CJ (2008). The binding sites for cocaine and dopamine in the dopamine transporter overlap. *Nature neuroscience* **11**(7): 780-789.

Bignon E, Ogita K, Kishimoto A, Gilbert J, Abecassis J, Miquel JF, Nishizuka Y (1989). Modes of inhibition of protein kinase C by triphenylacrylonitrile antiestrogens. *Biochemical and biophysical research communications* **163**(3): 1377-1383.

Brackins T, Brahm NC, Kissack JC (2011). Treatments for methamphetamine abuse: a literature review for the clinician. *Journal of Pharmacy Practice* **24**(6): 541-550.

Bramness JG, Gundersen OH, Guterstam J, Rognli EB, Konstenius M, Loberg EM, Medhus S, Tanum L, Franck J (2012). Amphetamine-induced psychosis--a separate diagnostic entity or primary psychosis triggered in the vulnerable? *BMC Psychiatry* **12**: 221.

Brody TM, Larner J, Minneman KP (1998). *Human Pharmacology: molecular to clinical.* Mosby, St Louis.

Carlsson A (1993). Thirty years of dopamine research. *Advances in neurology* **60**: 1-10.

Carvalho M, Carmo H, Costa VM, Capela JP, Pontes H, Remiao F, Carvalho F, Bastos Mde L (2012). Toxicity of amphetamines: an update. *Archives of toxicology* **86**(8): 1167-1231.

Chen R, Daining CP, Sun H, Fraser R, Stokes SL, Leitges M, Gnegy ME (2013). Protein kinase Cβ is a modulator of the dopamine D2 autoreceptor‐activated trafficking of the dopamine transporter. *Journal of neurochemistry* **125**(5): 663-672.

Chiueh CC, Moore KE (1975). D-amphetamine-induced release of "newly synthesized" and "stored" dopamine from the caudate nucleus in vivo. *The Journal of pharmacology and experimental therapeutics* **192**(3): 642-653.

Copeland BJ, Vogelsberg V, Neff NH, Hadjiconstantinou M (1996). Protein kinase C activators decrease dopamine uptake into striatal synaptosomes. *The Journal of pharmacology and experimental therapeutics* **277**(3): 1527-1532.

Cowell RM, Kantor L, Hewlett GH, Frey KA, Gnegy ME (2000). Dopamine transporter antagonists block phorbol ester-induced dopamine release and dopamine transporter phosphorylation in striatal synaptosomes. *European journal of pharmacology* **389**(1): 59-65.

Cubeddu LX, Lovenberg TW, Hoffman IS, Talmaciu RK (1989). Phorbol esters and D2-dopamine receptors. *The Journal of pharmacology and experimental therapeutics* **251**(2): 687-693.

Dahlström A, Fuxe K (1963). Evidence for the existence of monoamine-containing neurons in the central nervous system. I. Demonstration of monoamines in the cell bodies of brain stem neurons. *Acta Physiologica Scandinavica Supplementum*: SUPPL 232: 231-255.

de Medina P, Favre G, Poirot M (2004). Multiple targeting by the antitumor drug tamoxifen: a structure-activity study. *Current medicinal chemistry Anti-cancer agents* **4**(6): 491-508.

Dempsey EC, Newton AC, Mochly-Rosen D, Fields AP, Reyland ME, Insel PA, Messing RO (2000). Protein kinase C isozymes and the regulation of diverse cell responses. *American Journal of Physiology-Lung Cellular and Molecular Physiology* **279**(3): L429-L438.

Di Chiara G, Imperato A (1988). Drugs abused by humans preferentially increase synaptic dopamine concentrations in the mesolimbic system of freely moving rats. *Proceedings of the National Academy of Sciences of the United States of America* **85**(14): 5274-5278.

Dickinson SD, Sabeti J, Larson GA, Giardina K, Rubinstein M, Kelly MA, Grandy DK, Low MJ, Gerhardt GA, Zahniser NR (1999). Dopamine D2 receptor‐deficient mice exhibit decreased dopamine transporter function but no changes in dopamine release in dorsal striatum. *Journal of neurochemistry* **72**(1): 148-156.

Einat H, Yuan P, Szabo ST, Dogra S, Manji HK (2007). Protein kinase C inhibition by tamoxifen antagonizes manic-like behavior in rats: implications for the development of novel therapeutics for bipolar disorder. *Neuropsychobiology* **55**(3-4): 123-131.

Elazar Z, Fuchs S (1991). Phosphorylation by cyclic AMP‐dependent protein kinase modulates agonist binding to the D2 dopamine receptor. *Journal of neurochemistry* **56**(1): 75-80.

Elsworth JD, Roth RH (1997). Dopamine synthesis, uptake, metabolism, and receptors: relevance to gene therapy of Parkinson's disease. *Experimental neurology* **144**(1): 4-9.

Erreger K, Grewer C, Javitch JA, Galli A (2008). Currents in response to rapid concentration jumps of amphetamine uncover novel aspects of human dopamine transporter function. *The Journal of Neuroscience* **28**(4): 976.

Espelin DE, Done AK (1968). Amphetamine poisoning: Effectiveness of chlorpromazine. *New England Journal of Medicine* **278**(25): 1361-1365.

Fallah E, Arman S, Najafi M, Shayegh B (2016). Effect of tamoxifen and lithium on treatment of acute mania symptoms in children and adolescents. *Iranian journal of child neurology* **10**(2): 16.

Fleckenstein AE, Volz TJ, Riddle EL, Gibb JW, Hanson GR (2007). New insights into the mechanism of action of amphetamines. *Annual Review of Pharmacology and Toxicology* **47**: 681-698.

Fon EA, Pothos EN, Sun BC, Killeen N, Sulzer D, Edwards RH (1997). Vesicular transport regulates monoamine storage and release but is not essential for amphetamine action. *Neuron* **19**(6): 1271-1283.

Ford CP (2014). The role of D2-autoreceptors in regulating dopamine neuron activity and transmission. *Neuroscience* **282**: 13-22.

Freyberg Z, Sonders MS, Aguilar JI, Hiranita T, Karam CS, Flores J, Pizzo AB, Zhang Y, Farino ZJ, Chen A, Martin CA, Kopajtic TA, Fei H, Hu G, Lin YY, Mosharov EV, McCabe BD, Freyberg R, Wimalasena K, Hsin LW, Sames D, Krantz DE, Katz JL, Sulzer D, Javitch JA (2016). Mechanisms of amphetamine action illuminated through optical monitoring of dopamine synaptic vesicles in Drosophila brain. *Nature communications* **7**: 10652.

German CL, Baladi MG, McFadden LM, Hanson GR, Fleckenstein AE (2015). Regulation of the dopamine and vesicular monoamine transporters: Pharmacological targets and implications for disease. *Pharmacological reviews* **67**(4): 1005-1024.

Giambalvo CT (1992). Protein kinase C and dopamine transport--1. Effects of amphetamine in vivo. *Neuropharmacology* **31**(12): 1201-1210.

Giambalvo CT (2004). Mechanisms underlying the effects of amphetamine on particulate PKC activity. *Synapse (New York, NY)* **51**(2): 128-139.

Giros B, El Mestikawy S, Bertrand L, Caron MG (1991). Cloning and functional characterization of a cocaine-sensitive dopamine transporter. *FEBS letters* **295**(1-3): 149-154.

Giros B, el Mestikawy S, Godinot N, Zheng K, Han H, Yang-Feng T, Caron MG (1992). Cloning, pharmacological characterization, and chromosome assignment of the human dopamine transporter. *Molecular pharmacology* **42**(3): 383-390.

Gnegy ME, Khoshbouei H, Berg KA, Javitch JA, Clarke WP, Zhang M, Galli A (2004). Intracellular Ca2+ regulates amphetamine-induced dopamine efflux and currents mediated by the human dopamine transporter. *Molecular pharmacology* **66**(1): 137-143.

Gonzalez AM, Walther D, Pazos A, Uhl GR (1994). Synaptic vesicular monoamine transporter expression: distribution and pharmacologic profile. *Brain research Molecular brain research* **22**(1-4): 219-226.

Greene SL, Kerr F, Braitberg G (2008). Review article: amphetamines and related drugs of abuse. *Emergency Medicine Australasia* **20**(5): 391-402.

Griner EM, Kazanietz MG (2007). Protein kinase C and other diacylglycerol effectors in cancer. *Nature Reviews Cancer* **7**(4): 281-294.

Gundimeda U, Chen ZH, Gopalakrishna R (1996). Tamoxifen modulates protein kinase C via oxidative stress in estrogen receptor-negative breast cancer cells. *The Journal of biological chemistry* **271**(23): 13504-13514.

Heal DJ, Smith SL, Gosden J, Nutt DJ (2013). Amphetamine, past and present--a pharmacological and clinical perspective. *Journal of Psychopharmacology* **27**(6): 479-496.

Herman MA, Roberto M (2015). The addicted brain: understanding the neurophysiological mechanisms of addictive disorders. *Frontiers in Integrative Neuroscience* **9**(18).

Hersch SM, Yi H, Heilman CJ, Edwards RH, Levey AI (1997). Subcellular localization and molecular topology of the dopamine transporter in the striatum and substantia nigra. *The Journal of comparative neurology* **388**(2): 211-227.

Horgan K, Cooke E, Hallett MB, Mansel RE (1986). Inhibition of protein kinase C mediated signal transduction by tamoxifen. *Biochemical pharmacology* **35**(24): 4463-4465.

Huai-De S, Mazzei GJ, Vogler WR (1985). Effect of tamoxifen, a nonsteroidal antiestrogen, on phospholipid/calcium-dependent protein kinase and phosphorylation of its endogenous substrate proteins from the rat brain and ovary. *Biochemical pharmacology* **34**(20): 3649-3653.

Jang JY, Jang M, Kim SH, Um KB, Kang YK, Kim HJ, Chung S, Park MK (2011). Regulation of dopaminergic neuron firing by heterogeneous dopamine autoreceptors in the substantia nigra pars compacta. *Journal of neurochemistry* **116**(6): 966-974.

Johnson LA, Guptaroy B, Lund D, Shamban S, Gnegy ME (2005). Regulation of amphetamine-stimulated dopamine efflux by protein kinase C beta. *The Journal of biological chemistry* **280**(12): 10914-10919.

Jones SR, Gainetdinov RR, Hu X-T, Cooper DC, Wightman RM, White FJ, Caron MG (1999). Loss of autoreceptor functions in mice lacking the dopamine transporter. *Nature neuroscience* **2**(7): 649-655.

Jones SR, Gainetdinov RR, Wightman RM, Caron MG (1998). Mechanisms of amphetamine action revealed in mice lacking the dopamine transporter. *The Journal of neuroscience : the official journal of the Society for Neuroscience* **18**(6): 1979-1986.

Jordan VC (2003). Tamoxifen: a most unlikely pioneering medicine. *Nature reviews Drug discovery* **2**(3): 205-213.

Jordan VC (2007). New insights into the metabolism of tamoxifen and its role in the treatment and prevention of breast cancer. *Steroids* **72**(13): 829-842.

Kang HS, Park EK, Kim KH, Park J-Y, Choi J-Y, Shin H-I, Jun C-D, Kang S-S, Kim S-Y (2004). Receptor activator of nuclear factor-icB is induced by a Rottlerin-sensitive and p38 MAP kinase-dependent pathway during monocyte differentiation. *Molecules & Cells (Springer Science & Business Media BV)* **17**(3).

Kantor L, Gnegy ME (1998). Protein kinase C inhibitors block amphetamine-mediated dopamine release in rat striatal slices. *The Journal of pharmacology and experimental therapeutics* **284**(2): 592-598.

Kantor L, Hewlett GH, Park YH, Richardson-Burns SM, Mellon MJ, Gnegy ME (2001). Protein kinase C and intracellular calcium are required for amphetamine-mediated

dopamine release via the norepinephrine transporter in undifferentiated PC12 cells. *The Journal of pharmacology and experimental therapeutics* **297**(3): 1016-1024.

Kantor L, Zhang M, Guptaroy B, Park Y, Gnegy M (2004). Repeated amphetamine couples norepinephrine transporter and calcium channel activities in PC12 cells. *Journal of Pharmacology and Experimental Therapeutics* **311**(3): 1044-1051.

Kazi JU (2011). The mechanism of protein kinase C regulation. *Frontiers in Biology* **6**(4): 328-336.

Kilty JE, Lorang D, Amara SG (1991). Cloning and expression of a cocaine-sensitive rat dopamine transporter. *Science (New York, NY)* **254**(5031): 578-580.

Kimura M, Matsumoto N (1997). Nigrostriatal dopamine system may contribute to behavioral learning through providing reinforcement signals to the striatum. *European Neurology* **38**(Suppl. 1): 11-17.

Klawans HL, Jr. (1968). Chlorpromazine vs. amphetamine. *The New England journal of medicine* **279**(6): 329.

Lee FJ, Pei L, Moszczynska A, Vukusic B, Fletcher PJ, Liu F (2007). Dopamine transporter cell surface localization facilitated by a direct interaction with the dopamine D2 receptor. *The EMBO journal* **26**(8): 2127-2136.

Li L-B, Chen N, Ramamoorthy S, Chi L, Cui X-N, Wang LC, Reith ME (2004). The role of N-glycosylation in function and surface trafficking of the human dopamine transporter. *Journal of Biological Chemistry* **279**(20): 21012-21020.

Liang NY, Rutledge CO (1982). Evidence for carrier-mediated efflux of dopamine from corpus striatum. *Biochemical pharmacology* **31**(15): 2479-2484.

Loweth JA, Svoboda R, Austin JD, Guillory AM, Vezina P (2009). The PKC inhibitor Ro31-8220 blocks acute amphetamine-induced dopamine overflow in the nucleus accumbens. *Neuroscience letters* **455**(2): 88-92.

Luderman KD, Chen R, Ferris MJ, Jones SR, Gnegy ME (2015). Protein kinase C beta regulates the D(2)-like dopamine autoreceptor. *Neuropharmacology* **89**: 335-341.

Lüscher C (2012). Chapter 32. Drugs of Abuse. In: Katzung BG, Masters SB, Trevor AJ (eds). *Basic & Clinical Pharmacology, 12e*. The McGraw-Hill Companies: New York, NY.

Mantle TJ, Tipton KF, Garrett NJ (1976). Inhibition of monoamine oxidase by amphetamine and related compounds. *Biochemical pharmacology* **25**(18): 2073-2077.

Maxwell JC, Rutkowski BA (2008). The prevalence of methamphetamine and amphetamine abuse in North America: a review of the indicators, 1992-2007. *Drug and Alcohol Review* **27**(3): 229-235.

Meiser J, Weindl D, Hiller K (2013). Complexity of dopamine metabolism. *Cell Communication and Signaling* **11**(1): 34.

Messerschmidt A, Macieira S, Velarde M, Bädeker M, Benda C, Jestel A, Brandstetter H, Neuefeind T, Blaesse M (2005). Crystal structure of the catalytic domain of human atypical protein kinase C-iota reveals interaction mode of phosphorylation site in turn motif. *Journal of molecular biology* **352**(4): 918-931.

Miller GM (2011). The Emerging Role of Trace Amine Associated Receptor 1 in the Functional Regulation of Monoamine Transporters and Dopaminergic Activity. *Journal of neurochemistry* **116**(2): 164-176.

Miranda M, Wu CC, Sorkina T, Korstjens DR, Sorkin A (2005). Enhanced ubiquitylation and accelerated degradation of the dopamine transporter mediated by protein kinase C. *Journal of Biological Chemistry* **280**(42): 35617-35624.

Mochly-Rosen D, Das K, Grimes KV (2012). Protein kinase C, an elusive therapeutic target? *Nature reviews Drug discovery* **11**(12): 937-957.

Moritz AE, Rastedt DE, Stanislowski DJ, Shetty M, Smith MA, Vaughan RA, Foster JD (2015). Reciprocal phosphorylation and palmitoylation control dopamine transporter kinetics. *Journal of Biological Chemistry* **290**(48): 29095-29105.

Moscat J, Diaz-Meco MT, Albert A, Campuzano S (2006). Cell signaling and function organized by PB1 domain interactions. *Molecular cell* **23**(5): 631-640.

Mourits MJ, De Vries EG, Willemse PH, Ten Hoor KA, Hollema H, Van der Zee AG (2001). Tamoxifen treatment and gynecologic side effects: a review. *Obstetrics & Gynecology* **97**(5): 855-866.

Nakadate T, Jeng AY, Blumberg PM (1988). Comparison of protein kinase C functional assays to clarify mechanisms of inhibitor action. *Biochemical pharmacology* **37**(8): 1541-1545.

Namkung Y, Dipace C, Javitch JA, Sibley DR (2009). G protein-coupled receptor kinase-mediated phosphorylation regulates post-endocytic trafficking of the D2 dopamine receptor. *Journal of Biological Chemistry* **284**(22): 15038-15051.

Namkung Y, Sibley DR (2004). Protein kinase C mediates phosphorylation, desensitization, and trafficking of the D2 dopamine receptor. *Journal of Biological Chemistry* **279**(47): 49533-49541.

Nestler EJ (2004). Molecular mechanisms of drug addiction. *Neuropharmacology* **47**: 24-32.

Neve KA (1991). Regulation of dopamine D2 receptors by sodium and pH. *Molecular pharmacology* **39**(4): 570-578.

Neve KA, Ford CP, Buck DC, Grandy DK, Neve RL, Phillips TJ (2013). Normalizing dopamine D2 receptor-mediated responses in D2 null mutant mice by virus-mediated receptor restoration: comparing D2L and D2S. *Neuroscience* **248**: 479-487.

Neve KA, Seamans JK, Trantham-Davidson H (2004). Dopamine receptor signaling. *Journal of receptors and signal transduction* **24**(3): 165-205.

Newton AC (1995). Protein kinase C: structure, function, and regulation. *Journal of Biological Chemistry* **270**(48): 28495-28498.

O'Brian CA, Housey GM, Weinstein IB (1988). Specific and direct binding of protein kinase C to an immobilized tamoxifen analogue. *Cancer research* **48**(13): 3626-3629.

O'Brian CA, Liskamp RM, Solomon DH, Weinstein IB (1985). Inhibition of protein kinase C by tamoxifen. *Cancer research* **45**(6): 2462-2465.

O'Brian CA, Liskamp RM, Solomon DH, Weinstein IB (1986). Triphenylethylenes: a new class of protein kinase C inhibitors. *Journal of the National Cancer Institute* **76**(6): 1243-1246.

Opazo F, Schulz JB, Falkenburger BH (2010). PKC links Gq-coupled receptors to DAT-mediated dopamine release. *Journal of neurochemistry* **114**(2): 587-596.

Parker EM, Cubeddu LX (1986). Effects of d-amphetamine and dopamine synthesis inhibitors on dopamine and acetylcholine neurotransmission in the striatum. I. Release in the absence of vesicular transmitter stores. *The Journal of pharmacology and experimental therapeutics* **237**(1): 179-192.

Penmatsa A, Wang KH, Gouaux E (2013). X-ray structure of dopamine transporter elucidates antidepressant mechanism. *Nature* **503**(7474): 85-90.

Peter D, Jimenez J, Liu Y, Kim J, Edwards RH (1994). The chromaffin granule and synaptic vesicle amine transporters differ in substrate recognition and sensitivity to inhibitors. *The Journal of biological chemistry* **269**(10): 7231-7237.

Peto R, Group EBCTC (1993). Systemic treatment of early breast cancer by hormonal, cytotoxic, or immune therapy: 133 randomised trials involving 31 000 recurrences and 24 000 deaths among 75 000 women (summary). *Adjuvant Therapy of Breast Cancer IV*. Springer, pp 153-157.

Pifl C, Drobny H, Reither H, Hornykiewicz O, Singer EA (1995). Mechanism of the dopamine-releasing actions of amphetamine and cocaine: plasmalemmal dopamine transporter versus vesicular monoamine transporter. *Molecular pharmacology* **47**(2): 368-373.

Raiteri M, Cerrito F, Cervoni AM, Del Carmine R, Ribera MT, Levi G (1978). Release of dopamine from striatal synaptosomes. *Annali dell'Istituto superiore di sanita* **14**(1): 97-110.

Raiteri M, Cerrito F, Cervoni AM, Levi G (1979). Dopamine can be released by two mechanisms differentially affected by the dopamine transport inhibitor nomifensine. *Journal of Pharmacology and Experimental Therapeutics* **208**(2): 195.

Ramayya AG, Misra A, Baltuch GH, Kahana MJ (2014). Microstimulation of the Human Substantia Nigra Alters Reinforcement Learning. *The Journal of Neuroscience* **34**(20): 6887-6895.

Routtenberg A, Malsbury C (1969). Brainstem pathways of reward. *Journal of comparative and physiological psychology* **68**(1): 22-30.

Sarkis PTN, Ying S, Xu R, Yu X-F (2006). STAT1-independent cell type-specific regulation of antiviral APOBEC3G by IFN-α. *The Journal of Immunology* **177**(7): 4530-4540.

Schmid JA, Scholze P, Kudlacek O, Freissmuth M, Singer EA, Sitte HH (2001). Oligomerization of the human serotonin transporter and of the rat GABA transporter 1 visualized by fluorescence resonance energy transfer microscopy in living cells. *Journal of Biological Chemistry* **276**(6): 3805-3810.

Schmitt KC, Rothman RB, Reith ME (2013). Nonclassical pharmacology of the dopamine transporter: atypical inhibitors, allosteric modulators, and partial substrates. *The Journal of pharmacology and experimental therapeutics* **346**(1): 2-10.

Scholze P, Zwach J, Kattinger A, Pifl C, Singer EA, Sitte HH (2000). Transporter-mediated release: a superfusion study on human embryonic kidney cells stably expressing the human serotonin transporter. *The Journal of pharmacology and experimental therapeutics* **293**(3): 870-878.

Shan J, Javitch JA, Shi L, Weinstein H (2011). The substrate-driven transition to an inward-facing conformation in the functional mechanism of the dopamine transporter. *PloS one* **6**(1): e16350.

Shi L, Quick M, Zhao Y, Weinstein H, Javitch JA (2008). The mechanism of a neurotransmitter:sodium symporter – inward release of Na(+) and substrate is triggered by substrate in a second binding site. *Molecular cell* **30**(6): 667-677.

Shimada S, Kitayama S (1991). Cloning and expression of a cocaine-sensitive dopamine transporter complementary DNA. *Science (New York, NY)* **254**(5031): 576.

Sitte HH, Farhan H, Javitch JA (2004). Sodium-dependent neurotransmitter transporters: oligomerization as a determinant of transporter function and trafficking. *Molecular interventions* **4**(1): 38.

Sitte HH, Scholze P, Schloss P, Pifl C, Singer EA (2000). Characterization of carrier-mediated efflux in human embryonic kidney 293 cells stably expressing the rat serotonin transporter: a superfusion study. *Journal of neurochemistry* **74**(3): 1317-1324.

Soltoff SP (2007). Rottlerin: an inappropriate and ineffective inhibitor of PKCδ. *Trends in pharmacological sciences* **28**(9): 453-458.

Sorkina T, Doolen S, Galperin E, Zahniser NR, Sorkin A (2003). Oligomerization of dopamine transporters visualized in living cells by fluorescence resonance energy transfer microscopy. *The Journal of biological chemistry* **278**(30): 28274-28283.

Sotnikova TD, Beaulieu JM, Gainetdinov RR, Caron MG (2006). Molecular biology, pharmacology and functional role of the plasma membrane dopamine transporter. *CNS & Neurological Disorders-Drug Targets* **5**(1): 45-56.

Spano PF, Govoni S, Trabucchi M (1978). Studies on the pharmacological properties of dopamine receptors in various areas of the central nervous system. *Advances in biochemical psychopharmacology* **19**: 155-165.

Steinberg SF (2008). Structural basis of protein kinase C isoform function. *Physiological reviews* **88**(4): 1341-1378.

Substance Abuse and Mental Health Services Administration CfBHSaQ (2013). *The DAWN Report: Emergency department visits involving Attention Deficit/Hyperactivity Disorder stimulant medications*(Rockville, MD).

Sucic S, Dallinger S, Zdrazil B, Weissensteiner R, Jørgensen TN, Holy M, Kudlacek O, Seidel S, Cha JH, Gether U (2010). The N terminus of monoamine transporters is a lever required for the action of amphetamines. *Journal of Biological Chemistry* **285**(14): 10924-10938.

Sulzer D, Rayport S (1990). Amphetamine and other psychostimulants reduce pH gradients in midbrain dopaminergic neurons and chromaffin granules: a mechanism of action. *Neuron* **5**(6): 797-808.

UNODC (2012). World drug report. *United Nations publication, Sales No E12XI1*.

Usiello A, Baik JH, Rouge-Pont F, Picetti R, Dierich A, LeMeur M, Piazza PV, Borrelli E (2000). Distinct functions of the two isoforms of dopamine D2 receptors. *Nature* **408**(6809): 199-203.

Vaughan RA (2004). Phosphorylation and regulation of psychostimulant-sensitive neurotransmitter transporters. *Journal of Pharmacology and Experimental Therapeutics* **310**(1): 1.

Vaughan RA, Foster JD (2013). Mechanisms of dopamine transporter regulation in normal and disease states. *Trends in pharmacological sciences* **34**(9): 489-496.

Vaughan RA, Huff RA, Uhl GR, Kuhar MJ (1997). Protein kinase C-mediated phosphorylation and functional regulation of dopamine transporters in striatal synaptosomes. *Journal of Biological Chemistry* **272**(24): 15541-15546.

Vocci FJ, Montoya ID (2009). Psychological treatments for stimulant misuse, comparing and contrasting those for amphetamine dependence and those for cocaine dependence. *Current opinion in psychiatry* **22**(3): 263-268.

Wang HY, Friedman E (1996). Enhanced protein kinase C activity and translocation in bipolar affective disorder brains. *Biological psychiatry* **40**(7): 568-575.

Wang Y, Xu R, Sasaoka T, Tonegawa S, Kung MP, Sankoorikal EB (2000). Dopamine D2 long receptor-deficient mice display alterations in striatum-dependent functions. *The Journal of neuroscience : the official journal of the Society for Neuroscience* **20**(22): 8305-8314.

Wise RA (2009). Roles for nigrosriatal—not just mesocorticolimbic—dopamine in reward and addiction. *Trends in neurosciences* **32**(10): 517-524.

Wiseman H (1994). *Tamoxifen: Molecular basis of use in cancer treatment and prevention*, 4th edn. John Wiley & Sons, Ltd. Chichester, UK.

Woo C-H, Lim J-H, Kim J-H (2004). Lipopolysaccharide induces matrix metalloproteinase-9 expression via a mitochondrial reactive oxygen species-p38 kinase-activator protein-1 pathway in Raw 264.7 cells. *The Journal of Immunology* **173**(11): 6973-6980.

Wu-Zhang AX, Newton AC (2013). Protein kinase C pharmacology: refining the toolbox. *The Biochemical journal* **452**(2): 195-209.

Xu Z-B, Chaudhary D, Olland S, Wolfrom S, Czerwinski R, Malakian K, Lin L, Stahl ML, Joseph-McCarthy D, Benander C (2004). Catalytic domain crystal structure of protein kinase C-θ (PKCθ). *Journal of Biological Chemistry* **279**(48): 50401-50409.

Zarate CA, Jr., Singh JB, Carlson PJ, Quiroz J, Jolkovsky L, Luckenbaugh DA, Manji HK (2007). Efficacy of a protein kinase C inhibitor (tamoxifen) in the treatment of acute mania: a pilot study. *Bipolar disorders* **9**(6): 561-570.

Zestos AG, Mikelman SR, Kennedy RT, Gnegy ME (2016). PKCβ inhibitors attenuate amphetamine-stimulated dopamine efflux. *ACS Chemical Neuroscience* **7**(6): 757-766.

Zhou Z, Zhen J, Karpowich NK, Goetz RM, Law CJ, Reith ME, Wang DN (2007). LeuT-desipramine structure reveals how antidepressants block neurotransmitter reuptake. *Science (New York, NY)* **317**(5843): 1390-1393.

Zhu S-J, Kavanaugh MP, Sonders MS, Amara SG, Zahniser NR (1997). Activation of protein kinase C inhibits uptake, currents and binding associated with the human dopamine transporter expressed in Xenopus Oocytes. *Journal of Pharmacology and Experimental Therapeutics* **282**(3): 1358-1365.

Chapter 2. Design and synthesis of triarylacrylonitrile analogues of tamoxifen with improved binding selectivity to protein kinase C

Abstract

The clinical selective estrogen receptor modulator tamoxifen is also a modest inhibitor of protein kinase C (PKC), a target implicated in several untreatable brain diseases such as amphetamine (AMPH) abuse. This inhibition and tamoxifen's ability to cross the blood brain barrier make it an attractive scaffold to conduct further SAR studies toward uncovering effective therapies for such diseases. Utilizing the known compound **6a** as a starting template and guided by computational tools to derive physicochemical properties known to be important for CNS permeable drugs, the design and synthesis of a small series of novel triarylacrylonitrile analogues have been carried out providing compounds with enhanced potency and selectivity for PKC over the estrogen receptor (ER) relative to tamoxifen. Shortened synthetic routes compared to classical procedures have been developed for analogues incorporating a β- phenyl ring, which involve installing dialkylaminoalkoxy side chains first off the α and/or α' rings of a precursor benzophenone and then condensing the resultant ketones with phenylacetonitrile anion. A second novel, efficient and versatile route utilizing Suzuki chemistry has also been developed, which will allow for the introduction of a wide range of β-aryl or β-heteroaryl moieties and side-chain substituents onto the acrylonitrile core. For analogues possessing

a single side chain off the α- or α'- ring, novel 2D NMR experiments have been carried out that allow for unambiguous assignment of *E*- and *Z*- stereochemistry. From the SAR analysis, one compound, **6c**, shows markedly increased potency and selectivity for inhibiting PKC with an IC_{50} of 80 nM for inhibition of PKC protein substrate and >10 μM for binding to the ERα (tamoxifen IC_{50} = 20 μM and 222 nM, respectively). The data on **6c** provide support for further exploration of PKC as a druggable target for the treatment of AMPH abuse.

Introduction

Protein kinase C (PKC) is a pivotal enzyme in cell signaling pathways and has been implicated in numerous brain diseases such as Parkinson's disease (Zhang *et al*, 2007), Alzheimer's disease (Garrido *et al*, 2002), bipolar disease(Manji and Lenox, 2000; Wang and Friedman, 1996a) and substance abuse disorder (Olive and Messing, 2004; Schmitt and Reith, 2010). Although targeting PKC as a therapeutic target for these diseases has been proposed (Battaini, 2001; Manji and Chen, 2002; Mochly-Rosen *et al*, 2012), *in vivo* validation has been difficult due to lack of a PKC inhibitor that is permeable to the central nervous system. The only known PKC inhibitor that is permeable across the blood-brain barrier is the selective estrogen receptor modulator (SERM) tamoxifen, Figure 2.1 (Zarate *et al*, 2007), which inhibits cellular PKC activity reasonably potently, including that of PKCβ (O'Brian *et al*, 1985; Saraiva *et al*, 2003). Tamoxifen has been utilized to provide *in vivo* validation in rodents of PKC inhibition toward reducing the effects of AMPH, which is a model for bipolar mania (Dluzen *et al*, 2001; Einat *et al*, 2007; Sabioni *et al*, 2008), and clinically has demonstrated efficacy in the treatment of this disorder (Armani *et al*, 2014). The blockade of AMPH behavioral

effects can also be achieved by other traditional PKC inhibitors, but not by the selective ER inhibitors medroxyprogesterone or clomiphene, Figure 2.1 (Pereira *et al*, 2011). Inhibition of PKC reduces AMPH-stimulated dopamine efflux through the dopamine transporter (Kantor and Gnegy, 1998; Zestos *et al*, 2016), as well as AMPH-stimulated locomotor (Browman *et al*, 1998) and rewarding activities (Aujla and Beninger, 2003). Although the exact mechanism is not known, the dopamine transporter is a substrate for PKC (Moritz *et al*, 2013) and AMPH-stimulated dopamine efflux is regulated by transporter phosphorylation (Khoshbouei *et al*, 2004; Wang *et al*, 2016). Development of a potent PKC inhibitor that is permeable across the blood brain barrier would enhance exploration of the effect of PKC on numerous behavioral functions and could prove therapeutically useful.

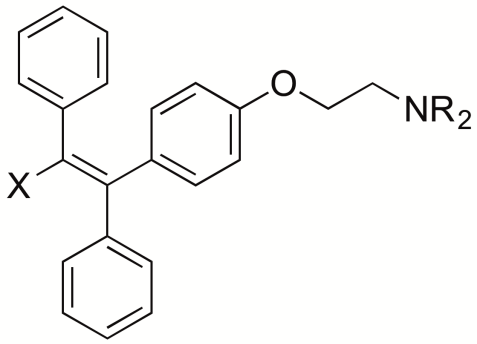

R = Me, X = Et: tamoxifen
R = Et, X = Cl: clomiphene

Figure 2.1. Clinical triphenylethylene SERMS.

Despite its wide use, tamoxifen is a drug with many sites of action. Its most common use is as a SERM to treat the recurrence of ER-positive breast cancer (Jordan, 2003). In addition to the ER and PKC, other identified binding sites for tamoxifen include calmodulin (O'Brian *et al*, 1990), voltage-dependent Ca^{2+} channels (Kuo *et al*, 2012) and

acyl-CoA:cholesterol acyl transferase (De Médina *et al*, 2004). Binding to all of these sites occurs at micromolar levels, which is greater than that required for binding to the ER.

Evidence suggests that although tamoxifen binds weakly to the catalytic subunit of PKC (O'Brian *et al*, 1988), its functional binding site is the Ca^{2+} and phospholipid-binding C2 regulatory subunit (Bignon *et al*, 1990). Inhibition of PKC by tamoxifen requires Ca^{2+} and phospholipid (O'Brian *et al*, 1985; Su *et al*, 1985), and is competitive with phospholipids and noncompetitive with Ca^{2+} (Gundimeda *et al*, 1996; Su *et al*, 1985). Tamoxifen inhibits PKC more potently in the presence of diolein and phorbol myristate acetate (PMA), but is not competitive with them (Gundimeda *et al*, 1996). The crystallographic structure of the phorbol ester and PKC regulatory site has been reported, but the mode of interaction between tamoxifen and its derivatives with PKC remains to be fully elucidated (Ochoa *et al*, 2001; Szallasi *et al*, 1996; Wang *et al*, 1996b).

There have been extensive structure-activity relationship (SAR) studies of the tamoxifen scaffold to dissect structural features that confer selective binding to ER relative to other targets such as PKC (Bignon *et al*, 1991; de Medina *et al*, 2004; Ohta *et al*, 2015). While tamoxifen can serve as an *in vivo* inhibitor of PKC, its high affinity for the ER and low affinity for PKC compromise its utility to selectively target PKC for brain disorders. To that end, our goal has been to use the triphenylethylene core of tamoxifen as a starting point to design analogues with increased affinity for PKC and decreased affinity for ER. A systematic study by Bignon *et al*, showed that PKC activity could be enhanced by substituting the tamoxifen ethyl moiety with a cyano function (Bignon *et al*, 1991). This paper delineates further SAR of this core change toward the

design and synthesis of a small series of novel triarylacrylonitrile derivatives with enhanced selectivity for PKC, and which have the potential for improved permeability across the blood brain barrier.

Analogue Design. Our goal was to design tamoxifen analogues that display enhanced selectivity for PKCβ versus ER binding and exhibit good CNS permeability. Compound **6a** (Table 2.1), previously synthesized and tested for PKC and ER binding (Bignon *et al*, 1989a; Bignon *et al*, 1989b; Dore *et al*, 1992), became our starting template for further SAR exploration. Our focus was to expand on **6a** with a small series of triarylacrylonitrile derivatives, listed in Table 2.1, which could dissect out structural features contributing to selectivity and potency for PKC over ER without a concomitant loss of molecular transport into the brain. The initial selection of **6a** and analogues was guided by computational tools (ChemAxon) to derive properties known to be important for CNS permeable drugs. The calculations for several key physicochemical descriptors are shown in Table 2.1, and reveal that our targeted analogues possess many of the critical parameters that track fairly closely with those for marketed CNS drugs (Abraham *et al*, 1997; Pan *et al*, 2004). While molecular weights tend to be greater than found for typical CNS drugs, cLogP and topological polar surface area (tPSA) values trend toward those favoring CNS penetration.

Chemistry. Our synthetic strategy to construct triphenylacrylonitrile compounds with variable aqueous solubilizing dialkylaminoalkoxy side chains is shown in Figure 2.2 (Scheme 1). The overall SAR trends for our small series of triarylacrylonitriles with respect to PKC activity are in general alignment with those summarized in a review in 2004 (de Medina *et al*, 2004), showing that the introduction of an additional basic side

chain of sufficient length off the 4-position of the α-phenyl ring and the nature of the terminal amine head group markedly increase potency for PKC inhibition relative to tamoxifen.

Materials and methods

General Chemistry Procedures. All starting materials were obtained from commercial suppliers and were used without further purification. Routine ^{1}H NMR spectra were recorded at 400 or 500 MHz on a Varian 400 or 500 instrument, respectively, with $CDCl_3$, CD_3OD, or DMSO-d_6 as solvent. ^{13}C NMR were recorded in DMSO-d_6 at 126 MHz on a Varian 400 instrument. Chemical shift values are recorded in δ units (ppm). The 1D ^{1}H, 1D ^{13}C, 2D ^{1}H-^{1}H TOCSY and 2D ^{1}H-^{13}C HSQC experiments were measured at 25 °C using a 600 MHz Bruker spectrometer equipped with a cryogenic probe. Compounds were dissolved either in DMSO-d_6 or a 1:1 DMSO-d_6:CD_3OD mixture. Mass spectra were recorded on a Micromass TofSpec-2E Matrix-Assisted, Laser-Desorption, Time-of-Flight Mass Spectrometer in a positive ESI mode ($TOFES^{+}$) unless otherwise noted. High resolution mass spectrometry (HRMS) analysis was performed on an Agilent Q-TOF system. Analytical HPLC was performed on an Agilent 1100 series instrument with an Agilent Zorbax Eclipse Plus C18 (4.6 mm × 75 mm, 3.5 μm particle size) column with the gradient 10% ACN/water (1 min), 10−90% ACN/water (6 min), and 90% ACN/water (2 min) flow = 1 ml/min. Thin-layer chromatography (TLC) was performed on silica gel GHLF plates (250 microns) purchased from Analtech. Column chromatography was carried out in the flash mode utilizing silica gel (220−240 mesh) purchased from Silicycle. Extraction solutions were dried over $MgSO_4$ prior to concentration.

(4-(2-Bromoethoxy)phenyl)(phenyl)methanone (1b), (Chen *et al*, 2014). A stirred suspension of 4-hydroxybenzophenone (**1a**; 700 mg, 3.53 mmol), 1,2-dibromoethane (3.04 ml, 35.3 mmol), cesium carbonate (2.3 g, 7.1 mmol) and acetonitrile (35 ml) was heated at reflux for 48 h. The mixture was diluted with 250 ml of water and extracted with dichloromethane (3x). The combined extracts were washed with water, sat. brine, dried, and concentrated to a solid that was purified by flash silica gel chromatography, eluting with chloroform. Product fractions were combined and concentrated to leave **1b** (750 mg, 70%) as a white solid, mp 74-75 °C. R_f 0.44 (chloroform). ^{1}H NMR (400 MHz, DMSO-d_6): δ 7.76 – 7.60 (m, 5H), 7.52 (t, J = 7.5 Hz, 2H), 7.10 (d, J = 8.7 Hz, 2H), 4.41 (t, J = 5.4 Hz, 2H), 3.83 (t, J = 5.3 Hz, 2H). MS TOFES$^+$: *m/z* 305.0, 307.0 $(M+H)^+$.

Bis(4-(2-bromoethoxy)phenyl)methanone (1d), (Tang *et al*, 2012) A stirred suspension of 4,4'-dihydroxybenzophenone (**1c**; 1.93 g. 9 mmol), 1,2-dibromoethane (15.5 ml, 180 mmol), cesium carbonate (11.77 g, 36.1 mmol) and acetonitrile (66 ml) was heated at reflux for 22 h. The suspension was filtered and the salts washed well with dichloromethane. The combined filtrate was filtered through a small pad of flash silica gel, washing the pad well with dichloromethane. The filtrate was concentrated to a semisolid that was diluted with 2-propanol. The suspension was heated for ~ 5 min and allowed to cool. The resulting solids were collected, washed with 2-propanol, and dried to leave 2.3 g of **1d**, mp 125-127 ºC. Upon standing for several days, additional product crystallized from the mother liquor and was collected to give 130 mg of **1d**, mp 120-125 ºC. Total yield = 2.43 g (63%). ^{1}H NMR (400 MHz, DMSO-d_6): δ 7.73 – 7.64 (m, 4H), 7.13 – 7.04 (m, 4H), 4.45 – 4.37 (m, 4H), 3.87 – 3.79 (m, 4H). MS TOFES$^+$: *m/z* 427.9

(M^+), 428.9 $(M+H)^+$.

(4-(2-Morpholinoethoxy)phenyl)(phenyl)methanone (2a), (Meegan *et al*, 2001). A stirred suspension of 4-hydroxybenzophenone (**1a**; 750 mg, 3.8 mmol), 4-(2-chloroethyl)morpholine hydrochloride, (739 mg, 4 mmol), cesium carbonate (3.7 g, 11.4 mmol) and acetonitrile (30 ml) was heated at reflux for 21 h. The mixture was poured into 250 ml of water and stirred overnight. The formed suspension was collected, washed with water, and dried to give **2a** (1.0 g, 85%) as an off-white powder, mp 64-66 °C. R_f 0.61 (85:15:2 ethyl acetate/methanol/triethylamine. ^{1}H NMR (400 MHz, DMSO-d_6): δ 7.75 – 7.60 (m, 5H), 7.53 (t, J = 7.5 Hz, 2H), 7.08 (d, J = 8.6 Hz, 2H), 4.17 (t, J = 5.7 Hz, 2H), 3.55 (t, J = 4.6 Hz, 4H), 2.70 (t, J = 5.7 Hz, 2H); remaining protons overlap DMSO peak. MS TOFES$^+$: *m/z* 312.1 $(M+H)^+$, 334.1 $(M+Na)^+$.

(4-(2-(Dimethylamino)ethoxy)phenyl)(phenyl)methanone (2b), (Meegan *et al*, 2001). A stirred mixture of (4-(2-bromoethoxy)phenyl)(phenyl)methanone (**1b**; 750 mg, 2.5 mmol), dimethylamine hydrochloride (301 mg, 3.7 mmol), potassium carbonate (1.36 g, 9.8 mmol), and acetone (10 ml) was heated at reflux for 16 h. The mixture was concentrated to a solid residue that was partitioned between ethyl acetate and water. The aqueous layer was further extracted with ethyl acetate and the combined organic phases were washed sequentially with water and sat. brine, dried and concentrated to an oil that was purified by flash silica gel chromatography eluting with 4:1 dichloromethane:methanol. Concentration of product fractions left **2b** (0.50 g, 76%) as a colorless syrup; R_f 0.25 (85:15:2 ethyl acetate/methanol/trimethylamine). ^{1}H NMR (400 MHz, DMSO-d_6): δ 7.71 (d, J = 8.3 Hz, 2H), 7.69 – 7.59 (m, 3H), 7.53 (t, J = 7.4 Hz, 2H), 7.07 (d, J = 8.3 Hz, 2H), 4.13 (t, J = 5.7 Hz, 2H), 2.63 (t, J = 5.8 Hz, 2H), 2.20 (s,

6H). MS TOF-ES$^+$: *m/z* 270.2 $(M+H)^+$.

(*E* and *Z*)-3-(4-(2-Morpholinoethoxy)phenyl)-2,3-diphenylacrylonitrile, hydrochloride (3a and 4a). Run 1: The anion of phenylacetonitrile (32.1 mmol) in THF (30 ml) was generated as described below for the synthesis of **6c**. A solution of (4-(2-morpholinoethoxy)phenyl)(phenyl)methanone (**2a**; 500 mg, 1.6 mmol) in THF (5 ml) was added over a period of 5 min. After 30 min the cooling bath was removed and the mixture warmed gradually to room temperature. After stirring for 48 h, the mixture was poured into 150 ml of 2N aq. HCl and further worked up as described below for **6c** below to leave a crude mixture by NMR of **3a** and **3b** (570 mg, 86%) as a syrup; R_f 0.44 (85:15:2 ethyl acetate/methanol/trimethylamine); R_f 0.18 (ethyl acetate). MS TOFES$^+$: *m/z* 411.1 $(M+H)^+$. Upon standing at room temperature (~1 month) the syrup crystallized. The solids were triturated in a few ml of ethanol with sonication, collected, washed with ethanol, and dried to leave an isomeric mixture of products (150 mg, 23%) as a cream-colored powder, mp 135-142 °C, shown by HPLC to be a 91:9 mixture of **3**a:**4**a. ^{1}H NMR (400 MHz, DMSO-d_6): δ 7.47 (m), 7.43 – 7.36 (m), 7.33 – 7.21 (m), 6.88 – 6.82 (m), 6.81 – 6.75 (m), 4.01 (t, J = 5.7 Hz), 3.53 (t, J = 4.7 Hz), 2.62 (t, J = 5.7 Hz), 2.41 (t, J = 4.7 Hz), remaining protons hidden under DMSO signal. The mother liquor was concentrated to leave ~400 mg of an isomeric mixture for further processing. Run 2: The above reaction was repeated on starting ketone **2a** (550 mg, 1.8 mmol) to give crude product (700 mg, 97%) that was processed as above to leave 164 mg (23%) of a powder, mp 136-142 °C, shown by HPLC to be a 82:18 mixture of **3**a:**4**a. The mother liquor was concentrated to leave ~530 mg of an isomeric mixture for further processing. To a stirred solution of 100 mg (0.24 mmol) of the 82:18 mixture of **3**a:**4**a from Run 2 in 5:1

ethanol/dichloromethane (6 ml) was added HCl in ether (0.26 ml of 1M solution). After 3 h the mixture was concentrated to a glassy residue that eventually crystallized after treatment with a few drops of methanol. The solids were collected, washed with 2-propanol, and dried to give **3a** hydrochloride (54 mg, 50%) as a white powder; mp 200-202 °C; R_f 0.85 (97:3 methanol/conc. ammonium hydroxide); R_f 0.66 (85:15:2 ethyl acetate/methanol/triethylamine). HPLC rt 6.1 min (98%), 6.3 min (2%). ^{1}H NMR (400 MHz, DMSO-d_6): δ 7.48 (m, 3H), 7.43 – 7.36 (m, 2H), 7.33 – 7.22 (m, 5H), 6.91 (d, J = 8.7 Hz, 2H), 6.85 (d, J = 8.7 Hz, 2H), 4.33 (t, J = 4.7 Hz, 2H), 3.93 (d, J = 13.0 Hz, 2H), 3.73 (t, J = 12.2 Hz, 2H), 3.55-3.39 (m, 4H), 3.15 (d, J = 5.2 Hz, 2H); ^{1}H NMR (600 MHz, DMSO-d_6): δ 3.02 - 3.18 (m, 2H, (C*H*H)$_2$N-), 3.29 - 3.48[a] (m, 2H, (CH*H*)$_2$N-)), 3.38 - 3.52[a] (m, 2H, NC*H*$_2$CH$_2$O), 3.69 - 3.98 (m, 4H, (C*H*$_2$)$_2$O), 4.25 – 4.44 (m, 2H, NCH$_2$C*H*$_2$O), 6.68 – 6.84 (m, 2H, Ar$_{\alpha'}$*H*), 6.84 – 6.93 (m, 2H, Ar$_{\alpha'}$*H*), 7.15 – 7.32 (m, 5H, Ar$_\beta$*H*), 7.33 - 7.51 (m, 5H, Ar$_\alpha$H); ^{1}H NMR (600 MHz, DMSO-d_6:CD$_3$OD, 1:1 v:v): δ 3.08 - 3.17 (m, 2H, (C*H*H)$_2$N-), 3.36 - 3.46 (m, 2H, (CH*H*)$_2$N-)), 3.46 - 3.52 (m, 2 H, NC*H*$_2$CH$_2$O), 3.65 - 3.78 (m, 2H, (C*H*H)$_2$O), 3.85 - 3.98 (m, 2H, (CH*H*)$_2$O), 4.22 – 4.28[a] (m, 2H, NCH$_2$C*H*$_2$O), 6.80 (d, J = 8.1 Hz, 2H, Ar$_{\alpha'}$*H*), 6.88 (d, J = 8.1 Hz, 2H, Ar$_{\alpha'}$*H*), 7.21 (m, 5H, Ar$_\beta$*H*), 7.31 - 7.49 (m, 5H, Ar$_\alpha$H); ^{13}C NMR (150 MHz, DMSO-d_6): δ 51.7, 54.9, 62.3, 63.2, 110.0, 114.4, 119.9, 128.5, 128.6, 128.8, 129.4, 129.6, 129.9, 131.2, 132.1, 134.7, 140.3, 157.1, 157.9; ([a]peaks overlapped with solvent, determined from HSQC). The sticky semisolid from the above combined mother liquors (~930 mg) was triturated in ethanol to leave solids that were collected, washed well with ethanol, and dried to leave 250 mg of a different mixture of isomers from above, as shown by tlc (95:5 dichloromethane/methanol), as an off-white powder; mp 123-135 °C. The mixture was

dissolved in 5 ml of 4:1 methanol/ dichloromethane, and anhydrous HCl in ether (0.7 ml of 1M solution) was added. The mixture was stirred at room temperature for 18 h and concentrated to a solid residue, which was triturated in several ml of 2-propanol, sonicated briefly, and stored overnight. The solids were collected, washed with 2-propanol, and dried to leave enriched **4a** (165 mg), mp 144-169 °C; R_f 0.72 (97:3 methanol/conc. ammonium hydroxide); R_f 0.55 (95:5 dichloromethane/methanol). The product was recrystallized from 2-3 ml of ethanol to leave highly pure **4a**, hydrochloride (45 mg) as a beige powder; mp 144-146 °C. HPLC: rt 6.1 min (6%), 6.3 min (94%). ^{1}H NMR (400 MHz, DMSO-d_6): δ 7.35 (d, J = 8.6 Hz, 2H), 7.27 - 7.17 (m, 8H), 7.04 (d, J = 8.4 Hz, 2H), 6.97 (dt, J = 6.8, 1.5 Hz, 2H), 4.25 - 4.15 (m, 2H), 3.65 – 3.58 (m, 4H), remaining protons hidden under DMSO signal. ^{1}H NMR (600 MHz, DMSO-d_6): δ 2.38 – 2.62[a] (m, 4H, (CH_2)$_2$N-), 2.64 – 2.88 (m, 2H, NCH_2CH$_2$O), 3.50 – 3.84 (m, 4H, (CH_2)$_2$O), 4.03 – 4.47 (m, 2H, NCH$_2$CH_2O), 6.95 – 7.04 (m, 2H, Ar$_\alpha H$), 7.05 - 7.12 (m, 2H, Ar$_{\alpha'}H$), 7.18 – 7.34 (m, 8H, Ar$_\alpha H$,Ar$_\beta H$), 7.35 - 7.44 (m, 2H, Ar$_{\alpha'}H$); ^{1}H NMR (600 MHz, DMSO-d_6:CD$_3$OD, 1:1 v:v): δ 2.70 – 2.86 (m, 4H, (CH_2)$_2$N-), 2.94 - 3.04 (m, 2H, NCH_2CH$_2$O), 3.60 – 3.73 (m, 4H, (CH_2)$_2$O), 4.17 – 4.25[a] (m, 2H, NCH$_2$CH_2O), 6.95 (d, J = 7.0 Hz, 2H, Ar$_\alpha H$), 7.01 (d, J = 8.4 Hz, 2H, Ar$_{\alpha'}H$), 7.12 – 7.26 (m, 8H, Ar$_\alpha H$,Ar$_\beta H$), 7.34 (d, J=8.4 Hz, 2H, Ar$_{\alpha'}H$); ^{13}C NMR (150 MHz, DMSO-d_6): δ 53.1[b], 56.5[b], 64.6[b], 65.5[b], 109.7, 114.6, 120.2, 128.4, 128.4, 128.7, 129.1, 129.4, 130.4, 131.3, 132.1, 134.8, 138.9, 157.6; ([a]peaks overlapped with solvent, determined from HSQC, [b]due to broad signals the chemical shifts have been extracted from the HSQC experiment); MS TOFES$^+$: m/z 411.1 (M+H)$^+$; TOFES$^-$: m/z 409.2 (M-H)$^+$.

(*E* and *Z*)-3-(4-(2-(Dimethylamino)ethoxy)phenyl)-2,3-diphenylacrylonitrile,

hydrochloride (3b and 4b), (Lashley *et al*, 2003). The anion of phenylacetonitrile (33.4 mmol) in THF (45 ml) was generated as described below for the synthesis of **6c**. After 30 minutes at 0-5 °C, the anion was cooled to -78 °C and a solution of the ketone **2b** (450 mg, 1.7 mmol) in THF (15 ml) was added over a period of 5 min. Cooling was removed and the red-brown mixture was stirred at room temperature for 5 d. The mixture was poured into ice-cold 3N aq. HCl and further worked up as described for the preparation of **6c** below to leave a solid residue (600 mg, 97%) that was triturated in 2-propanol, collected, washed with ether and dried to leave crude **3b**, **4b** (98 mg, 16%), confirmed by NMR and MS, as a tan powder. The combined mother liquor and washes were concentrated to a residue that was dissolved in methanol and treated with an excess of anhydrous 1N HCl in ether. After stirring for 20 h the solution was concentrated leaving a glassy residue that was triturated in 2-propanol. The precipitate was collected and dried to leave an 84:16 mixture (by hplc) of **3b**:**4b** hydrochloride (0.14 g, 20%) as a cream-colored powder, mp 217-230 °C. R_f 0.69 (99:1 dichloromethane/methanol). ^{1}H NMR (400 MHz, DMSO-d_6): δ 10.47 (s, 1H), 7.49 - 6.83 (m, 14H), 4.42, 4.29 (m, 2H), 3.51, 3.44 (m, 2H), 2.83, 2.78 (s, 6H). MS TOFES$^+$: *m/z* 369.1 $(M+H)^+$.

Bis(4-(2-(diethylamino)ethoxy)phenyl)methanone (5a), (Palopoli *et al*, 1966). A mixture of bis(4-hydroxyphenyl)methanone (**1c**; 1.07 g, 5 mmol), 2-chloro-*N*,*N*-diethylethylamine hydrochloride (1.76 g, 10.2 mmol), cesium carbonate (8 g, 24.6 mmol) and acetonitrile (52 ml) was stirred at reflux for 18 h. The mixture was poured into 500 ml of water and then extracted with ethyl acetate (3x). The combined extracts were washed with sat. brine, dried and concentrated to leave 1.93 g (92%) of **5a** as a free-flowing pale orange oil, 91% pure by HPLC, that solidified in the refrigerator. The

compound was used directly in the next step. ^{1}H NMR (400 MHz, DMSO-d_6): δ 7.71 – 7.61 (m, 4H), 7.09 – 7.00 (m, 4H), 4.09 (t, J = 6.1 Hz, 4H), 2.78 (t, J = 6.1 Hz, 4H), 2.53 (q, J = 7.1 Hz, 8H), 0.95 (t, J = 7.1 Hz, 12H); MS TOFES$^+$: *m/z* 413.3 $(M+H)^+$.

Bis(4-(2-morpholinoethoxy)phenyl)methanone (5b). A stirred mixture of 4,4'-dihydroxybenzophenone (**1c**; 500 mg, 2.3 mmol), 4-(2-chloroethyl)morpholine hydrochloride (864 mg, 4.6 mmol), cesium carbonate (3.69 g, 11.3 mmol) and acetonitrile (25 ml) was heated at reflux for 18 h. The mixture was diluted with 250 ml of water and the resulting solution was stirred at room temperature for 18 h. The precipitated solids were collected, washed with water, and dried to leave **5b** (0.9 g, 90%) as a white powder, mp 119-120 °C. R_f 0.33 (ethyl acetate/methanol/triethylamine, 85:15:2]. ^{1}H NMR (400 MHz, DMSO-d_6): δ 7.67 (d, J = 8.7 Hz, 4H), 7.06 (d, J = 8.7 Hz, 4H), 4.17 (t, J = 5.6 Hz, 4H), 3.59 – 3.52 (m, 8H), 2.70 (t, J = 5.6 Hz, 4H); remaining protons overlap DMSO peak. MS TOFES$^+$: *m/z* 441.2 $(M+H)^+$.

Bis(4-(2-(4-methylpiperazin-1-yl)ethoxy)phenyl)methanone (5c). A suspension of the bis-bromoethoxy compound (**1d**; 1.3 g, 3.0 mmol), *N*-methylpiperazine (1.52 ml, 13.7 mmol), and acetonitrile (6 ml) was stirred at reflux for 2 h. The mixture was cooled and distributed between 5% aq. $NaHCO_3$ and dichloromethane, using NaCl to break up the emulsion. The layers were separated and the aqueous phase was further extracted with dichloromethane (2x). The combined extracts were dried and concentrated to a semisolid that was dissolved in a minimum volume of hot 2-propanol (5-6 ml). The solution was refrigerated for several hours and the precipitated solids were collected, washed with 2-propanol, and dried to leave 1.17 g of **5c**, mp 129-130 ºC. Concentration of the mother liquor and further processing as above gave 45 mg of a second crop, mp 129-130 ºC.

Total yield = 1.22 g (86%). ^{1}H NMR (400 MHz, DMSO-d_6): δ 7.68 (d, J = 8.8 Hz, 4H), 7.08 (d, J = 8.9 Hz, 4H), 4.17 (t, J = 5.7 Hz, 4H), 2.71 (t, J = 5.6 Hz, 4H), 2.32 (m, 6H), 2.14 (s, 6H), remaining protons hidden under solvent signal. MS TOFES$^+$: *m/z* 467.3 $(M+H)^+$.

3,3-Bis(4-(2-(diethylamino)ethoxy)phenyl)-2-phenylacrylonitrile, dihydrochloride (6a), (Dore *et al*, 1992). A solution of commercially available lithium diisopropylamide (1M in THF/hexanes, 30 ml, 30 mmol) under nitrogen at -78 °C was treated dropwise with phenylacetonitrile (3.46 ml, 30 mmol) over ~5 min. The cooling bath was removed and the temperature was allowed to come to 0 - 10 °C. The deep yellow anion suspension was re-cooled to -78 °C and diluted with THF (17 ml). Ketone **5a** (619 mg, 1.5 mmol) in 5 ml THF was added over a ~1 min and the resultant suspension was maintained at -78 °C for 3-3.5 h (beige suspension) and then allowed to slowly warm to room temperature overnight. After stirring for a total of 19 h from the point of ketone addition, the violet mixture was poured into 2N aq. HCl (125 ml), stirred for 2.5 h, and extracted with ethyl acetate (2x). The combined organic extracts were discarded. The acidic aqueous phase was ice-cooled and treated portion-wise with 10.5 g of NaOH dissolved in minimal water. The cloudy aqueous solution (pH ~12) was extracted with ethyl acetate (3x), with small aliquots of aq. NaOH added to keep the aqueous phase basic. The combined extracts were washed with sat. brine, dried, and concentrated to a viscous oil that was pumped *in vacuo* 2 h to leave 700 mg (91%) of **6a** as a pale orange viscous oil, shown by HPLC to be 94% pure. Processing a small amount of product by re-dissolving it in 2N aq. HCl followed by further treatment as above provided **6a** that was 96% pure by HPLC. R_f ~0.35 (95:5 methanol/conc. ammonium

hydroxide). ^{1}H NMR (400 MHz, DMSO-d_6): δ 7.36 –7.16 (m, 7H), 7.04 – 6.96 (m, 2H), 6.91 – 6.80 (m, 2H), 6.79 – 6.71 (m, 2H), 4.11 – 3.96 (m, 2H), 3.93 (t, J = 6.1 Hz, 2H), 2.78 (t, J = 6.1 Hz, 2H), 2.69 (t, J = 6.1 Hz, 2H), 2.59 – 2.43 (m, 8H), 0.94 (dt, J = 18.2, 7.1 Hz, 12H). ^{1}H NMR (500 MHz, CD_3OD): δ 7.39 (d, J = 8.8 Hz, 2H), 7.25 (s, 5H), 7.02 (d, J = 8.8 Hz, 2H), 6.93 (d, J = 8.7 Hz, 2H), 6.77 (d, J = 8.8 Hz, 2H), 4.19 (t, J = 5.6 Hz, 2H), 4.07 (t, J = 5.6 Hz, 2H), 3.07 – 2.95 (m, 2H), 2.95 – 2.84 (m, 2H), 2.75 (m, 4H), 2.69 (m, 4H), 1.14 (t, J = 7.2 Hz, 6H), 1.09 (t, J = 7.2 Hz, 6H); The dihydrochloride salt was made as follows: **6a** free base (90 mg) was dissolved in minimal dichloromethane and the solution was treated with 800 µl of anhydrous 1N HCl in ether. The mixture was stirred for 10 min and then filtered through a cotton plug to remove a few insolubles. The filtrate was concentrated to a residue that was redissolved in dichloromethane/hexane and then concentrated to a yellow solid that was triturated in hexane. The solids were collected and dried to leave 100 mg (97%) of **6a** dihydrochloride. ^{1}H NMR (400 MHz, DMSO-d_6): δ 10.02 (s, 2H), 7.37 (d, J = 8.2 Hz, 2H), 7.30-7.19 (m, 5H), 7.08 (d, J = 8.3 Hz, 2H), 6.90 (d, J = 8.4 Hz, 2H), 6.84 (d, J = 8.4 Hz, 2H), 4.39 (t, J = 5.8 Hz, 2H), 4.28 (t, J = 5.2 Hz, 2H), 3.51 (t, J = 6.7 Hz, 2H), 3.43 (t, J = 6.2 Hz, 2H), 3.25-3.08 (m, 8H), 1.25-1.17 (m, 12H). MS TOFES$^+$: *m/z* 512.4 $(M+H)^+$.

3,3-Bis(4-(2-morpholinoethoxy)phenyl)-2-phenylacrylonitrile, dihydrochloride (6b). The anion of phenylacetonitrile (36.2 mmol) was generated in THF (45ml) as described below for the synthesis of **6c**. The ketone **5b** (800 mg, 1.8 mmol) in THF (15 ml) was added over a period of 5 min, the solution allowed to gradually warm to room temperature over 2-3 h and maintained there for 18 h. The

mixture was poured into 100 ml of ice-cold 3N aq. HCl, stirred for 30 min, and washed with ether (2x). The aqueous phase was made strongly basic with 15% aq. NaOH, and extracted with ethyl acetate (3x). The combined extracts were washed with water and then sat. brine, dried, and concentrated to leave a clear amber syrup (960 mg, 98%), which crystallized upon standing at room temperature over several days. The solids were triturated in ethanol with sonication, collected, washed with ethanol, and dried to leave **6b** (0.54g, 55%) as a pale yellow powder, mp 130-131 °C. R_f 0.15 (85:15:2 ethyl acetate/methanol/trimethylamine). HPLC: rt 4.9 min (96% purity). ^{1}H NMR (400 MHz, DMSO-d_6) δ 7.35 – 7.17 (m, 7H), 7.02 (d, J = 8.5 Hz, 2H), 6.85 (d, J = 8.6 Hz, 2H), 6.78 (d, J = 8.6 Hz, 2H), 4.13 (t, J = 5.6 Hz, 2H), 4.01 (t, J = 5.6 Hz, 2H), 3.60 – 3.45 (m, 8H), 2.69 (t, J = 5.6 Hz, 2H), 2.62 (t, J = 5.7 Hz, 2H); 2.47-2.40 (m, 8H). MS TOFES$^+$: m/z 540.0 $(M+H)^+$. The dihydrochloride salt was prepared as follows: A solution of **6b** (100 mg, 0.19 mmol) in dichloromethane at room temperature was treated dropwise with anhydrous HCl (0.39 ml, 1M in ether) and the resulting gummy suspension was concentrated. The residue was triturated in ether to give a glassy solid that was collected, rinsed thoroughly with ether and dried to leave **6b** dihydrochloride (0.10 g, 82%) as a yellow powder and solvated with ~0.6 equivalents of ether. R_f 0.77 (95:5 methanol/conc. ammonium hydroxide). ^{1}H NMR (400 MHz, DMSO-d_6): δ 11.22 (br s, 3H), 7.40 - 7.21 (m, 7H), 7.09 (d, J = 8.5 Hz, 2H), 6.91 - 6.84 (m, 4H), 4.51-4.32 (m, 6H), 4.08 – 3.65 (m, 8H), 3.60 – 3.00 (remaining protons overlapping water peak).

3,3-Bis(4-(2-(4-methylpiperazin-1-yl)ethoxy)phenyl)-2-phenylacrylonitrile, 2.5 hydrochloride salt (6c). To a solution of diisopropylamine (10.03 ml, 71.6 mmol) in THF (50 ml) under nitrogen at -78 °C was added dropwise n-BuLi (44.7 ml of 1.6 M

solution in hexane, 71.6 mmol). The solution was stirred for 10 min and then treated dropwise with phenylacetonitrile (8.26 ml, 71.6 mmol) over 20 min. The bath was removed and the temperature was allowed to come to ~0 °C. The pale yellow anion suspension was recooled to -78 °C and diluted with THF (40 ml). The solid ketone (**5c**; 1.67 g, 3.6 mmol) was added all at once and the resultant suspension was maintained at -78 °C for 2-2.5 h and then allowed to slowly warm to room temperature. During this time there was a deepening orange suspension, which became a deep purple solution that remained while the solution was stirred at room temperature for 18 h. The solution was poured into ice-cold 2N aq. HCl (300 ml), stirred for 1.5 h, and extracted with ethyl acetate (2x). The combined extracts were washed with sat. brine and discarded. The brine was combined with the aq. acid phase, the solution ice-cooled and treated portion-wise with 25 g of NaOH dissolved in minimal water. The cloudy aqueous solution (pH ~12) was extracted with ethyl acetate (3x), checking after each extraction to ensure the aqueous phase was basic. The combined extracts were washed with sat. brine, dried, and concentrated to a viscous oil that was pumped *in vacuo* overnight to leave 2 g (100%) of partially crystalline **6c** as a golden solid. R_f ~0.35 (95:5 methanol/conc. ammonium hydroxide).^{1}H NMR (400 MHz, DMSO-d_6): δ 7.50 – 7.18 (m, 6H), 7.09 – 6.85 (m, 3H), 6.85 – 6.70 (m, 4H), 4.12 (t, J = 5.7 Hz, 2H), 3.99 (t, J = 5.7 Hz, 2H), 2.69 (t, J = 5.8 Hz, 2H), 2.61 (t, J = 5.7 Hz, 2H), 2.50 – 2.16 (m, 9H), 2.13 (s, 3H), 2.11 (s, 3H), remaining protons hidden under solvent signal; MS TOFES$^+$: *m/z* 566.2 $(M+H)^+$. The residue was dissolved in minimal 2-propanol and while stirring vigorously the solution was treated with anhydrous HCl (12 ml, 1N in ether) resulting in precipitation of a gum. After stirring for 18 h, the supernatant liquid was decanted and the residue washed once with ether by

decantation. The residue was then immersed in fresh ether and stirred vigorously at room temp for 20 h leaving a fine filterable pale yellow solid that was collected, washed with portions of ether, and then once with 1% methanol in dichloromethane, resulting in conversion to a thick gummy syrup, which was collected and dissolved in methanol. The solution was concentrated *in vacuo* and the resulting glass was immersed in ether and stirred vigorously at room temperature overnight. The resulting yellow solid was collected, rinsed with ether and dried *in vacuo* over P_2O_5 at 55-60 °C for 36 h to leave **6c** dihydrochloride (1.35 g, 53%) as a pale yellow slightly hygroscopic powder, mp >135 °C. HPLC: rt 4.8 min (90% purity). ^{1}H NMR (400 MHz, DMSO-d_6): δ 10.36 (bs, 3H), 7.35 - 7.18 (m, 7H), 7.03 (d, J = 8.4 Hz, 2H), 6.86 (d, J = 8.4 Hz, 2H), 6.79 (d, J = 8.5 Hz, 2H), 4.15 (bs, 2H), 4.02 (bs, 2H), 2.99 (m, 8H), 2.80 – 2.60 (m, 10H); remaining protons overlap DMSO peak; ^{13}C NMR (126 MHz, DMSO-d_6) δ 157.48, 135.57, 132.71, 131.93, 131.40, 129.79, 129.17, 128.64, 120.92, 114.85, 114.71, 108.69, 55.93, 52.72, 49.95, 42.51. Anal. Calcd. for $C_{35}H_{43}N_5O_2 \cdot 2.5\ HCl \cdot 3.3\ H_2O$ (MW 716.36): C, 58.68; H, 7.33; N, 9.78; Cl^-, 12.37. Found: C, 59.06; H, 7.20; N, 9.60; Cl^-, 12.17.

3,3-Bis(4-methoxyphenyl)acrylonitrile (8). A solution of diethyl (cyanomethyl)phosphonate (8.77 g, 49.5 mmol) in THF (10 ml) was added dropwise to a stirred suspension of sodium hydride (1.98 g of 60 wt %, 49.5 mmol) in THF (50 ml) under nitrogen at room temperature. After 30 min a solution of 4,4'-dimethoxybenzophenone (**7**; 2.0 g, 8.3 mmol) in THF (30 ml) was slowly added, and the resulting solution was heated at reflux for 20 h. The mixture was poured into 300 ml of ice water, stirred, and acidified with 4N aq. HCl. After 1 h the mixture was concentrated to ~75 % volume and extracted with ethyl acetate (3x). The combined extracts were

washed with sat. aq. $NaHCO_3$, then sat. brine, dried and concentrated to a solid that was triturated in 2-propanol. The solids were collected, washed with 2-propanol and then hexane, and dried to leave **8** (1.96g, 89%) as a white powder, mp 104-106 °C. R_f 0.68 (98:2 dichloromethane/ethyl acetate). ^{1}H NMR (400 MHz, $CDCl_3$): δ 7.40 (d, J = 8.0 Hz, 2H), 7.25 (d, J = 8.6 Hz, 2H), 7.18 – 6.93 (m, 2H), 6.88 (d, J = 8.3 Hz, 2H), 5.55 (s, 1H), 3.87 (s, 3H), 3.84 (s, 3H). MS TOFES$^+$: *m/z* 266.0 $(M+H)^+$.

2-Bromo-3,3-bis(4-methoxyphenyl)acrylonitrile (9). A solution of bromine (0.55 ml, 10.7 mmol) in 1,2-dichloroethane (12 ml) was added dropwise to a stirred solution of 3,3-bis(4-methoxyphenyl)acrylonitrile (**8**; 1.9 g, 7.2 mmol) in 1,2-dichloroethane (15 ml) at -25 °C. After a few minutes the mixture was warmed slowly to room temperature where it was stirred for 4 h. The mixture was diluted with dichloromethane and then washed successively with sat. aq. $NaHCO_3$, aq. sodium thiosulfate, sat. brine, and dried. Concentration left a solid that was recrystallized from 3-4 ml of ethanol to give **9** (1.45 g, 59%) as an off-white powder; mp 105-107 °C. ^{1}H NMR (400 MHz, $CDCl_3$): δ 7.34 – 7.23 (m, 4H), 6.93 – 6.84 (m, 4H), 3.85 (s, 3H), 3.84 (s, 3H). MS TOFES$^+$: *m/z* 344.0, 346.0 $(M+H)^+$.

3,3-Bis(4-methoxyphenyl)-2-(thiophen-2-yl)acrylonitrile (10). A stirred mixture of 2-bromo-3,3-bis(4-methoxyphenyl)acrylonitrile (**9**; 500 mg, 1.5 mmol), thiophen-2-ylboronic acid (195 mg, 1.5 mmol), $Pd(PPh_3)_4$ (84 mg, 7.3 mmol), potassium carbonate (1.0 g, 7.3 mmol), toluene (7.3 ml), and 2-propanol (7.3 ml) was heated at reflux for 42 h, and then treated with additional Pd catalyst (84 mg). After heating 18 h more, the mixture was diluted with water and extracted with ethyl acetate. The combined organic phases were washed with sat. brine, dried and concentrated to an oil that was

purified by flash silica gel chromatography, eluting with 4:1 hexane/ethyl acetate. Product fractions were combined and concentrated to give **10** (440 mg, 87%) as a yellow syrup. ^{1}H NMR (400 MHz, DMSO-d_6): δ 7.45 (dd, J = 5.1, 1.2 Hz, 1H), 7.33 (d, J = 8.8 Hz, 2H), 7.17 (dd, J = 3.7, 1.2 Hz, 1H), 7.09 (d, J = 8.7 Hz, 2H), 7.02 – 6.89 (m, 5H), 3.79 (s, 3H), 3.76 (s, 3H). MS TOFES$^+$: *m/z* 348.0 $(M+H)^+$, 370.0 $(M+Na)^+$.

3,3-Bis(4-hydroxyphenyl)-2-(thiophen-2-yl)acrylonitrile (11). BBr_3 (0.86 ml of a 1M solution in dichloromethane) was added to a stirred solution of 3,3-bis(4-methoxyphenyl)-2-(thiophen-2-yl)acrylonitrile (**10**; 100 mg, 0.3 mmol) in dichloromethane at room temperature. The mixture was stirred for 16 h, and then poured into water, stirred vigorously for 5 min, and extracted with ether (2x). The combined extracts were washed with sat. brine, dried and concentrated to leave **11** (90 mg, 98%) as an amber syrup. ^{1}H NMR (400 MHz, DMSO-d_6): δ 9.99 (s, 1H), 9.89 (s, 1H), 7.42 (d, J = 3.9 Hz, 1H), 7.22 (d, J = 8.6 Hz, 2H), 7.13 (dd, J = 3.7, 1.3 Hz, 1H), 6.95 (d, J = 8.7 Hz, 2H), 6.79 (d, J = 8.7 Hz, 2H), 6.87-6.78 (m, 3H). MS TOFES$^+$: *m/z* 320.1 $(M+H)^+$.

3,3-Bis(4-(2-(dimethylamino)ethoxy)phenyl)-2-(thiophen-2-yl)acrylonitrile (12). A stirred mixture of 3,3-bis(4-hydroxyphenyl)-2-(thiophen-2-yl)acrylonitrile (**11**; 30 mg, 0.1 mmol), 2-bromo-*N*,*N*-dimethylethylamine hydrobromide (328 mg, 1.4 mmol), cesium carbonate (612 mg, 1.9 mmol), and acetonitrile (3 ml) was heated at reflux for 18 h. The mixture was diluted with water and extracted with ethyl acetate (3x). The combined extracts were washed successively with water and sat. brine, dried and concentrated to a syrup that was purified by flash silica gel chromatography, eluting first with 4-5 column volumes of 3:1 dichloromethane/methanol and then with 95:5 methanol/conc. ammonium hydroxide to elute the product. Combined product fractions

were concentrated to leave **12** (18 mg, 42%) as an amber gum. HPLC: rt 5.1 min (89% purity). ^{1}H NMR (400 MHz, DMSO-d_6): δ 7.46 (d, J = 5.2 Hz, 1H), 7.32 (d, J = 8.9 Hz, 2H), 7.17 (d, J = 2.5 Hz, 1H), 7.08 (d, J = 8.8 Hz, 2H), 7.03 – 6.87 (m, 5H), 4.15 – 3.97 (m, 4H), 2.65 – 2.53 (m, 4H), 2.20 (s, 12H). MS TOFES$^+$: *m/z* 462.1 $(M+H)^+$.

Preparation of compounds for biological testing. Stock solutions of tamoxifen and triarylacrylonitrile analogues (12.5 or 25 mM) were made up in DMSO and stored at 20 °C for no longer than 3 weeks.

PKC assay. To evaluate the ability of tamoxifen and the triarylacrylonitrile analogues to inhibit PKC activity, SHSY5Y cells were incubated in Krebs Ringer HEPES (KRH) buffer (25 mM HEPES, 125 mM NaCl, 4.8 mM KCl, 1.2 mM KH_2PO4, 1.3 mM $CaCl_2$, 1.2 mM $MgSO_4$, pH 7.4) at 37 °C for 15 min followed by a 1 h treatment with 3 and 10 μM of each compound in KRH. PKC was activated by adding a final concentration of 333 nM phorbol 12-myristate 13-acetate (PMA) in KRH to the samples for 15 minutes and the reaction quenched with 1 ml cold KRH. The samples were pelleted at 3000 rpm for 2 min. The pellets were washed twice in cold KRH and lysed in solubilization buffer (1% Triton X-100, 50 mM Tris HCl, 150 mM NaCl, pH 7.4). Lysates were rotated at 4 °C for 1 h and centrifuged at 14000 rpm for 15 min to remove debris. Protein assays were conducted using the Biorad DC Protein Assay Kit. PKC activity was quantified using western blot analysis of the phosphorylation of myristoylated alanine-rich C kinase substrate (MARCKS). To obtain the IC_{50} for **6c** and tamoxifen, the PKC assay was carried out by treating the SHSY5Y cells with 0.1-10 μM **6c** or 0.03-30 μM tamoxifen in KRH for 1 h.

Western blot analysis. Lysates were resolved (50 μg/lane) on a 12%

polyacrylamide gel using SDS-PAGE. The proteins were transferred onto a nitrocellulose membrane at 0.1 A for 12-16 h. Membranes were incubated in blocking buffer (5% w/v milk, 150 mM NaCl, 10 mM Tris, 0.05% Tween 20). The membranes were probed with anti-phospho-MARCKS Ser 152/156 antibody (1:1000, catalogue # 2741, Cell Signaling Technology Inc, Danvers, MA) and anti-glyceraldehyde 3-phosphate dehydrogenase (GAPDH) 14C10 (1:10000, catalogue # 2118, Cell Signaling Technology Inc, Danvers, MA) antibodies for 24 h at 4 °C. Primary phospho-MARCKS antibody binding was detected using goat-anti rabbit antibody (1:2000, catalogue # sc-2054, Santa Cruz Biotechnology, Inc., Santa Cruz, CA) for 1 h at room temperature and ECL Western Blotting Substrate (catalogue #32106, ThermoFisher Scientific, Waltham, MA). Primary GAPDH antibody binding was detected using donkey-anti rabbit antibody (1:20000, catalogue # sc-2054, Santa Cruz Biotechnology, Inc., Santa Cruz, CA) for 1 h at room temperature and Chemiluminescent Western Substrate (catalogue # WBKLS0500, EMD Millipore, Darmstadt, Germany). Band densities were quantified using Image J software. PKC activity of each compound was calculated as the ratio of phosphorylated MARCKS to GAPDH as a percentage of that ratio for the PMA control sample. The results are displayed in Table 2.1 as percent inhibition of PMA-stimulated PKC activity.

ERα binding assay. ER binding of tamoxifen and triarylacrylonitrile analogues was evaluated using a commercially available competitive binding assay (PolarScreen™ ER Beta Competitor Assay Kit, Green, catalogue # 15883, ThermoFisher Scientific, Waltham, MA). Compounds were loaded in triplicates.

Statistical analysis. Statistical differences were calculated by one-way analysis of variants (ANOVA) using GraphPad Prism 6. Statistical significance was set at $p \leq 0.05$.

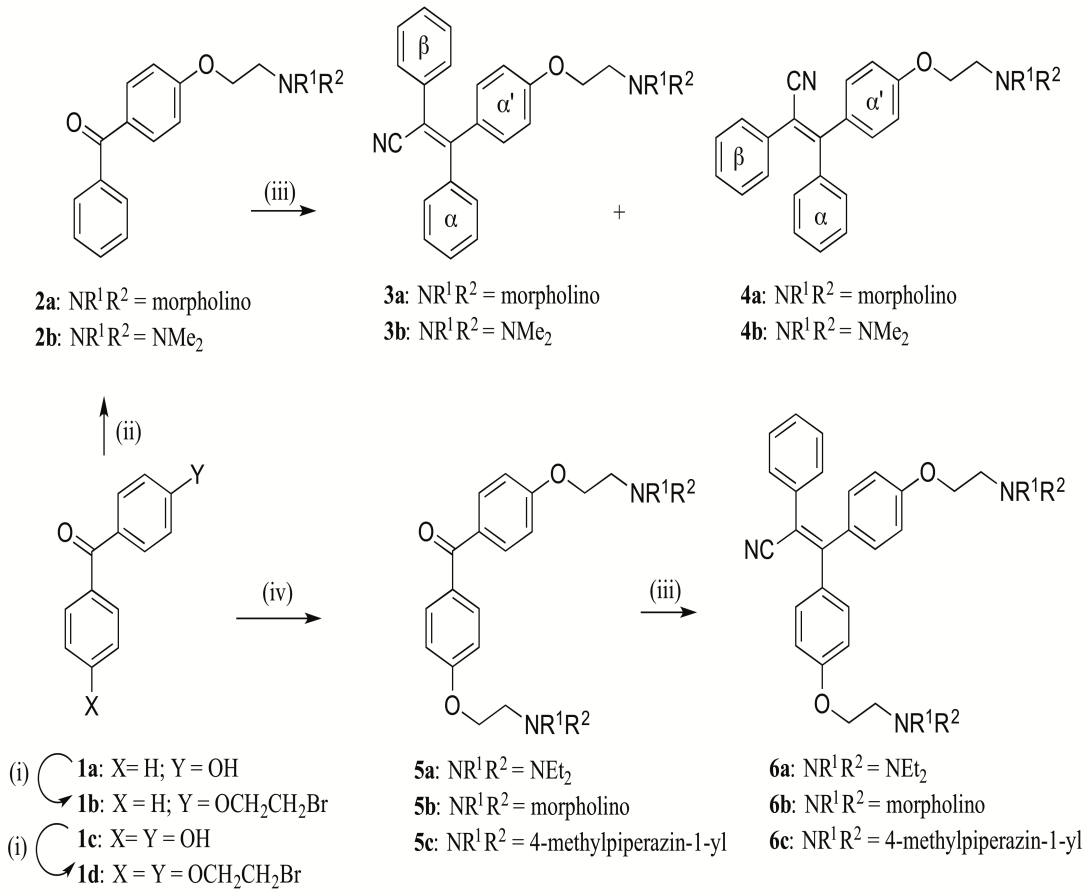

Figure 2.2. Scheme 1.

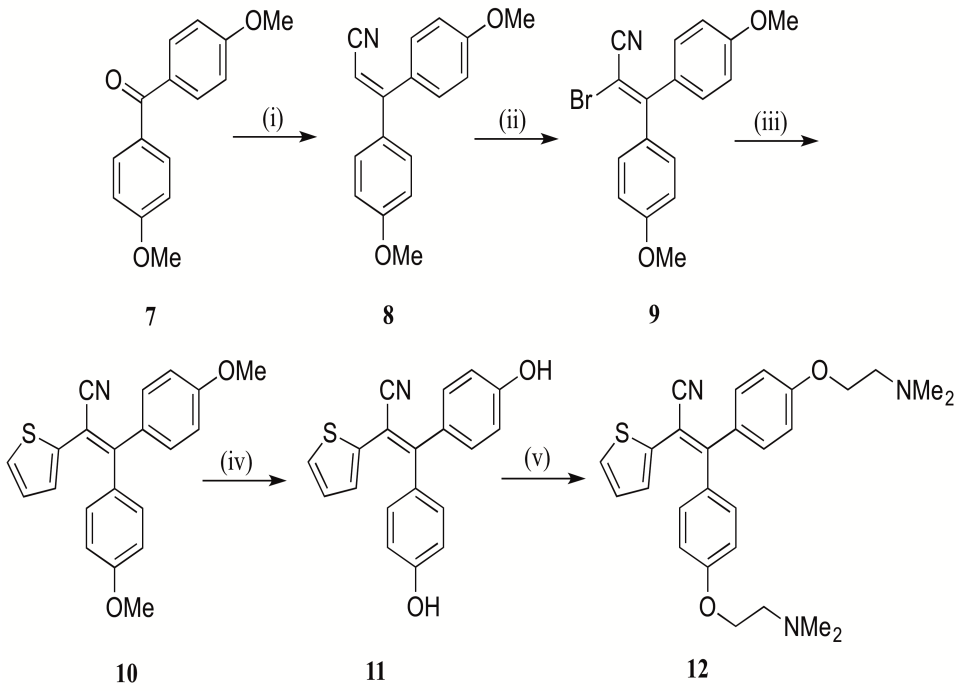

Figure 2.3. Scheme 2.

Results

Bignon *et al.* carried out a systematic study of a series of triphenylacrylonitrile derivatives for their effects on PKC (Bignon *et al*, 1991). One sub-series of compounds, substituted with at least one basic dialkylaminoethoxy side chain, inhibited type α, β, and γ PKC subspecies activated by Ca^{2+} and phosphatidylserine (PS) at micromolar concentrations, with or without diolein, but did not inhibit protamine sulfate phosphorylation. One compound (**6a**, Table 2.1) was one of the most potent tested (IC_{50} ~3 μM with PS; tamoxifen ~75 μM, (Bignon *et al*, 1991)). Based on an earlier study in which **6a** also displayed a lowered binding affinity to calf uterus cytosolic ER relative to tamoxifen (Bignon *et al*, 1989b), we decided to utilize it as a starting point for further SAR investigation.

Compound	Physicochemical Descriptor[a]			Inhibition of PKC-specific MARCKS Phosphorylation (% inhibition ± SEM), n = 3		ERα Binding IC_{50} (nM) [95% CI], n = 2-3[b]
	MW[c]	cLogP	tPSA	3 μM	10 μM	
Tamoxifen	371.52	6.74	12.47	27 ± 9	52 ± 7	222 [48-1035]
3a · HCl	410.52	5.57	45.49	43 ± 13	57 ± 9	224 [38-1326]
4a · HCl	410.52	5.57	45.49	37 ± 18	70 ± 11	97 [14-665]
3b:**4b** · HCl (17:3**)**	368.48	5.91	36.26	22 ± 10	67 ± 16	86 [18-405]
6a	511.71	7.01	48.73	12 ± 5	68 ± 8	>10,000
6b · 2 HCl	539.68	4.96	67.19	62 ± 8	72 ± 7	553 [101-3015]
6c · 2.5 HCl[d]	565.76	5.24	55.21	83 ± 4	78 ± 13	>10,000
12	461.62	5.46	48.73	39 ± 7	68 ± 5	>10,000

Table 2.1. Computed physicochemical properties and binding of compounds to PKC and ER.
Computed physicochemical properties and binding of compounds to PKC and ER. [a]Calculations utilizing ChemAxon/Marvin Sketch software. [b]For comparison, β-estradiol binding to ERα has IC_{50} = 4.4 nM [95% CI, 1-17]; n = 10. [c]Free base. [d]PKC IC_{50} = 160 nM; n = 6.

To determine the effectiveness of compounds against PKC, SHSY5Y cells were pre-incubated with vehicle or two concentrations (3 μM and 10 μM) of tamoxifen or triarylacrylonitrile analogue at 37 °C followed by a 15 min treatment with the phorbol ester PMA. These concentrations were chosen because in cellular models, tamoxifen inhibits PKC with an IC_{50} of approximately 1-10 μM (Horgan *et al*, 1986; O'Brian *et al*, 1985). Therefore, we tested tamoxifen and its analogues in our PKC activity assay at both 3 μM and 10 μM to rapidly evaluate whether the analogues had improved PKC inhibitory activity compared to tamoxifen. The inhibition of phosphorylation of myristoylated alanine-rich C kinase substrate (MARCKS), a known PKC target, was quantified using western blotting. To assess effects against the ER, a complex of full length ERα and a proprietary fluorescent estrogen ligand were added to various concentrations of estradiol, tamoxifen and triarylacrylonitrile analogue for up to 4 h. Relative binding affinities were determined from changes in fluorescence polarization.

Inhibition data against PKC and ERα for synthesized triarylacrylonitrile analogues versus tamoxifen as control are shown in Table 2.1. The results are displayed in Table 2.1 as percent inhibition of PMA-stimulated PKC activity. Representative western blots for all compounds except for **6c**, which is shown in Figure 2.4, are shown in Figure 2.5. In our ERα binding assay, tamoxifen displaced estradiol binding with an IC_{50} of 222 nM. Additionally, we observed a 27 ± 9% and 52 ± 7% inhibition of PKC activity by tamoxifen at 3 μM and 10 μM, respectively. This was nearly equivalent to the inhibition of PKC by the isomeric compounds **3a** and **4a**, which possess a single morpholinoethoxy side chain, with each showing nearly equivalent inhibition of PKC relative to tamoxifen at the two concentrations tested. These compounds also display essentially equivalent affinity for binding to ERα, which is within the same range as tamoxifen. The same pattern holds for the direct nitrile congener of tamoxifen, **3b**, which was tested as a mixture highly enriched in the *E*-isomer. More specifically, **3b:4b** caused a 22 ± 10% and 67 ± 16% reduction in PKC activity at 3 μM and 10 μM, respectively. Analogues **6a-6c** with solubilizing dialkylaminoalkoxy side chains attached to both the α and α' rings show a different pattern of inhibition. In general, there is a trend for greater potency toward inhibition of PKC at both concentrations tested relative to tamoxifen, and/or reduced affinity to the ERα. Compound **6a** with the (diethylamino)ethoxy side chains shows essentially equivalent potency to tamoxifen for inhibition of PKC, but with negligible binding to ERα. In contrast, compound **6b** with the less basic morpholinoethoxy side chains shows much greater sensitivity toward PKC, with 3 μM and 10 μM of **6b** causing a 62 ± 8% and 72 ± 7% decrease in PKC activity respectively. However, **6b** displays equivalent potency for ERα relative to tamoxifen. Compared to **6a**,

6b showed significantly more inhibition of PKC at 3 μM (one-way ANOVA, *p < 0.05; see Table 2.1). Compound **6c** with the more basic (4-methylpiperazin-1-yl)ethoxy side chains shows the best selectivity profile relative to tamoxifen for all analogues synthesized with excellent potency toward inhibition of PKC and undetected binding to ERα. Similar to **6b**, **6c** inhibited PKC more significantly at 3 μM when compared to **6a** (one-way ANOVA, **p < 0.01; see Table 2.1). Dose response experiments with **6c** shows that it inhibits PKC activity with an IC_{50} of 80 nM, but does not bind ERα at concentrations up to at least 10 μM. A representative blot with a calculated dose response curve demonstrating the inhibition of PMA-stimulated MARCKS phosphorylation is shown in Figure 2.4. By comparison, tamoxifen in our cell-based PKC inhibition assay has an IC_{50} of 20 μM against PKC and an IC_{50} of 222 nM for binding to ERα.

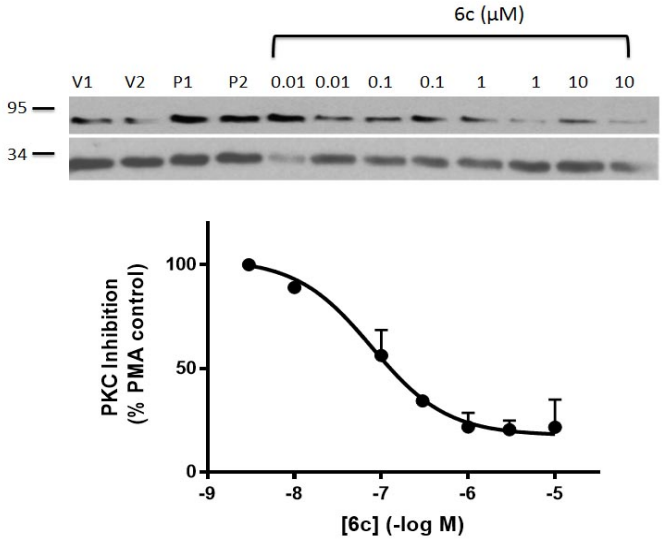

Figure 2.4. Compound 6c dose dependently inhibits PMA-stimulated MARCKS phosphorylation.
A. Representative western blot of pMARCKS (top row) with GAPDH loading control (bottom row). Concentrations in μM are given above the lanes. V1 and V2 are vehicle; P1and P2 are PMA control. The molecular weight markers of 95 and 34 kDa are shown. **B**. Dose response curve calculated from pMARCKS western blot analysis. PMA control is calculated as PMA values minus vehicle control and set at 100%. n=4-6.

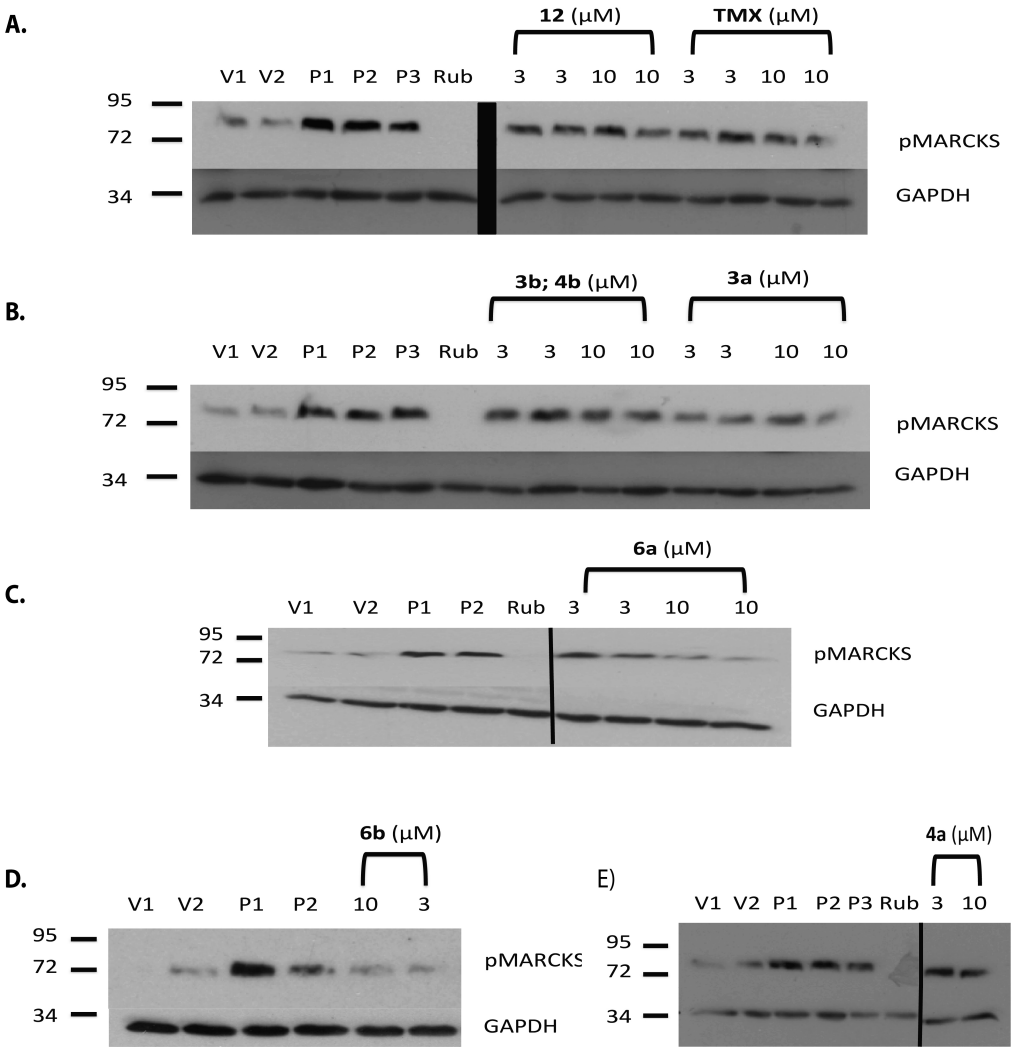

Figure 2.5. The effect of tamoxifen and the tamoxifen analogues on PKC activity.
SHSY5Y cells were incubated in the presence or absence (vehicle) of the compounds for 1 h at 37 ˚C. PMA (333 nM) was used to stimulate PKC for 15 min and then the samples were lysed and probed for phosphorylated MARCKS (pMARCKS). GAPDH served as the loading control. Representative blots show actions of A: **tamoxifen** (TMX) and **12** (cropped blots), B: **3b:4b** and **3a**, C: **6a** (cropped), D: **6b**. E: **4a** (cropped). V1, V2: vehicle; P1, P2, P3: PMA control, Rub = 500 nM ruboxistaurin (positive control).

The data for a single congener, **12**, in which the β-phenyl ring has been replaced with a thiophen-2-yl ring, show a similar selectivity pattern to **6c** but with reduced potency for inhibition of PKC. More specifically, unlike **6c** which causes a 83 ± 4 % reduction in PKC activity at 3 μM, **12** inhibits only at 39 ± 7 %. More work needs to be carried out to fully map out a β-heteroaryl ring SAR.

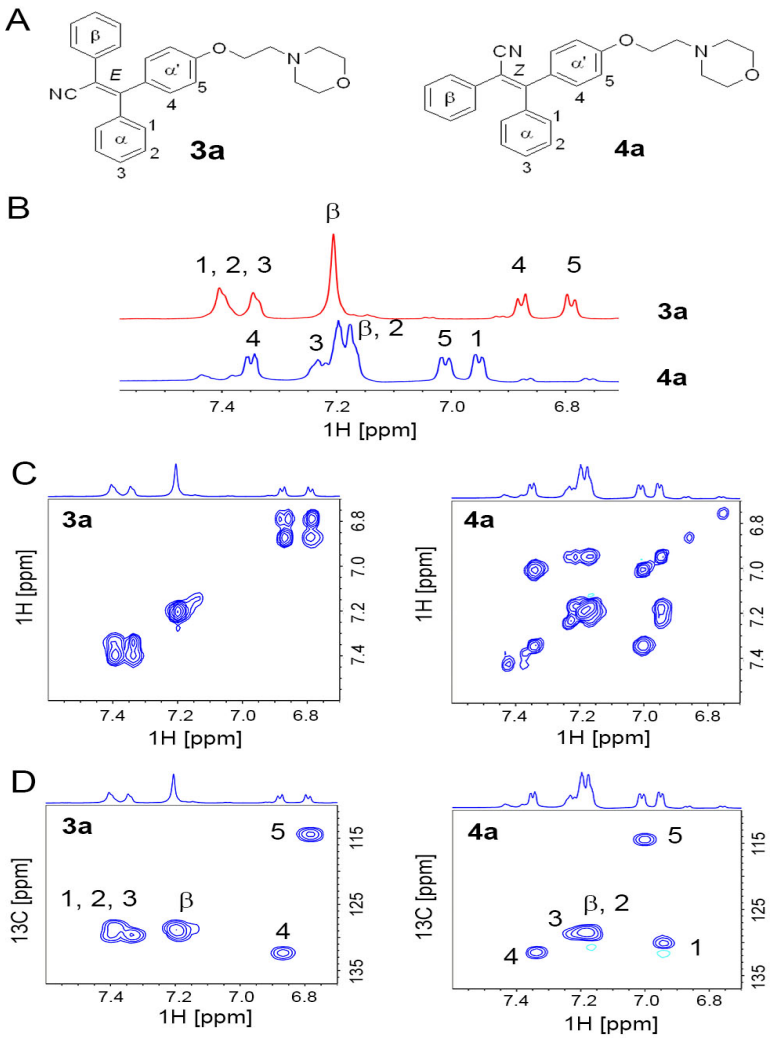

Figure 2.6. Assignment of aromatic regions of NMR spectra compounds 3a and 4a hydrochloride salts. Assignment of aromatic regions of NMR spectra for compounds 3a and 4a hydrochloride salts. A. Structures of 3a and 4a with labeled aromatic protons; B. Assigned 1H aromatic regions for 3a and 4a; C. 2D ^{1}H-^{1}H TOCSY spectra for 3a (left) and 4a (right); D. 2D ^{1}H-^{13}C HSQC spectra for 3a (left) and 4a (right).

Discussion

Protocol optimization

The classical procedure to construct the triphenylacrylonitrile compounds used for this study is through condensation of a methoxy benzophenone precursor and phenyl-acetonitrile anion, generated either with NaH or sodium amide in refluxing benzene,

followed by pyridinium hydrochloride demethylation (Gilbert *et al*, 1983) and phenolic alkylation with an appropriate dialkylaminoalkyl halide (Dore *et al*, 1992). In order to shorten the sequence and provide the option of introducing variable β-ring aryl or heteroaryl moieties, we decided to install our dialkylaminoalkoxy side chains first off the α and/or α' rings and then condense the resultant ketones with a phenylacetonitrile anion.

Toward that end, we generated a small set of mono- and bis-(dialkylaminoalkoxy)benzophenones either through a one-step phenolic alkylation of **1a** or **1c** with readily available dialkylaminoalkyl halides to give **2a**, **5a**, **5b** in 85-92% yield, or in two steps via mono bromo displacement with excess 1,2-dibromoethane to give **1b** and **1d**, followed by a second bromo displacement with a chosen dialkylamine to give **2b** and **5c** in an overall ~55% yield. The latter method, while longer, is especially suited toward installing a wide range of distal amino headpieces onto the alkoxy side chain, which otherwise would not be readily accessible from aminoalkyl halides. We then examined condensation of these elaborated benzophenones with phenylacetonitrile by screening a range of anion forming conditions. Notably, reaction of **5a** with 1 – 5 equivalents of NaH under a variety of solvent (THF, *p*-dioxane, toluene, DMSO) and temperature (25 ºC – 110 ºC) conditions resulted in recovery of starting ketone or the generation of complex mixtures showing only trace amounts of product **6a**. Reaction with potassium *t*-butoxide in DMSO at 25 ºC left starting material. We then progressed to stronger bases such as *n*-BuLi and LDA at low temperature. Anion generation in THF at -78 ºC with 5 equivalents of *n*-BuLi followed by addition of ketone **5a** and warming to 25 ºC provided the desired product **6a** contaminated with a small amount of by-product, whereas the use of LDA under the same conditions resulted in a cleaner condensation.

Optimization of reaction conditions, utilizing 20 equivalents of LDA, and application to ketones **2a**, **2b**, **5a-5c** provided condensation products (**3a** – **4b**, **6a** – **6c**) in 86-100% yields prior to crystallization. Unsymmetrical ketones **2a** and **2b** generated mixtures of *E* and *Z* isomers (**3a**/**4a** and **3b**/**4b**) in an *E*/*Z* ratio of 9:1 to 5:1 by HPLC. Partial separation of isomers **3a** and **4a** was achieved through fractional crystallization/trituration of the free base. Further fractional crystallization of the formed hydrochloride salts of each enriched mixture then provided individual isomers in ≥ 94% purity by HPLC. No attempt was made to purify each isomer of the **3b**/**4b** mixture, which was tested as such.

Having developed condensation conditions to add phenylacetonitrile to a range of dialkylaminoalkoxy-substituted benzophenones, we were interested in applying the same anion generating conditions to provide target compounds in which the β-aryl moiety is derived from representative heterocyclic acetonitriles. Thus, LDA treatment of 2- or 4-pyridylacetonitrile or 2-thienylacetonitrile under the optimum conditions discussed above followed by addition of ketone **5c** resulted either in recovered starting ketone (for pyridylacetonitriles) or a very low yield of product (for 2-thienylacetonitrile), along with intractable side products. This necessitated the development of a completely novel approach ("Suzuki strategy") for this type of scaffold. Its reduction to practice, which is exemplified with a test heteroaryl boronic acid, is shown in Figure 2.3 (Scheme 2).

Accordingly, Horner-Wadsworth-Emmons (HWE) reaction of diethyl (cyanomethyl)phosphonate with benzophenone **7** proceeded under literature conditions to provide the elaborated acrylonitrile **8** in 89% yield. Selective olefin bromination of **8** was patterned after an analogous literature reaction to give **9** in 59% yield. Heteroarylation of

9 with thiophen-2-ylboronic acid proceeded under standard Suzuki conditions (Lone and Bhat, 2014) to give the core scaffold **10** in 87% yield incorporating the β-heteroaryl moiety (similar reaction of furan-2-ylboronic acid proceeded also in high yield). Installation of the bis-(2-dimethylamino)ethoxy side chains was then accomplished by a standard sequence of methoxy ether demethylation (BBr_3) followed by alkylation with 2-bromo-*N*,*N*-dimethylethylamine to give target compound **12** in 41% yield. Attempts to further shorten the sequence were evaluated with elaborated ketone **5c** and found to be unsuccessful. While HWE reaction proceeded successfully, attempted bromination of the resultant product under several conditions left only starting cyano olefin.

Most compounds could be rigorously purified by flash chromatography and/or crystallization, except for except for **6a**-**6c**. Each of these shows a spot on silica gel TLC that overlaps with its respective precursor ketone **5**, and requires an extremely polar eluant (95:5 methanol: concentrated ammonium hydroxide) to develop the plate to a reasonable R_f (~0.35). Hence, standard flash chromatography or preparative thick layer chromatography was not useful, so hydrochloride salts were formed and crystallized for further purification. Structural assignments for all compounds were supported by diagnostic peaks in the ^{1}H NMR spectra and by mass spectrometry. For purified unsymmetrical *E*- and *Z*-isomers, **3a** and **4a** hydrochloride salts, respectively, structural assignments were based on 1D ^{1}H, 1D ^{13}C, 2D ^{1}H-^{1}H TOCSY and 2D ^{1}H-^{13}C HSQC experiments. Chemical shift analysis revealed that **3a** is the *E*-isomer while **4a** is the *Z*-isomer. These assignments are based on significant differences between proton chemical shifts for protons in the *α*-ring of each isomer (Figure 2.6). In **4a** (*Z*-isomer) the C-1 proton of the α-phenyl ring has a strong upfield shift (6.95 ppm) due to its location above

the plane of either the α'- or β-phenyl ring. By contrast, the C-1 proton of the α-phenyl ring in **3a** shows a downfield shift (~7.4 ppm), which is consistent with *E*-stereochemistry. Such a strong conformational effect on chemical shifts allows for unambiguous assignment of *Z*- and *E*-isomers, which is more convenient than the classical methods of isomeric assignments by x-ray crystallography (Gilbert *et al*, 1983).

Lead compound

Overall, we are interested in pursuing the effects of the tamoxifen analogues, **6c**, on AMPH neurochemical and behavioral effects *in vivo*. **6c** proved to be 250 times more potent than tamoxifen in inhibiting PKC in our cellular assay and displayed no affinity at the ER, and therefore was the most promising tamoxifen analogues generated from this study. There are many quantifiable traits of drugs that successfully cross the blood-brain barrier. These include good lipophilicity (calculated logP <5), a total polar surface area (tPSA) <60-70 $Å^2$ and a molecular weight <450 Da (Pajouhesh and Lenz, 2005). Compared to tamoxifen (molecular weight 371 Da; tPSA, 12 $Å^2$; calculated logP, 6.8), **6c** has improved calculated logP (5.2), increased tPSA (55 $Å^2$) and molecular weight (566 Da; free base). Although, the molecular weight is slightly higher than desired, we believe the other physicochemical properties of the compound will allow it to cross the blood-brain barrier.

Conclusion

Utilizing the known compound **6a** as a starting template, we have designed and synthesized a small series of novel triarylacrylonitrile analogues with some possessing enhanced potency and selectivity for PKC over the ER. For analogues incorporating a β-phenyl ring, we have shortened the classical synthetic route by installing

dialkylaminoalkoxy side chains first off the α- and/or α'- rings of a precursor benzophenone, and then condensing the resultant ketones with phenylacetonitrile anion. Additionally, we have developed a completely novel, efficient, and versatile route utilizing Suzuki chemistry, which will allow for the introduction of a wide range of β-aryl or β-heteroaryl moieties and side-chain substituents onto the acrylonitrile scaffold. For analogues possessing a single side chain off the α- or α'- ring, we have developed novel 2D NMR experiments that allow for unambiguous assignment of *E*- and *Z*-stereochemistry. From our SAR, we have successfully uncovered a compound, **6c**, with markedly increased potency and selectivity for inhibiting PKC and reduced ER binding compared to tamoxifen. Future publications will detail studies that show that **6c** significantly inhibits AMPH-induced dopamine release using both *in vitro* and *in vivo* models. Additional studies investigating the effects of **6c** on AMPH reinforcement using self-administration in rats as well as current studies to determine CNS penetration will also be reported. These, in addition to the binding data reported herein, support further SAR exploration of the triphenylacrylonitrile scaffold, and heteroaryl congeners, toward the development of potential clinical agents to treat AMPH abuse.

Acknowledgement

The Vahlteich Medicinal Chemistry Core at the University of Michigan synthesized the compounds used in this study.

References

Abraham MH, Takács‐Novák K, Mitchell RC (1997). On the partition of ampholytes: application to blood‐brain distribution. *Journal of pharmaceutical sciences* **86**(3): 310-315.

Armani F, Andersen ML, Galduróz JCF (2014). Tamoxifen use for the management of mania: a review of current preclinical evidence. *Psychopharmacology* **231**(4): 639-649.

Aujla H, Beninger RJ (2003). Intra-accumbens protein kinase C inhibitor NPC 15437 blocks amphetamine-produced conditioned place preference in rats. *Behavioural Brain Research* **147**(1–2): 41-48.

Battaini F (2001). Protein kinase C isoforms as therapeutic targets in nervous system disease states. *Pharmacological research* **44**(5): 353-361.

Bignon E, Ogita K, Kishimoto A, Gilbert J, Abecassis J, Miquel JF, Nishizuka Y (1989a). Modes of inhibition of protein kinase C by triphenylacrylonitrile antiestrogens. *Biochemical and biophysical research communications* **163**(3): 1377-1383.

Bignon E, Pons M, Crastes de Paulet AC, Dore JC, Gilbert J, Abecassis J, Miquel JF, Ojasoo T, Raynaud JP (1989b). Effect of triphenylacrylonitrile derivatives on estradiol-receptor binding and on human breast cancer cell growth. *Journal of medicinal chemistry* **32**(9): 2092-2103.

Bignon E, Pons M, Dore JC, Gilbert J, Ojasoo T, Miquel JF, Raynaud JP, Crastes de Paulet A (1991). Influence of di- and tri-phenylethylene estrogen/antiestrogen structure on the mechanisms of protein kinase C inhibition and activation as revealed by a multivariate analysis. *Biochemical pharmacology* **42**(7): 1373-1383.

Bignon E, Pons M, Gilbert J, Nishizuka Y (1990). Multiple mechanisms of protein kinase C inhibition by triphenylacrylonitrile antiestrogens. *FEBS letters* **271**(1-2): 54-58.

Browman KE, Kantor L, Richardson S, Badiani A, Robinson TE, Gnegy ME (1998). Injection of the protein kinase C inhibitor Ro31-8220 into the nucleus accumbens attenuates the acute response to amphetamine: tissue and behavioral studies. *Brain research* **814**(1-2): 112-119.

Chen J, Wang Y, Li W, Zhou H, Li Y, Yu C (2014). Nucleic acid-induced tetraphenylethene probe noncovalent self-assembly and the superquenching of aggregation-induced emission. *Analytical chemistry* **86**(19): 9866-9872.

de Medina P, Favre G, Poirot M (2004). Multiple targeting by the antitumor drug tamoxifen: a structure-activity study. *Current medicinal chemistry Anti-cancer agents* **4**(6): 491-508.

De Médina P, Payré BL, Bernad J, Bosser I, Pipy B, Silvente-Poirot S, Favre G, Faye J-C, Poirot M (2004). Tamoxifen is a potent inhibitor of cholesterol esterification and prevents the formation of foam cells. *Journal of Pharmacology and Experimental Therapeutics* **308**(3): 1165-1173.

Dluzen D, McDermott J, Anderson L (2001). Tamoxifen diminishes methamphetamine‐induced striatal dopamine depletion in intact female and male mice. *Journal of neuroendocrinology* **13**(7): 618-624.

Dore JC, Gilbert J, Bignon E, Crastes de Paulet A, Ojasoo T, Pons M, Raynaud JP, Miquel JF (1992). Multivariate analysis by the minimum spanning tree method of the structural determinants of diphenylethylenes and triphenylacrylonitriles implicated in estrogen receptor binding, protein kinase C activity, and MCF7 cell proliferation. *Journal of medicinal chemistry* **35**(3): 573-583.

Einat H, Yuan P, Szabo ST, Dogra S, Manji HK (2007). Protein kinase C inhibition by tamoxifen antagonizes manic-like behavior in rats: implications for the development of novel therapeutics for bipolar disorder. *Neuropsychobiology* **55**(3-4): 123-131.

Garrido JL, GODOY JA, Alvarez A, Bronfman M, Inestrosa NC (2002). Protein kinase C inhibits amyloid β peptide neurotoxicity by acting on members of the Wnt pathway. *The FASEB journal* **16**(14): 1982-1984.

Gilbert J, Miquel JF, Precigoux G, Hospital M, Raynaud JP, Michel F, Crastes de Paulet A (1983). Inhibition of prostaglandin synthetase by di-and triphenylethylene derivatives: a structure-activity study. *Journal of medicinal chemistry* **26**(5): 693-699.

Gundimeda U, Chen ZH, Gopalakrishna R (1996). Tamoxifen modulates protein kinase C via oxidative stress in estrogen receptor-negative breast cancer cells. *The Journal of biological chemistry* **271**(23): 13504-13514.

Horgan K, Cooke E, Hallett MB, Mansel RE (1986). Inhibition of protein kinase C mediated signal transduction by tamoxifen. *Biochemical pharmacology* **35**(24): 4463-4465.

Jordan VC (2003). Tamoxifen: a most unlikely pioneering medicine. *Nature reviews Drug discovery* **2**(3): 205-213.

Kantor L, Gnegy ME (1998). Protein kinase C inhibitors block amphetamine-mediated dopamine release in rat striatal slices. *The Journal of pharmacology and experimental therapeutics* **284**(2): 592-598.

Khoshbouei H, Sen N, Guptaroy B, Johnson LA, Lund D, Gnegy ME, Galli A, Javitch JA (2004). N-terminal phosphorylation of the dopamine transporter is required for amphetamine-induced efflux. *PLoS Biology* **2**(3).

Kuo J-R, Wang C-C, Huang S-K, Wang S-J (2012). Tamoxifen depresses glutamate release through inhibition of voltage-dependent Ca 2+ entry and protein kinase Cα in rat cerebral cortex nerve terminals. *Neurochemistry international* **60**(2): 105-114.

Lashley M, Dicus C, Brown K, Nantz MH (2003). Synthesis of α-hydroxytamoxifen and its 4-hydroxy analog. *Organic preparations and procedures international* **35**(2): 231-238.

Lone AM, Bhat BA (2014). Metal free stereoselective synthesis of functionalized enamides. *Organic & biomolecular chemistry* **12**(2): 242-246.

Manji H, Chen G (2002). PKC, MAP kinases and the bcl-2 family of proteins as long-term targets for mood stabilizers. *Molecular Psychiatry* **7**(S1): S46.

Manji HK, Lenox RH (2000). Signaling: cellular insights into the pathophysiology of bipolar disorder. *Biological psychiatry* **48**(6): 518-530.

Meegan MJ, Hughes RB, Lloyd DG, Williams DC, Zisterer DM (2001). Flexible estrogen receptor modulators: design, synthesis, and antagonistic effects in human MCF-7 breast cancer cells. *Journal of medicinal chemistry* **44**(7): 1072-1084.

Mochly-Rosen D, Das K, Grimes KV (2012). Protein kinase C, an elusive therapeutic target? *Nature reviews Drug discovery* **11**(12): 937-957.

Moritz AE, Foster JD, Gorentla BK, Mazei-Robison MS, Yang J-W, Sitte HH, Blakely RD, Vaughan RA (2013). Phosphorylation of dopamine transporter serine 7 modulates cocaine analog binding. *Journal of Biological Chemistry* **288**(1): 20-32.

O'Brian CA, Housey GM, Weinstein IB (1988). Specific and direct binding of protein kinase C to an immobilized tamoxifen analogue. *Cancer research* **48**(13): 3626-3629.

O'Brian CA, Ioannides CG, Ward NE, Liskamp RM (1990). Inhibition of protein kinase C and calmodulin by the geometric isomers cis‐and trans‐tamoxifen. *Biopolymers* **29**(1): 97-104.

O'Brian CA, Liskamp RM, Solomon DH, Weinstein IB (1985). Inhibition of protein kinase C by tamoxifen. *Cancer research* **45**(6): 2462-2465.

Ochoa WF, Garcia-Garcia J, Fita I, Corbalan-Garcia S, Verdaguer N, Gomez-Fernandez JC (2001). Structure of the C2 domain from novel protein kinase Cϵ. A membrane binding model for Ca 2+-independent C2 domains. *Journal of molecular biology* **311**(4): 837-849.

Ohta K, Chiba Y, Kaise A, Endo Y (2015). Structure–activity relationship study of diphenylamine-based estrogen receptor (ER) antagonists. *Bioorganic & medicinal chemistry* **23**(4): 861-867.

Olive MF, Messing RO (2004). Protein kinase C isozymes and addiction. *Molecular neurobiology* **29**(2): 139-153.

Pajouhesh H, Lenz GR (2005). Medicinal chemical properties of successful central nervous system drugs. *NeuroRx* **2**(4): 541-553.

Palopoli FP, Holtkamp DE, Schaar JL (1966). Bis(aminoalkoxy)triphenylethanols.

Pan D, Iyer M, Liu J, Li Y, Hopfinger AJ (2004). Constructing optimum blood brain barrier QSAR models using a combination of 4D-molecular similarity measures and cluster analysis. *Journal of chemical information and computer sciences* **44**(6): 2083-2098.

Pereira M, Martynhak BJ, Baretta IP, Correia D, Siba IP, Andreatini R (2011). Antimanic-like effect of tamoxifen is not reproduced by acute or chronic administration of medroxyprogesterone or clomiphene. *Neuroscience letters* **500**(2): 95-98.

Sabioni P, Baretta IP, Ninomiya EM, Gustafson L, Rodrigues ALS, Andreatini R (2008). The antimanic-like effect of tamoxifen: behavioural comparison with other PKC-inhibiting and antiestrogenic drugs. *Progress in Neuro-Psychopharmacology and Biological Psychiatry* **32**(8): 1927-1931.

Saraiva L, Fresco P, Pinto E, Gonçalves J (2003). Isoform-selectivity of PKC inhibitors acting at the regulatory and catalytic domain of mammalian PKC-α,-βI,-δ,-η and-ζ. *Journal of enzyme inhibition and medicinal chemistry* **18**(6): 475-483.

Schmitt KC, Reith ME (2010). Regulation of the dopamine transporter. *Annals of the New York Academy of Sciences* **1187**(1): 316-340.

Su HD, Mazzei GJ, Vogler WR, Kuo JF (1985). Effect of tamoxifen, a nonsteroidal antiestrogen, on phospholipid/calcium-dependent protein kinase and phosphorylation of its endogenous substrate proteins from the rat brain and ovary. *Biochemical pharmacology* **34**(20): 3649-3653.

Szallasi Z, Bogi K, Gohari S, Biro T, Acs P, Blumberg PM (1996). Non-equivalent roles for the first and second zinc fingers of protein kinase Cδ effect of their mutation on phorbol ester-induced translocation in NIH 3T3 cells. *Journal of Biological Chemistry* **271**(31): 18299-18301.

Tang B, Hong Y, Chen S, Kwok RTK (2012). Water-soluble conjugated polyene-based aggregation-induced emission luminogen for monitoring and retardation of amyloid fibrillation of insulin. Vol US Patent 0172296 A1.

Wang HY, Friedman E (1996a). Enhanced protein kinase C activity and translocation in bipolar affective disorder brains. *Biological psychiatry* **40**(7): 568-575.

Wang Q, Bubula N, Brown J, Wang Y, Kondev V, Vezina P (2016). PKC phosphorylates residues in the N-terminal of the DA transporter to regulate amphetamine-induced DA efflux. *Neuroscience letters* **622**: 78-82.

Wang S, Kazanietz MG, Blumberg PM, Marquez VE, Milne G (1996b). Molecular modeling and site-directed mutagenesis studies of a phorbol ester-binding site in protein kinase C. *Journal of medicinal chemistry* **39**(13): 2541-2553.

Zarate CA, Jr., Singh JB, Carlson PJ, Quiroz J, Jolkovsky L, Luckenbaugh DA, Manji HK (2007). Efficacy of a protein kinase C inhibitor (tamoxifen) in the treatment of acute mania: a pilot study. *Bipolar disorders* **9**(6): 561-570.

Zestos AG, Mikelman SR, Kennedy RT, Gnegy ME (2016). PKCβ inhibitors attenuate amphetamine-stimulated dopamine efflux. *ACS Chemical Neuroscience* **7**(6): 757-766.

Zhang D, Anantharam V, Kanthasamy A, Kanthasamy AG (2007). Neuroprotective effect of protein kinase C delta inhibitor rottlerin in cell culture and animal models of Parkinson's disease. *The Journal of pharmacology and experimental therapeutics* **322**(3): 913-922.

Chapter 3. Direct and systemic administration of a CNS-permeant tamoxifen analogue reduces amphetamine-induced dopamine release and reinforcing effects

Abstract

Amphetamines (AMPHs) are globally abused. With no effective treatment for AMPH addiction to date, there is urgent need for the identification of druggable targets that mediate the reinforcing action of this stimulant class. AMPH-stimulated dopamine efflux is modulated by protein kinase C (PKC) activation. Inhibition of PKC reduces AMPH-stimulated dopamine efflux and locomotor activity. The only known CNS-permeant PKC inhibitor is the selective estrogen receptor modulator tamoxifen. In this study we demonstrate that a tamoxifen analogue, **6c**, which more potently inhibits PKC than tamoxifen but lacks affinity for the estrogen receptor, reduces AMPH-stimulated increases in extracellular dopamine and reinforcement-related behavior. In rat striatal synaptosomes, **6c** was almost fivefold more potent at inhibiting AMPH-stimulated dopamine efflux than [^{3}H]dopamine uptake through the dopamine transporter (DAT). The compound did not compete with [^{3}H]WIN35,428 binding or affect surface DAT levels. Using microdialysis, direct accumbal administration of 1 μM **6c** reduced dopamine overflow in freely moving rats. Using LC-MS, we demonstrate that **6c** is CNS-permeant. Systemic treatment of rats with 6 mg/kg of **6c** either simultaneously or 18 h

prior to systemic AMPH administration reduced both AMPH-stimulated dopamine overflow and AMPH-induced locomotor effects. Finally, 18 h pretreatment of rats with 6 mg/kg of **6c** *s.c.* reduces AMPH-self administration but not food self-administration. These results demonstrate the utility of tamoxifen analogues in reducing AMPH effects on dopamine and reinforcement-related behaviors and suggest a new avenue of development for therapeutics to reduce AMPH abuse.

Introduction

Amphetamine (AMPH) and its congeners are highly addictive stimulants and their abuse remains a significant health, social and economic burden (Berman *et al*, 2008; Carvalho *et al*, 2012). Yet an effective treatment for AMPH abuse remains elusive. Like other drugs of abuse, the reinforcing effects of AMPH are attributed to its ability to significantly increase extracellular dopamine in the nucleus accumbens (Di Chiara and Imperato, 1988; Wise and Bozarth, 1985). AMPH achieves this effect through its action at the dopamine transporter (DAT). The primary role of DAT is to clear extracellular dopamine, thereby terminating pre- and post-synaptic dopamine signaling (Zhu and Reith, 2008). AMPH, a substrate of DAT, disrupts this process by competitively blocking dopamine reuptake and also promoting reverse transport of dopamine via DAT (McMillen, 1983). Unlike stimulants such as cocaine, whose actions are more reliant on storage pools of monoamines, the release of newly synthesized dopamine also contributes to AMPH action (Chiueh and Moore, 1975; Parker and Cubeddu, 1986).

We found that protein kinase C (PKC) enhances AMPH-stimulated dopamine efflux. AMPH increases striatal particulate PKC activity (Giambalvo, 1992, 2004) and PKC stimulates the phosphorylation of N-terminal DAT residues (Foster *et al*, 2002).

Phosphorylation of DAT is permissive for AMPH-stimulated dopamine release (Khoshbouei *et al*, 2004; Wang *et al*, 2016). Selective PKC inhibitors and genetic deletion of PKC significantly reduce AMPH-stimulated dopamine release from striatal synaptosomes and slices (Chen *et al*, 2009; Kantor and Gnegy, 1998). PKC inhibition, however, does not alter the normal uptake functioning of the transporter (Johnson *et al*, 2005; Kantor *et al*, 1998; Zestos *et al*, 2016). Therefore PKC represents a novel therapeutic target for the treatment of AMPH abuse.

The selective estrogen receptor modulator tamoxifen stands as the only commercially available central nervous system (CNS)-permeant PKC inhibitor (Zarate and Manji, 2009). Tamoxifen is commonly used to reduce estrogen receptor (ER)-positive breast cancer recurrence and to prevent breast cancer in high-risk women (Fisher *et al*, 1998; Jordan, 2003). Early reports using purified PKC show that tamoxifen inhibits the calcium- and phospholipid- dependent activity of classical PKC isoforms, with IC_{50}s between 25-100 μM (Su *et al*, 1985). In cells, tamoxifen inhibits PKC at more pharmacologically relevant concentrations (1-5 μM) (Gundimeda *et al*, 1996; Horgan *et al*, 1986; Lien *et al*, 1991; O'Brian *et al*, 1985). There are findings that suggest PKC activity is elevated in patients suffering from bipolar mania, a disorder modeled by repeated AMPH administration in animals (Wang and Friedman, 1996). Interestingly, systemic tamoxifen reduces manic symptoms in patients with bipolar mania and this effectiveness is believed to stem from the action of tamoxifen at PKC (Kulkarni *et al*, 2006; Zarate *et al*, 2007). These data point to the clinical relevance of tamoxifen as a CNS-permeant PKC inhibitor. Although tamoxifen is well tolerated overall, it can cause ER-mediated adverse effects including increased risk of hot flashes, thromboembolisms

and endometrial cancers (Fisher *et al*, 1998; Gradishar, 2004). Therefore a CNS-permeant tamoxifen analogue lacking ER activity could be useful in the context of AMPH abuse treatment.

Extensive structure-activity relationship (SAR) studies have investigated tamoxifen substructures that contribute to its ability to bind to the ER and inhibit PKC (de Medina *et al*, 2004). We used this wealth of knowledge to synthesize a new generation of tamoxifen analogues with increased selectivity for PKC over ER (Carpenter *et al*, 2016). In this paper we investigate the effect of our most promising novel compound, **6c** (Figure 3.1A), at DAT and also on the neurochemical, behavioral and reinforcing actions of AMPH. Our key findings show that **6c** modulates DAT asymmetrically, in that it is more potent in reducing dopamine efflux than uptake. Importantly, intra-accumbal and systemic administration of the tamoxifen analogue significantly reduces dopamine overflow and locomotion stimulated by AMPH. Finally, our self-administration studies demonstrate that **6c** effectively reduces AMPH self-administration but not food self-administration. This work supports the repurposing of the tamoxifen scaffold as a treatment for AMPH abuse and elucidates an effective route for blocking AMPH reinforcement.

Materials and methods

Compounds. **6c** (6c•2.5 HCl) was synthesized and provided by the Vahlteich Medicinal Chemistry Core at the University of Michigan (Carpenter *et al*, 2016). *D*-AMPH hemi-sulfate, dopamine, nomifensine maleate salt and phorbol-12-myristate-13-acetate (PMA) were purchased from Sigma-Aldrich. Ruboxistaurin and cocaine hydrochloride were provided by NIDA-NIH. [^{3}H]Dopamine and [^{3}H]WIN35,428 ((−)-2-

β-carbomethoxy-3-β-(4-fluorophenyl)tropane-1,5-napthalenedisulfonate) were purchased from Perkin Elmer. Heparin was purchased from Sagent Pharmaceuticals.

Animals. Animal use and procedures were approved by the Institutional Animal Care and Use Committee at the University of Michigan and followed the guidelines put forth by the National Institutes of Health. Male Sprague Dawley rats were purchased from Envigo laboratories and were maintained on a 12-h light cycle with lights on at 0700 (or 7 am) and all experiments were performed during the light phase. For *in vitro* experiments the rats were 7-12 wks. The age of rats for microdialysis and self-administration ranged from 7 wks-10 months. During self-administration, the rats were food restricted to 80-85% of their free-feeding body weight and given free access to water.

*Synaptosome preparation***.** Rat striata were dissected on ice and homogenized in 10 volumes of homogenization buffer comprised of 0.32 M sucrose, 1 mM EDTA, cocktail of protease inhibitors (Complete Mini, Roche), pH 7.4. Homogenates were centrifuged at 3000 rpm for 10 min and the supernatant saved. The supernatant fractions were then centrifuged at 14000 rpm for 15 min. For the PKC activity experiments, the supernatants were aspirated and the pellets resuspended in Kreb's Ringer buffer (KRB) made of 145 mM NaCl, 2.7 mM KCl, 1.2 mM KH_2PO_4, 1.2 mM $CaCl_2$, 1.0 mM $MgCl_2$, 10 mM glucose, 24.9 mM $NaHCO_3$, pH 7.4. For dopamine uptake and suprafusion experiments, the pellets were resuspended in KRB that included 0.05 mM ascorbic acid and 0.05 mM pargyline.

*PKC activity assay***.** Synaptosomes were incubated in KRB at 37 °C for 15 min followed by a 1 h treatment with 0-3 μM **6c** and 500 nM ruboxistaurin (PKC inhibitor;

positive control). The final percentage of DMSO in all samples was 0.01%. PKC was activated by adding 100 nM PMA to the samples for 15 min and the reaction quenched with 1 ml cold KRB. The samples were pelleted at 3000 rpm for 3 min. The pellets were washed once in cold KRB and lysed in solubilization buffer (1% Triton X-100, 50 mM Tris HCl, 150 mM NaCl, pH 7.4). Lysates were rotated at 4 °C for 1 h and centrifuged at 14000 rpm for 15 min to remove debris. Protein assays were conducted using the Biorad DC Protein Assay Kit.

Western blotting. Samples (20 μg) were resolved on a 12% polyacrylamide gel using SDS-PAGE. The proteins were transferred onto a nitrocellulose membrane at 100 mA for 12-16 h. Membranes were incubated in blocking buffer (5% w/v milk, 150 mM NaCl, 10 mM Tris, 0.05% Tween 20) and probed with either anti-phospho- $ser^{152/156}$ MARCKS antibody (1:1000, catalogue # 2741, Cell Signaling Technology Inc, Danvers, MA), or anti-phospho-ser^{41}-GAP43 (1:1000, catalogue # sc-135697, Santa Cruz Biotechnology, Inc., Santa Cruz, CA) anti-GAPDH 14C10 (1:10000, catalogue # 2118, Cell Signaling Technology Inc, Danvers, MA) antibodies for 24 h at 4 °C. Primary phospho-MARCKS and phospho-GAP-43 antibody binding were detected using goat-anti rabbit antibody (1:2000, catalogue # sc-2054, Santa Cruz Biotechnology, Inc., Santa Cruz, CA) for 1 h at room temperature and ECL Western Blotting Substrate (catalogue #32106, ThermoFisher Scientific, Waltham, MA). Primary GAPDH antibody binding was detected using goat-anti rabbit antibody (1:20000, catalogue # sc-2054, Santa Cruz Biotechnology, Inc., Santa Cruz, CA) for 1 h at room temperature and Chemiluminescent Western Substrate (catalogue # WBKLS0500, EMD Millipore, Darmstadt, Germany). Band densities were quantified using Image J software.

[^{3}H]Dopamine uptake. Synaptosomes were treated with 0-3 μM **6c** at 37 °C for 1 h. [^{3}H]Dopamine (PerkinElmer Life Sciences) was added for 3 min and [^{3}H]dopamine uptake was terminated with 5 ml cold KRB. The samples were then rapidly filtered on Fisherbrand GF/C filters and washed with 5 ml of cold KRB twice. Non-specific uptake was determined using 100 μM cocaine. Once dried, the filters were counted in a Beckman LS 5801 liquid scintillation counter.

Biotinylation. The effect of **6c** on DAT surface levels in synaptosomes was investigated with sulfo-NHS-SS-biotin using a method previously described (Furman *et al*, 2009). Rat striatal synaptosomes were incubated with 3 μM **6c** or vehicle in KRB for at 37 °C for 1 h. Synaptosomes were washed twice with cold PBS/Ca–Mg buffer pH 7.3 (138 mM NaCl, 2.7 mM KCl, 1.5 mM K_2PO_4, 9.6 mM Na_2PO_4, 1 mM $MgCl_2$ and 0.1 mM $CaCl_2$), before treating with sulfo-NHS-SS-biotin (2.0 mg/ml) at 4 °C for 1 h in PBS/Ca–Mg. 1 M glycine was added for 15 min to quench the biotinylation reaction and then the samples were washed twice with 100 mM glycine in PBS/Ca–Mg. The synaptosomes were lysed in solubilization buffer (25 mM, Tris, 150 mM NaCl, 1 mM EDTA, 5 mM N-ethylmalemeide, and 1% triton-X 100) and protease inhibitors (Roche, Indianapolis, IN) for 1 h at 4 °C. Lysates were centrifuged at 20000 × g for 30 min at 4 °C and protein concentration determined using a Bio-Rad Dc protein assay kit. Samples (~200 μg) were incubated with streptavidin beads (50 μl) for 1 h at room temperature. The beads were washed three times with solubilization buffer and then eluted in 2X sample buffer. Proteins were resolved by 10% SDS-PAGE and immunoblotted using 1:1000 dilution MAB16, anti-DAT donated by Dr. Roxanne Vaughn, Department of

Biochemistry, University of North Dakota. Quantification of the bands was performed with Image J software.

[^{3}H]WIN35,428 Binding. Radioligand saturation binding assays were performed by incubating synaptosomes with 3 μM **6c** at 37 °C for 1 h followed by 0-200 nM of the cocaine analogue [^{3}H]WIN35,428 for 2 h at 4 °C. Five ml cold KRB was then added to samples followed by rapid filtration on Fisherbrand GF/C filters and washed twice with 5 ml of cold KRB. Non-specific binding was determined using 30 μM nomifensine.

*Suprafusion***.** Synaptosomes were loaded onto filters in chambers of a Brandel perfusion apparatus (Brandel SF-12, Gaithersburg, MD) and perfused with 0-3 μM **6c** at 37 °C for 1 h at a rate of 400 μl/min. Following this wash, 16 fractions were collected in 2 min increments in vials containing internal standard solution (final concentration 50 mM perchloric acid, 25 μM EDTA, and 10 nM 2-aminophenol). Dopamine efflux was stimulated by the addition of 10 μM AMPH from fractions 6-11. The vehicle control or **6c** was also present during collection. Dopamine was quantified using high performance liquid chromatography coupled to electrochemical detection (Thermo Scientific/ESA, Sunnyvale, CA).

Microdialysis and locomotor behavior. Probes were prepared and implanted as previously described (Zestos *et al*, 2016). Rats were anesthetized with 5% isofluorane and fixed on a stereotaxic frame. Probes were implanted bilaterally (+1.7 A/P, ±1.4 M/L, -7.5 D/V in reference to bregma) to sample from the nucleus accumbens core. Measurements attained from both probes in each rat were averaged to represent a single replicate. The perfusion flow rate through the probe for all experiments was 1 μl/min and

fractions were collected in 3 min increments. After the experiments, cannula placement was confirmed using histology.

*Acute **6c** preteatment.* After probe implantation, rats were allowed to recover and habituate to the Raturn testing chamber (Bioanalytical Systems, Inc., West Lafayette, IN) for 24 h. Immediately before the experiment, the probe was perfused with aCSF for 1 h and then baseline fractions were collected for 30 min. Next, 1 μM **6**c or saline was administered directly to the nucleus accumbens core using retrodialysis for 30 min, with fractions being collected during this time. Two mg/kg of AMPH *i.p.* was then administered and fractions collected for another 1 h.

*Detection of **6c** and AMPH.* 6 mg/kg of **6c** was given *s.c.* and the presence of the compound was monitored in accumbal dialysate from 0 to 18 h. The presence of AMPH was only monitored for 60 min.

*Simultaneous administration of 6 mg/kg of **6c** and AMPH.* After probe implantation, rats were allowed to recover and habituate to the Raturn testing chamber (Bioanalytical Systems, Inc., West Lafayette, IN) for 24 h. Immediately before the experiment, the probe was perfused with aCSF for 60 min and then baseline fractions were collected for 30 min. Then 6 mg/kg of **6c** or saline was given with 1 mg/kg of AMPH subcutaneously and fractions were collected for another hour.

*18 h 6 mg/kg of **6c** pretreatment.* After probe insertion, the rats were given 6 mg/kg of **6c** or saline subcutaneously and were placed in the Raturn testing chamber (Bioanalytical Systems, Inc., West Lafayette, IN) for 18 h. Immediately before the experiment, the probe was perfused with aCSF for 1 h and then baseline fractions were

collected for 30 min. Two mg/kg of AMPH *i.p.* was then given and fractions collected for another hour.

Sample derivatization and neurotransmitter analysis. Standards and fractions were derivatized with benzoyl chloride and analyzed on a Thermo TSQ LCMS as previously described (Zestos *et al*, 2016). In experiments monitoring the presence of **6c**, samples were not derivatized since the compound has no primary amine.

Locomotor behavior. During microdialysis, locomotor behavior was recorded using Logitech webcams (Apples, Switzerland) placed above the Raturns chambers (Bioanalytical Systems, Inc., West Lafayette, IN). Webcams were connected via USB port to analysis PC running Matlab 2009 (Mathworks, Natick, MA, USA) software. The data were collected using the image acquisition toolbox in Matlab via a custom designed motion-monitoring program (Mark Dow, University of Oregon) and quantified as previously described (Zestos *et al*, 2016).

Apparatus for self-administration. Self-administration studies were conducted in operant chambers (ENV-008CT, Med Associates, St. Albans VT) inside sound-attenuating cubicles (ENV-018V, Med Associates). Each box contained two nose poke devices with yellow lights (ENV-114BM, Med Associates Inc) on the left and right sides of the front wall and a pellet receptacle in between the nose pokes (ENV-200R7M, Med Associates Inc). The pellet receptacle was attached to a dispenser (ENV-203-45, Med Associates Inc) that delivered 45 mg sucrose pellets. A white house light was at the top of the wall opposite the nose poke devices. Drug solutions were delivered by variable infusion rate syringe pumps (PHM-107, Med Associates Inc) through Tygon tubing attached to single channel plastic swivel (375/22PS, Instech Laboratories, Plymouth

Meeting, PA) on a counterbalanced arm (PHM-110-SAI, Med Associates). Tygon tubing connected the swivel to the implanted backplate (313-000BM-15-5UP/1/SPC, Plastics One, Roanoke, VA) and was protected by a stainless steel spring. Data was collected using MED-PC software (SOF-735, Med Associates).

18 h 6 mg/kg of ***6c*** *pretreatment on AMPH self-administration.* Rats were surgically implanted with intravenous catheters in their left or right femoral vein under ketamine/xylazine anesthesia (90:10 mg/kg *i.p.*). Catheters were attached to backplates made of stainless steel tubing and polyester mesh (313-000BM-15-5UP/1/SPC, Plastics One, Roanoke, VA) that exited between the scapula. Rats recovered for a minimum of 7 days following the surgery and were flushed with 0.3 ml of heparinized-saline (50 U/ml) during recovery and before and after each self-administration session. The rats were trained to respond in the nose poke device for 0.1 mg/kg/infusion AMPH during 60 min sessions under a fixed-ratio 1 (FR1) schedule of reinforcement. One nose poke, the "active" nose poke, was illuminated with a yellow light; and the "inactive" nose poke was not illuminated and responses in this nose poke were recorded but had no scheduled consequences. Ratio completion resulted in an infusion (100 μl/kg/1 sec), turning of the nose poke light, and 1 sec illumination of the house light. All stimuli were turned off for a 10 sec period following the infusion and responses during blackout period were recorded but had no consequences. Upon acquisition of stable responding (defined as 3 consecutive sessions with less than a 20% difference in infusions earned and no increasing or decreasing trend in the number of infusions earned), the response requirement was gradually increased to FR5 and then the AMPH dose was decreased to

0.032 mg/kg/infusion. The training data depict average responses for each group at each FR schedule.

Following stable AMPH self-administration under the FR5 schedule, saline was substituted repeatedly for AMPH for 1-3 consecutive sessions until responding dropped to less than 30% of stable responding levels within a single substitution session. Once responding rapidly extinguished in the absence of AMPH, baseline AMPH responding was re-established for a minimum of 3 days prior to evaluating the effects of **6c** pretreatment on AMPH self-administration. Injections of vehicle (5% tween in saline) or 6 mg/kg of **6c** were administered subcutaneously 18 h prior to an AMPH self-administration session.

*18 h 6 mg/kg of **6c** pretreatment on food self-administration.* Food self-administration studies were carried out with a similar design to the AMPH self-administration studies but for a few differences. The rats were not implanted with intravenous catheters and the sessions lasted for 20 min. Responses on the active nose poke were reinforced with 45 mg sucrose pellets instead of AMPH. Stable responding was defined as 2-3 consecutive sessions with less than a 20% difference in food pellets earned and no increasing or decreasing trend in the number of food pellets earned. Instead of saline substitution, responding was extinguished by removing delivery of the sucrose pellets only (cues remained).

Statistics. The results were analyzed using GraphPad Prism 6 software (San Diego, CA) and are plotted as mean ± SEM. Statistical significance was determined using 2-way repeated measures (RM) ANOVA, 1-way ANOVA or a 2-tailed Students *t* test. When concentration response curves were compared, comparison of fits in non-

linear regression was used to determine whether curves differed from each other. The null hypothesis was that the best-fit parameters for the values did not differ. A conclusion of statistical significance represents a rejection of the null hypothesis and indicates a difference between designated values.

Results

***6c** inhibits PKC in synaptosomes.* Previously, we showed that **6c** inhibits PKC activity 250 times more potently than tamoxifen in the human neuroblastoma cell line SHSY5Y and displayed a K_i > 10 μM at the ERα (Carpenter *et al*, 2016). Here we examined the effect of **6c** on PKC activity in striatal synaptosomes that contain dopaminergic terminals. To do this, we determined the effect of **6c** on the phosphorylation of the PKC substrates growth associated protein-43 (GAP-43) and myristoylated alanine-rich C-kinase substrate (MARCKS) at the PKC-specific phosphorylation sites ser^{41} and $ser^{152/156}$ respectively (Heemskerk *et al*, 1993; Nielander *et al*, 1990). **6c** decreased both GAP-43 and MARCKS phosphorylation in a concentration dependent manner up to 3 μM but showed greater potency in inhibition of GAP-43 phosphorylation as compared to MARCKS (3.1B). The IC_{50} of **6c** for inhibition of PMA-stimulated $phosphoser^{41}$-GAP-43 was 30 nM [95% confidence interval (CI), 9 nM to 98 nM, n=4] while that for inhibition of $phophoser^{152/156}$-MARCKS was 189 nM [95% CI, 25 nM – 1460 nM, n=5]. A comparison of fits in Prism 6 showed the two IC_{50}s were significantly different ($F_{(2,45)}$=7.7, p<0.01).

***6c** asymmetrically blocks AMPH-stimulated dopamine efflux and uptake.* We showed that selective PKC inhibitors reduce AMPH-stimulated dopamine release *in vitro* (Kantor *et al*, 1998). Using suprafusion of striatal synaptosomes, the effect of the PKC

inhibitor **6c** on AMPH-stimulated dopamine efflux was tested. Synaptosomes were incubated with **6c** for 1 h before AMPH exposure. **6c** effectively and dose-dependently reduced dopamine efflux induced by 10 μM AMPH (Figure 3.2A). No concentration of

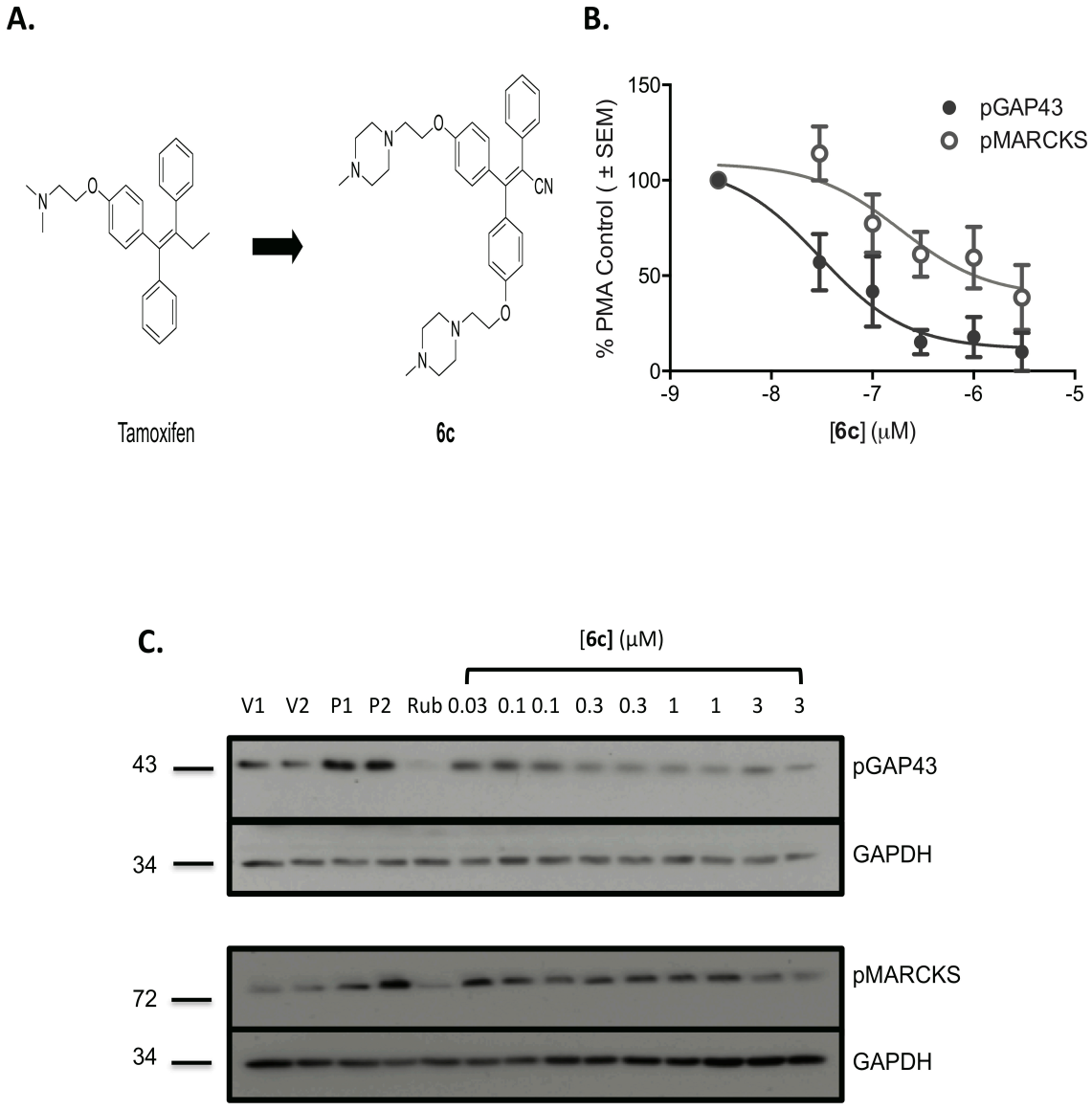

Figure 3.1. Structure of tamoxifen analogue, 6c, and its effect on PMA-induced PKC activity in synaptosomes. **A**. Structures of tamoxifen and its analogue, **6c**. **B-C**. Rat striatal synaptosomes were incubated in the presence or absence of **6c** for 1 h at 37 °C. 100 nM PMA was added for 15 min to stimulate PKC and the samples were lysed and probed for phosphoser^{41}-GAP-43 (n=4) and phosphoser$^{152/156}$-MARCKS (n=5). GAPDH served as the loading control. **B.** Data are represented as percent of vehicle optical density and each data set represents mean ± SEM. **C.** Representative western blots. V1, V2: vehicle; P1, P2: PMA control; Rub: 500 nM ruboxistaurin, a control PKC inhibitor.

6c tested affected basal dopamine release (Figure 3.3). Our group has shown that PKC inhibitors exhibit asymmetry in their effects on DAT activity, where the compounds preferentially block dopamine efflux without having significant effects on [^{3}H]dopamine uptake (Johnson *et al*, 2005; Zestos *et al*, 2016). The effect of a 1 h pretreatment of 0.3-3 μM **6c** on [^{3}H]dopamine uptake was determined in striatal synaptosomes. Only 3 μM **6c** had a significant effect on dopamine uptake, reducing [^{3}H]dopamine uptake by 60% compared to the vehicle treatment (Figure 3.2B). Calculation of the dose-dependent percent inhibition of dopamine efflux and uptake (0.35 μM and 1.60 μM respectively) demonstrates a 4.6-fold selectivity for efflux over influx (Figure 3.2C).

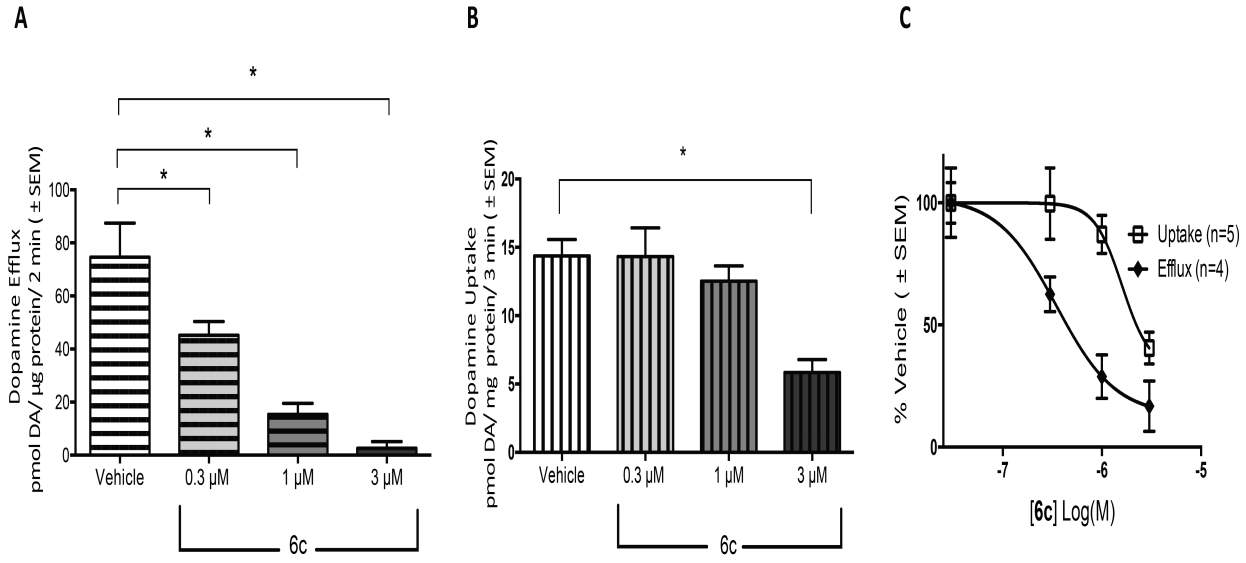

Figure 3.2. 6c modulation of DAT efflux and uptake processes.
A. Rat striatal synaptosomes were incubated in the presence or absence of **6c** for 1 h at 37 °C, efflux was stimulated with 10 μM AMPH (n=4). *Post hoc* Dunnett multiple comparison test, * $p \leq 0.05$. **B.** Synaptosomes were incubated with vehicle or **6c** for 1 h at 37 °C and [^{3}H]dopamine uptake was quantified (n=5). *Post hoc* Dunnett multiple comparison test, *$p < 0.01$. **C.** Efflux and uptake results represented as % vehicle. All points are mean ± SEM.

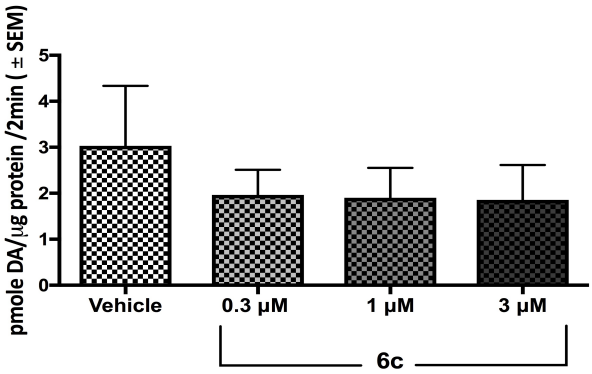

Figure 3.3. The effect of 6c on basal dopamine release in synaptosomes.
Rat striatal synaptosomes were incubated in the presence or absence of **6c** for 1 h at 37 °C and at a flow rate of 400 µl/min, six fractions were collected and basal dopamine release was quantified using HPLC coupled to electrochemical detection (n=4).

***6c** does not affect DAT trafficking and does not displace [^{3}H]WIN35,428 binding.*

Two potential explanations for the effect of **6c** on dopamine uptake or efflux are that the compound is altering surface transporter levels or that it is directly binding to DAT. After incubating rat striatal synaptosomes with 3 µM **6c** for 1 h at 37 °C, our biotinylation studies showed that the compound did not cause a change in DAT surface levels as compared to vehicle (Figure 3.4). Many dopamine uptake blockers, such as cocaine, interact with a binding site close to the substrate site and hence reduce the normal uptake functioning at DAT (Beuming *et al*, 2008). To investigate whether **6c** is directly binding at this site, we tested the ability of the compound to alter binding of the cocaine analogue [^{3}H]WIN35,428. We found that treating synaptosomes with 3 µM **6c** for 1 h at 37 °C caused no changes in the subsequent equilibrium binding of [^{3}H]WIN35,428. The K_d for [^{3}H]WIN35,428 in the absence or presence of **6c** in nM ± SEM was 77±17 and 71±19 respectively. The B_{max} for [^{3}H]WIN35,428 binding in the absence or presence of **6c** in pmol/mg protein ± SEM was 2.4±0.4 and 2.2±0.3, respectively, n=3.

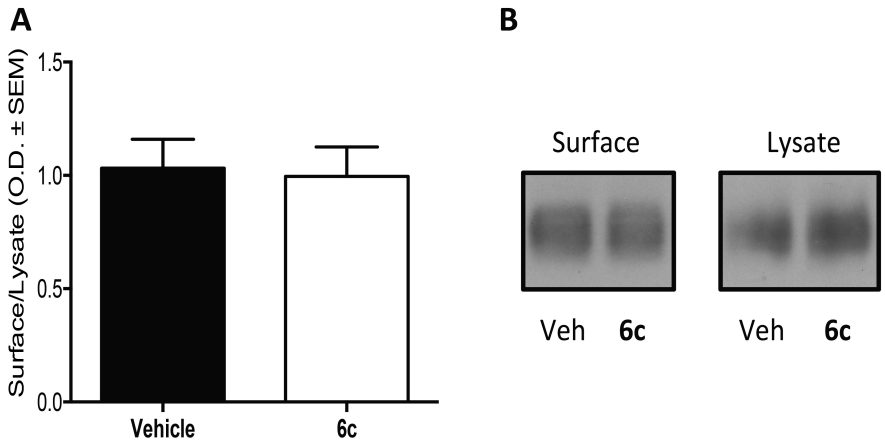

Figure 3.4. The action of 6c on DAT surface expression.
A. Rat striatal synaptosomes were incubated in the presence or absence of 3 μM **6c** for 1 h at 37 °C, followed by the biotinylation of surface DAT as previously described in Methods. **B.** Representative western blots. Data shown as mean ± SEM (n=5).

*Direct accumbal and systemic administration of **6c** decreases AMPH-stimulated dopamine overflow and locomotion.* To assess if the effect of **6c** on reduction of AMPH-stimulated dopamine efflux in synaptosomes would occur *in vivo*, we conducted a series of microdialysis experiments in which dopamine overflow and locomotor activity were measured simultaneously. In the first experiment, we collected baseline samples for 30 min, then 1 μM **6c** was perfused directly into the nucleus accumbens core 30 min prior to the peripheral administration of 2 mg/kg of AMPH. As shown in Figure 3.5A, **6c** significantly reduced AMPH-stimulated dopamine overflow in freely moving rats at a concentration that did not reduce dopamine uptake (2-way RM ANOVA, $F_{(39, 507)}$=22.42, $p<0.0001$ for time; $F_{(1, 13)}$=7.23, $p<0.05$ for drug; and $F_{(39, 507)}$=4.04, $p<0.0001$ for time-drug interaction). Similarly, as depicted in Figure 3.5B, locomotor activity in response to the injection of AMPH was significantly reduced (2-way RM ANOVA, $F_{(39, 546)}$=19.15, $p<0.0001$ for time; $F_{(1, 14)}$=4.26, $p=0.058$ for drug; and $F_{(39,546)}$=1.92, $p<0.01$ for interaction of drug and time).

Because **6c** was designed on the scaffold of the CNS-permeant drug, tamoxifen, there was some expectation that it might cross the blood-brain barrier. To test this possibility, we administered the compound systemically and checked for its presence in the nucleus accumbens using microdialysis coupled to LC-MS. 6 mg/kg of **6c** *s.c.* resulted in detectable levels of the compound in the nucleus accumbens (Figure 3.5G, 2-way RM ANOVA, $F_{(1,4)}=22.53$, $p<0.01$ for drug). The data demonstrate that **6c** peaks in the brain within 10 min and remains relatively steady at concentrations between 10 nM and 20 nM over the next hour. Estimated percent recovery through the probe was 10-15% and was used to calculate the concentration of **6c** *in vivo*.

Based upon the rapid appearance of **6c** in the brain after peripheral injection, we examined if subcutaneous administration of **6c** with AMPH would reduce the effects of AMPH on dopamine overflow and locomotion. As shown in Figure 3.5C, simultaneous subcutaneous injection of 6 mg/kg of **6c** and 1 mg/kg of AMPH resulted in a significant decrease in dopamine overflow as compared to AMPH alone (2 way RM ANOVA $F_{(29, 116)}=5.17$, $p<0.0001$ for time; $F_{(1, 4)}=16.15$, $p<0.05$ for drug; and $F_{(29, 116)}=2.85$, $p<0.0001$ for interaction of drug and time). Figure 3.5D demonstrates that administration of **6c** elicited a corresponding significant decrease in AMPH-stimulated locomotor behavior compared to AMPH alone (2 way RM ANOVA, $F_{(29, 174)}=6.45$, $p<0.0001$ for time; $F_{(1, 6)}=15.82$, $p<0.01$ for drug; and $F_{(29, 174)}=1.95$, $p<0.01$ for drug and time interaction). To rule out whether **6c** was simply reducing the amount of AMPH getting into the brain, we tested the concentrations of AMPH in the brain after **6c** was given subcutaneously with AMPH. Subcutaneous administration of **6c** with 1 mg/kg of AMPH had no effect on the

AMPH levels achieved in the nucleus accumbens when compared to rats treated with vehicle and 1 mg/kg of AMPH (Figure 3.6).

We next queried if pretreatment with **6c** had extended effects. A subcutaneous injection of 6mg/kg of **6c** was given 18 h prior to AMPH and AMPH-stimulated dopamine overflow and locomotor behavior were measured. As shown in Figure 3.5E, pretreatment with 6 mg/kg of **6c** *s.c.* 18 h prior to an injection of 2 mg/kg of AMPH *i.p.* significantly decreased AMPH-stimulated dopamine overflow (in 2-way RM ANOVA, $F_{(29, 319)}$=9.05, $p<0.0001$ for time; $F_{(1, 11)}$=5.05, $p<0.05$ for drug; and $F_{(29, 319)}$=2.87, $p<0.0001$ for drug and time interaction). Again, there was a corresponding decrease in the locomotor response to AMPH (Figure 3.5F) following **6c** pretreatment (in 2-way RM ANOVA, $F_{(29, 319)}$=7.97, $p<0.0001$ for time; $F_{(1, 11)}$=9.87, $p<0.01$ for drug; and $F_{(29, 319)}$=2.56, $p<0.0001$ for interaction of time and drug). Although higher than null value, only low picomolar levels of **6c** were detected in accumbal dialysate 18 h after *s.c.* administration (data not shown).

*Systemic **6c** reduces AMPH-self administration but not food self-administration.* Since **6c** effectively reduced AMPH neurochemical and behavioral effects *in vivo*, we next investigated whether the tamoxifen analogue could effectively reduce the reinforcing effects of AMPH in a rat model of self-administration. Rats were trained to administer AMPH *i.v.* on a FR5 schedule of reinforcement and both groups of rats in the AMPH self-administration studies demonstrated similar patterns of responding for AMPH during training (Figure 3.7A). As shown in Figure 3.7C, 18 h following *s.c.* injection of **6c**, the number of infusions of AMPH earned over a 1 h session significantly decreased compared to the vehicle-treated animals (in 2-way RM ANOVA, $F_{(2, 20)}$ =76.56, $p<0.0001$

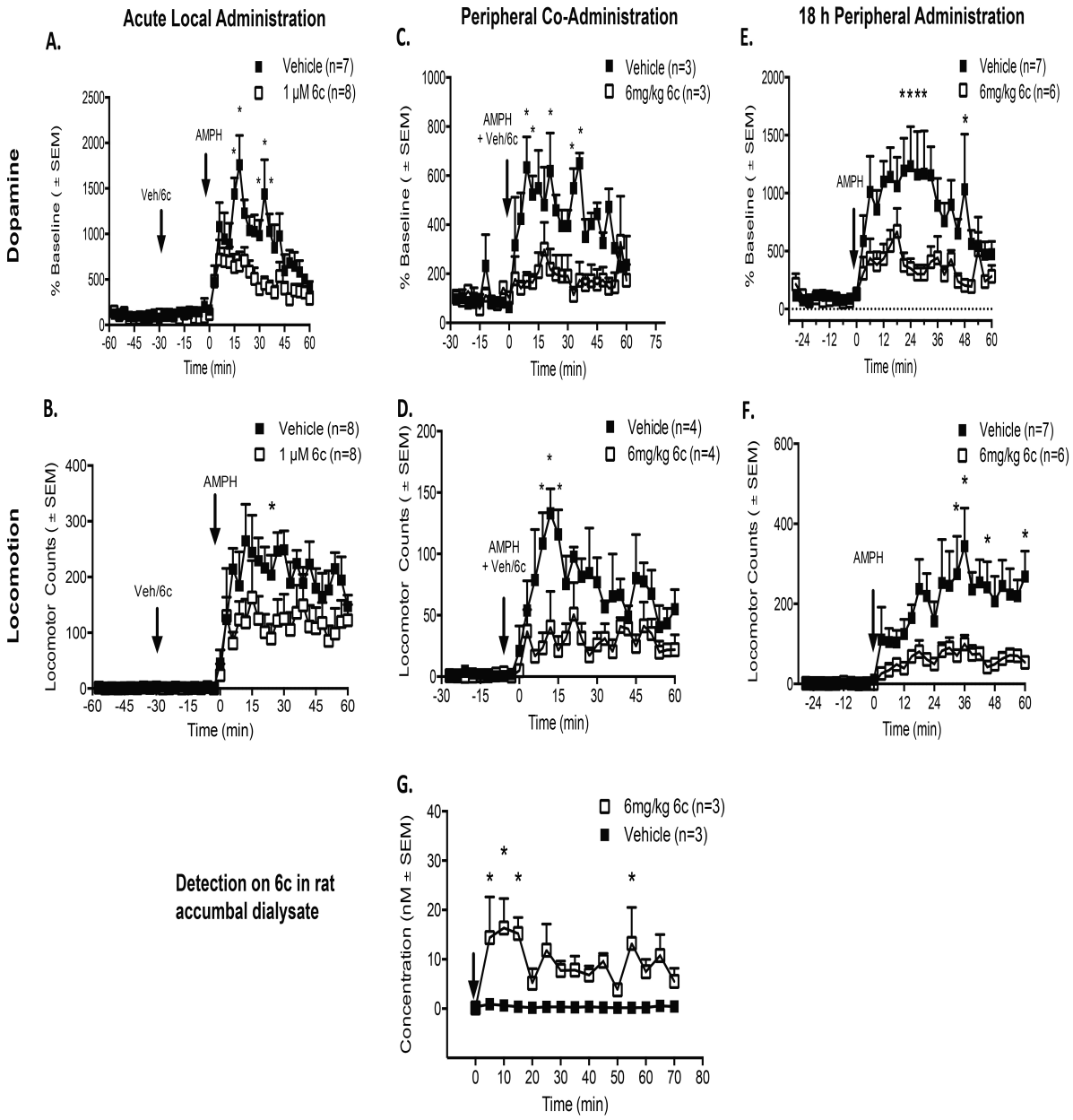

Figure 3.5. The effect of 6c on *in vivo* AMPH-induced dopamine overflow and locomotion.
A. and **B.**, 1 µM **6c** or vehicle was perfused into the nucleus accumbens using retrodialysis 30 min prior to the administration of 2 mg/kg of AMPH *i.p.* **A.** Dopamine overflow; vehicle (n=7) and **6c** (n=8). *Post hoc* Sidak's multiple comparison test, *p<0.05. **B.** Locomotion; in *post hoc* Sidak's multiple comparison test, *p<0.05; vehicle (n=8), **6c** (n=8). **C.** and **D.**, 6 mg/kg of **6c** or vehicle were given to rats *s.c.* simultaneously with 1 mg/kg of AMPH *i.p.* **C**. Dopamine overflow; *post hoc* Sidak's multiple comparison test, *p<0.05; vehicle (n=3), **6c** (n=3). **D**. Locomotor activity; *post hoc* Sidak's multiple comparison test, *p<0.01; vehicle (n = 4), **6c** (n=4). **E.** and **F.**, 6 mg/kg of **6c** or vehicle was given 18 h prior to the administration of 2 mg/kg of AMPH *i.p.*. In *post hoc* Sidak's multiple comparison test, **E**, *p<0.05 for dopamine overflow. **F**. *Post hoc* Sidak's multiple comparison test, *p<0.05 for locomotion. For dopamine and locomotor activity, vehicle (n=7) and **6c** (n=6)**. G**. 6 mg/kg of **6c** or vehicle (n=3) was administered *s.c.*, and dialysate collected from time 0 to 80 min. *Post hoc* Sidak's multiple comparison test, *p<0.05. Levels of **6c** were quantified using LC-MS and corrected for recovery.

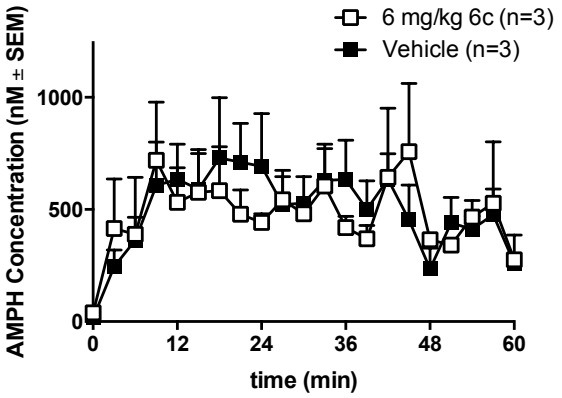

Figure 3.6. The effect of 6c on AMPH entry in the brain.
Vehicle or 6 mg/kg of **6c** were given to rats *s.c* simultaneously with 1 mg/kg of AMPH *i.p.* Using microdialysis coupled to LC-MS, the levels of AMPH were quantified from accumbal dialysate from time 0 to 60 min.

for responses; $F_{(1,10)}$=12.90, p<0.01 for drug; and $F_{(2, 20)}$ =7.25, p<0.01 for interaction of infusion and drug). In a similar procedure, rats were trained to self-administer sucrose pellets on a FR5 schedule of reinforcement in 20 min daily sessions. Again, both groups of rats in the food self-administration studies demonstrated similar patterns of responding for food pellets during training (Figure 3.7B). We found that 18 h pretreatment with 6 mg/kg of **6c** did not alter the number of active nose poke responses as compared with vehicle pretreatment (Figure 3.7D). There were no significant differences in the rats responding at the inactive nose poke for either the AMPH or food self-administration experiments (Figures 3.7E and 3.7F).

Discussion

In this paper, we report our findings on a novel tamoxifen analogue and PKC inhibitor that modulates DAT functioning. It is well known that phosphorylation serves as a major regulator of DAT expression and activity (Foster *et al*, 2006). Enhanced PKC activity results in internalization of DAT, although a direct mechanism linking DAT phosphorylation and internalization has not been elucidated (Zahniser and Doolen, 2001).

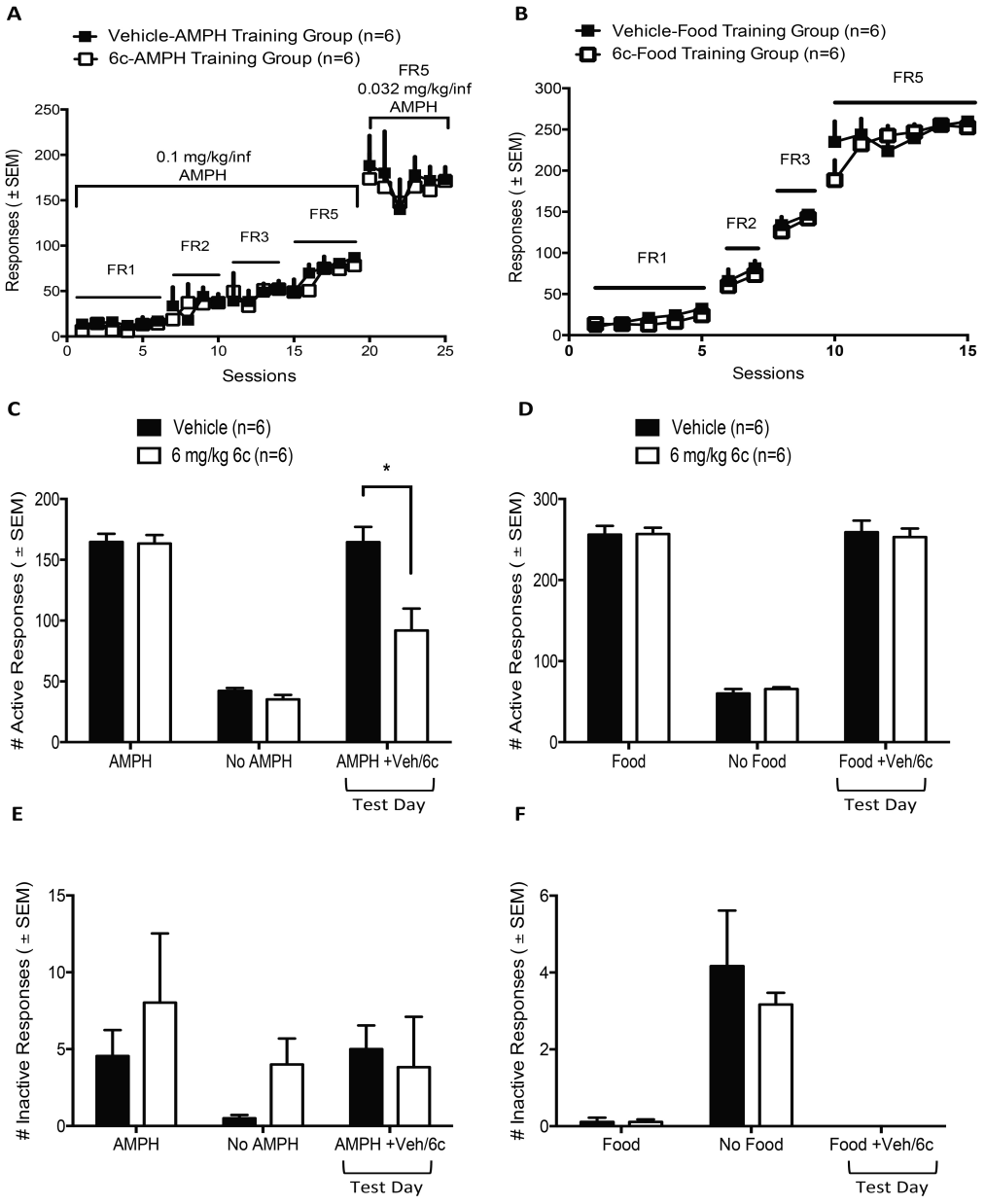

Figure 3.7. The effect of 6 mg/kg of 6c *s.c.* on AMPH and food self-administration.

A. Training data for rats used in AMPH self-administration experiments. Rats were escalated from a FR1 to a FR5 schedule with 0.1 mg/kg/infusion of AMPH. Finally rats were trained to stably administer on the FR5 schedule with 0.032 mg/kg/infusion of AMPH. **B.** Training data for rats used in food self-administration. Rats escalated from a FR1 to a FR5 schedule for food pellets. **C.** On test day, 6 mg/kg of **6c** or vehicle was given 18 h prior to AMPH self-administration session. *Post hoc* Sidak's multiple comparison test, * $p<0.0001$, a significant difference between vehicle- and **6c**-treated rats. **D.** On test day 6 mg/kg of **6c** or vehicle was given 18 h prior to food self-administration session. **E.** and **F.** Inactive nose poke responses during AMPH and food self-administration sessions respectively. All data sets are represented as mean ± SEM.

DAT contains PKC consensus sites (Foster *et al*, 2002) in its N-terminal domain and truncation of this region attenuates DAT phosphorylation induced by the PKC activator phorbol 12-myristate 13-acetate (Granas *et al*, 2003). Phosphorylation of DAT in the N-terminus has been reported to be permissive for AMPH-stimulated dopamine efflux with no effect on dopamine influx (Khoshbouei *et al*, 2004; Wang *et al*, 2016). Several reports have shown that PKC inhibitors reduce dopamine release (Kantor *et al*, 1998; Loweth *et al*, 2009; Zestos *et al*, 2016) while treatment of striatal synaptosomes with PKC activators stimulates dopamine efflux (Cowell *et al*, 2000; Opazo *et al*, 2010). We previously demonstrated that specific inhibitors of PKCβ inhibit AMPH-stimulated dopamine overflow and locomotor activity when administered directly into the core of the nucleus accumbens (Zestos *et al*, 2016).

In vitro studies

AMPH-induced dopamine efflux is central to the abuse-liability of the stimulant. Therefore we hypothesize that a CNS-permeant PKC inhibitor may be therapeutically beneficial in the treatment of AMPH abuse. Since the only CNS-permeant PKC inhibitor, tamoxifen, causes undesirable ER-mediated side effects, we used previously available SAR information to create a CNS-permeant PKC inhibitor lacking ER affinity (Carpenter *et al*, 2016). As shown in Figure 3.1B-C, **6c** reduced PMA-stimulated PKC activity in striatal synaptosomes. Moreover, the compound demonstrated selectivity for PKC substrates, in that its inhibitory activity was more potent for phospho-GAP-43 than for phospho-MARCKS. Tamoxifen acts as an allosteric inhibitor of PKC by interacting with its regulatory domain and competing with phospholipids (O'Brian *et al*, 1985). It is possible that the mechanism of action of **6c** at PKC is also at the regulatory site but

further studies must be undertaken to confirm this. An action at a regulatory subunit of PKC, similar to that of tamoxifen, could explain the differential effect on substrates.

There was also a differential potency of **6c** on the direction of dopamine transport in that **6c** more potently inhibited reverse transport of dopamine than inward transport. This observation is comparable to, but not identical to our previous studies examining the effects of PKCβ inhibitors on DAT. We and others have reported that PKC inhibitors, including specific PKCβ inhibitors, reduce AMPH-stimulated dopamine efflux but have no effect on dopamine uptake (Browman *et al*, 1998; Loweth *et al*, 2009; Zestos *et al*, 2016). The asymmetric regulation of DAT is possible because forward and reverse transport appear to be mediated by different factors (Sitte and Freissmuth, 2015). For example, the DAT ligand SoRI-20041 inhibited substrate uptake with no significant effects on efflux (Rothman *et al*, 2009; Schmitt *et al*, 2013). **6c** has different effects on DAT from the standard PKC inhibitors, however, because at higher concentrations it will inhibit dopamine uptake. This suggests that the compound might interact directly with DAT, although not at the cocaine binding site since up to 3 μM **6c** had no effect on the binding of [^{3}H]WIN35,428. Although the cocaine and dopamine binding sites on DAT overlap, they are not the same (Beuming *et al*, 2008). Therefore it is possible, albeit unlikely, that **6c** can affect substrate but not cocaine binding.

The biotinylation experiments showed that the inhibition of dopamine uptake could not be attributed to a reduction in cell-surface DAT. It is possible that the diphenyl structural motif in **6c** could partially account for its blockade of dopamine uptake because this motif also exists in atypical DAT blockers such as modafinil and benztropine which appear to bind preferentially to the inward-facing conformation of DAT (Reith *et al*,

2015; Schmitt *et al*, 2013). In addition to the well-characterized substrate site (S1), crystal structures of the bacterial leucine transporter (Zhen and Reith, 2016), the drosophila DAT and the serotonin transporter show the presence of secondary allosteric sites (S2 and S3), where compounds can bind and modify the conformation and function of DAT (Reith *et al*, 2015; Schmitt *et al*, 2013). It is possible that **6c** could occupy one of these allosteric sites. Alternatively, the effect on uptake effect could be through an as yet unidentified mediator.

In vivo studies

We previously demonstrated that direct administration of specific inhibitors of PKCβ via retrodialysis into the nucleus accumbens inhibit AMPH-stimulated dopamine overflow and locomotor activity (Zestos *et al*, 2016). This result was recapitulated with the structurally unrelated **6c**, using a concentration (1 μM) that did not disrupt inward transport in our *in vitro studies*. A notable advantage of **6c** over the other inhibitors, however, is that it can cross the blood brain barrier, like its parent compound tamoxifen. We found that giving 6 mg/kg of **6c** subcutaneously led to detectable levels of the compound in the brain within the first 5 min following administration. The maximally measured concentration of **6c** in the brain was approximately 15 nM; but it appeared biologically active even at that concentration. Simultaneous subcutaneous injection of 6 mg/kg of **6c** with 1 mg/kg of AMPH resulted in a rapid reduction in both dopamine overflow and locomotor behavior. Therefore, despite the seemingly low level, the compound was active. Also, the low concentration of **6c** in the nucleus accumbens was comparable to the IC_{50} of **6c** for inhibition of GAP-43 phosphorylation in synaptosomes (Figure 3.1B).

Our ultimate goal is to determine if **6c** would alter the reinforcing properties of AMPH. Therefore, we measured the effect of subcutaneous administration of the compound on AMPH self-administration. As previously mentioned, giving **6c** 18 h prior to AMPH significantly decreased AMPH induced-dopamine overflow and locomotion. In agreement with this, we found that administering 6 mg/kg of **6c** 18 h prior to an AMPH self-administration session significantly reduced responding on the active nose poke manipulandum as compared with vehicle pretreatment (Figure 3.7C). This finding serves as direct evidence that **6c** decreases on-going AMPH self-administration. Ultimately, we are interested in investigating how **6c** affects the inverted U-shaped dose-response curve for AMPH self-administration and whether the results obtained in this current study translate to other schedules of reinforcement, such as a progressive ratio schedule. The lack of effect of **6c** on sucrose self-administration demonstrates that the drug did not alter responding for all reinforcers and did not suppress all operant responding.

We are in the process of performing time-course studies documenting the onset and duration of the ability of **6c** to reduce the neurochemical and behavioral effects of AMPH *in vivo*. Nonetheless, it is highly interesting that 18 h after *s.c.* administration, **6c** can still produce a reduction in AMPH-stimulated dopamine overflow and locomotor activity. Our measurement of **6c** in the nucleus accumbens showed that it is still present, albeit at extremely low levels. Nothing is known of the metabolism of this compound, but it is possible that there is a long-lasting metabolite that remains active. Another explanation is that the initial action of the compound, perhaps PKC inhibition, elicits a long-term change in downstream signaling that maintains inhibition of AMPH action. A limitation to our methodology for measuring **6c** levels in the brain is that it only reflects

extracellular concentrations. It is therefore also conceivable that the long-term effects of **6c** could be due to intracellular accumulation of the compound, which we did not sample.

PKC is widely expressed in the body and is involved in a diverse collection of GPCR and growth factor-dependent cellular pathways. Therefore, there are concerns that targeting the enzyme could lead to significant, unwanted side effects. However, clinical work with PKC inhibitors proves otherwise. For instance, chronic tamoxifen administration is generally well-tolerated by women and selective PKC inhibitors have not caused severe toxicities in clinical studies (Mochly-Rosen *et al*, 2012). Recent findings suggest that PKC inhibitors would be useful in other central nervous system disorders, such as Alzheimer's disease where activating forms of PKCα support Aβ activity (Alfonso *et al*, 2016). A total block of PKC activity is likely not required for adequate treatment; if increases in PKC activity are involved in a particular pathology, reduction to normal levels could be effective. Repeated treatment with AMPH, for example, leads to an increase in striatal PKC activity in rats (Iwata *et al*, 1997). Development of inhibitors selective for specific isozymes or substrate-specific inhibitors would increase the utility of PKC inhibitors. Our data showing greater potency by **6c** for inhibition of phosphorylation of GAP-43 over that of MARCKS demonstrates that substrate selectivity is possible, especially if the drug does not act directly at the ATP-substrate binding site on the PKC isozyme. We are hopeful in the possibility of creating even more selective CNS permeant-tamoxifen analogues and also implementing tools that will allow site-specific targeting of these compounds.

Conclusion

In summary, this study presents a new CNS permeant PKC inhibitor, **6c**, which attenuated *in vitro* and *in vivo* neurochemical and behavioral effects of AMPH. Furthermore, systemic administration of **6c** significantly reduced AMPH self-administration without generally suppressing behavior. These findings further support the targeting of PKC for the treatment of AMPH abuse and also illuminate the use of tamoxifen as a scaffold to create a new generation of CNS-permeant PKC inhibitors. Additionally, **6c**, may serve as a useful tool for investigating other PKC-related brain disorders such as bipolar mania (Mochly-Rosen *et al*, 2012).

Acknowledgement

Special thanks to Bipasha Guptaroy, PhD, for helping with the biotinylation experiments, Alexander Zestos, PhD, for performing the microdialysis studies and Rachel Altshuler, for conducting the self-administration studies.

References

Alfonso SI, Callender JA, Hooli B, Antal CE, Mullin K, Sherman MA, Lesne SE, Leitges M, Newton AC, Tanzi RE, Malinow R (2016). Gain-of-function mutations in protein kinase Calpha (PKCalpha) may promote synaptic defects in Alzheimer's disease. *Science signaling* **9**(427): ra47.

Berman S, O'Neill J, Fears S, Bartzokis G, London ED (2008). Abuse of amphetamines and structural abnormalities in the brain. *Annals of the New York Academy of Sciences* **1141**: 195-220.

Beuming T, Kniazeff J, Bergmann ML, Shi L, Gracia L, Raniszewska K, Newman AH, Javitch JA, Weinstein H, Gether U, Loland CJ (2008). The binding sites for cocaine and dopamine in the dopamine transporter overlap. *Nature neuroscience* **11**(7): 780-789.

Browman KE, Kantor L, Richardson S, Badiani A, Robinson TE, Gnegy ME (1998). Injection of the protein kinase C inhibitor Ro31-8220 into the nucleus accumbens attenuates the acute response to amphetamine: tissue and behavioral studies. *Brain research* **814**(1-2): 112-119.

Carpenter C, Sorenson RJ, Jin Y, Klossowski S, Cierpicki T, Gnegy M, Showalter HD (2016). Design and synthesis of triarylacrylonitrile analogues of tamoxifen with improved binding selectivity to protein kinase C. *Bioorganic & medicinal chemistry* **24**(21): 5495-5504.

Carvalho M, Carmo H, Costa VM, Capela JP, Pontes H, Remiao F, Carvalho F, Bastos Mde L (2012). Toxicity of amphetamines: an update. *Archives of toxicology* **86**(8): 1167-1231.

Chen R, Furman CA, Zhang M, Kim MN, Gereau RW, Leitges M, Gnegy ME (2009). Protein kinase Cβ is a critical regulator of dopamine transporter. *The Journal of pharmacology and experimental therapeutics* **328**(3): 912-920.

Chiueh CC, Moore KE (1975). D-amphetamine-induced release of "newly synthesized" and "stored" dopamine from the caudate nucleus in vivo. *The Journal of pharmacology and experimental therapeutics* **192**(3): 642-653.

Cowell RM, Kantor L, Hewlett GH, Frey KA, Gnegy ME (2000). Dopamine transporter antagonists block phorbol ester-induced dopamine release and dopamine transporter phosphorylation in striatal synaptosomes. *European journal of pharmacology* **389**(1): 59-65.

de Medina P, Favre G, Poirot M (2004). Multiple targeting by the antitumor drug tamoxifen: a structure-activity study. *Current medicinal chemistry Anti-cancer agents* **4**(6): 491-508.

Di Chiara G, Imperato A (1988). Drugs abused by humans preferentially increase synaptic dopamine concentrations in the mesolimbic system of freely moving rats. *Proceedings of the National Academy of Sciences of the United States of America* **85**(14): 5274-5278.

Fisher B, Costantino JP, Wickerham DL, Redmond CK, Kavanah M, Cronin WM, Vogel V, Robidoux A, Dimitrov N, Atkins J, Daly M, Wieand S, Tan-Chiu E, Ford L, Wolmark N, Breast oNSA, Investigators BP (1998). Tamoxifen for prevention of breast cancer: Report of the national surgical adjuvant breast and bowel project P-1 study. *Journal of the National Cancer Institute* **90**(18): 1371-1388.

Foster JD, Cervinski MA, Gorentla BK, Vaughan RA (2006). Regulation of the dopamine transporter by phosphorylation. In: Sitte HH, Freissmuth M (eds). *Neurotransmitter Transporters*. Springer Berlin Heidelberg: Berlin, Heidelberg, pp 197-214.

Foster JD, Pananusorn B, Vaughan RA (2002). Dopamine transporters are phosphorylated on N-terminal serines in rat striatum. *The Journal of biological chemistry* **277**(28): 25178-25186.

Furman CA, Chen R, Guptaroy B, Zhang M, Holz RW, Gnegy M (2009). Dopamine and amphetamine rapidly increase dopamine transporter trafficking to the surface: live cell imaging using total internal reflection fluorescence microscopy. *The Journal of neuroscience : the official journal of the Society for Neuroscience* **29**(10): 3328-3336.

Giambalvo CT (1992). Protein kinase C and dopamine transport--1. Effects of amphetamine in vivo. *Neuropharmacology* **31**(12): 1201-1210.

Giambalvo CT (2004). Mechanisms underlying the effects of amphetamine on particulate PKC activity. *Synapse (New York, NY)* **51**(2): 128-139.

Gradishar WJ (2004). Tamoxifen--what next? *The oncologist* **9**(4): 378-384.

Granas C, Ferrer J, Loland CJ, Javitch JA, Gether U (2003). N-terminal truncation of the dopamine transporter abolishes phorbol ester- and substance P receptor-stimulated phosphorylation without impairing transporter internalization. *The Journal of biological chemistry* **278**(7): 4990-5000.

Gundimeda U, Chen ZH, Gopalakrishna R (1996). Tamoxifen modulates protein kinase C via oxidative stress in estrogen receptor-negative breast cancer cells. *The Journal of biological chemistry* **271**(23): 13504-13514.

Heemskerk FM, Chen HC, Huang FL (1993). Protein kinase C phosphorylates Ser152, Ser156 and Ser163 but not Ser160 of MARCKS in rat brain. *Biochemical and biophysical research communications* **190**(1): 236-241.

Horgan K, Cooke E, Hallett MB, Mansel RE (1986). Inhibition of protein kinase C mediated signal transduction by tamoxifen. *Biochemical pharmacology* **35**(24): 4463-4465.

Iwata SI, Hewlett GH, Ferrell ST, Kantor L, Gnegy ME (1997). Enhanced dopamine release and phosphorylation of synapsin I and neuromodulin in striatal synaptosomes after repeated amphetamine. *The Journal of pharmacology and experimental therapeutics* **283**(3): 1445-1452.

Johnson LA, Guptaroy B, Lund D, Shamban S, Gnegy ME (2005). Regulation of amphetamine-stimulated dopamine efflux by protein kinase C beta. *The Journal of biological chemistry* **280**(12): 10914-10919.

Jordan VC (2003). Tamoxifen: a most unlikely pioneering medicine. *Nature reviews Drug discovery* **2**(3): 205-213.

Kantor L, Gnegy ME (1998). Protein kinase C inhibitors block amphetamine-mediated dopamine release in rat striatal slices. *The Journal of pharmacology and experimental therapeutics* **284**(2): 592-598.

Khoshbouei H, Sen N, Guptaroy B, Johnson LA, Lund D, Gnegy ME, Galli A, Javitch JA (2004). N-terminal phosphorylation of the dopamine transporter is required for amphetamine-induced efflux. *PLoS Biology* **2**(3).

Kulkarni J, Garland KA, Scaffidi A, Headey B, Anderson R, de Castella A, Fitzgerald P, Davis SR (2006). A pilot study of hormone modulation as a new treatment for mania in women with bipolar affective disorder. *Psychoneuroendocrinology* **31**(4): 543-547.

Lien EA, Wester K, Lønning PE, Solheim E, Ueland PM (1991). Distribution of tamoxifen and metabolites into brain tissue and brain metastases in breast cancer patients. *British Journal of Cancer* **63**(4): 641-645.

Loweth JA, Svoboda R, Austin JD, Guillory AM, Vezina P (2009). The PKC inhibitor Ro31-8220 blocks acute amphetamine-induced dopamine overflow in the nucleus accumbens. *Neuroscience letters* **455**(2): 88-92.

McMillen BA (1983). CNS stimulants: two distinct mechanisms of action for amphetamine-like drugs. *Trends in pharmacological sciences* **4**: 429-432.

Mochly-Rosen D, Das K, Grimes KV (2012). Protein kinase C, an elusive therapeutic target? *Nature reviews Drug discovery* **11**(12): 937-957.

Nielander HB, Schrama LH, van Rozen AJ, Kasperaitis M, Oestreicher AB, Gispen WH, Schotman P (1990). Mutation of serine 41 in the neuron-specific protein B-50 (GAP-43) prohibits phosphorylation by protein kinase C. *Journal of neurochemistry* **55**(4): 1442-1445.

O'Brian CA, Liskamp RM, Solomon DH, Weinstein IB (1985). Inhibition of protein kinase C by tamoxifen. *Cancer research* **45**(6): 2462-2465.

Opazo F, Schulz JB, Falkenburger BH (2010). PKC links Gq-coupled receptors to DAT-mediated dopamine release. *Journal of neurochemistry* **114**(2): 587-596.

Parker EM, Cubeddu LX (1986). Effects of d-amphetamine and dopamine synthesis inhibitors on dopamine and acetylcholine neurotransmission in the striatum. I. Release in the absence of vesicular transmitter stores. *The Journal of pharmacology and experimental therapeutics* **237**(1): 179-192.

Reith ME, Blough BE, Hong WC, Jones KT, Schmitt KC, Baumann MH, Partilla JS, Rothman RB, Katz JL (2015). Behavioral, biological, and chemical perspectives on atypical agents targeting the dopamine transporter. *Drug and alcohol dependence* **147**: 1-19.

Rothman RB, Dersch CM, Ananthan S, Partilla JS (2009). Studies of the biogenic amine transporters. 13. Identification of "agonist" and "antagonist" allosteric modulators of amphetamine-induced dopamine release. *The Journal of pharmacology and experimental therapeutics* **329**(2): 718-728.

Schmitt KC, Rothman RB, Reith ME (2013). Nonclassical pharmacology of the dopamine transporter: atypical inhibitors, allosteric modulators, and partial substrates. *The Journal of pharmacology and experimental therapeutics* **346**(1): 2-10.

Sitte HH, Freissmuth M (2015). Amphetamines, new psychoactive drugs and the monoamine transporter cycle. *Trends in pharmacological sciences* **36**(1): 41-50.

Su HD, Mazzei GJ, Vogler WR, Kuo JF (1985). Effect of tamoxifen, a nonsteroidal antiestrogen, on phospholipid/calcium-dependent protein kinase and phosphorylation of its endogenous substrate proteins from the rat brain and ovary. *Biochemical pharmacology* **34**(20): 3649-3653.

Wang HY, Friedman E (1996). Enhanced protein kinase C activity and translocation in bipolar affective disorder brains. *Biological psychiatry* **40**(7): 568-575.

Wang Q, Bubula N, Brown J, Wang Y, Kondev V, Vezina P (2016). PKC phosphorylates residues in the N-terminal of the DA transporter to regulate amphetamine-induced DA efflux. *Neuroscience letters* **622**: 78-82.

Wise RA, Bozarth MA (1985). Brain mechanisms of drug reward and euphoria. *Psychiatric medicine* **3**(4): 445-460.

Zahniser NR, Doolen S (2001). Chronic and acute regulation of Na+/Cl- -dependent neurotransmitter transporters: drugs, substrates, presynaptic receptors, and signaling systems. *Pharmacology & therapeutics* **92**(1): 21-55.

Zarate CA, Jr., Singh JB, Carlson PJ, Quiroz J, Jolkovsky L, Luckenbaugh DA, Manji HK (2007). Efficacy of a protein kinase C inhibitor (tamoxifen) in the treatment of acute mania: a pilot study. *Bipolar disorders* **9**(6): 561-570.

Zarate CA, Manji HK (2009). Protein Kinase C Inhibitors: Rationale for Use and Potential in the Treatment of Bipolar Disorder. *CNS drugs* **23**(7): 569-582.

Zestos AG, Mikelman SR, Kennedy RT, Gnegy ME (2016). PKCβ inhibitors attenuate amphetamine-stimulated dopamine efflux. *ACS Chemical Neuroscience* **7**(6): 757-766.

Zhen J, Reith ME (2016). Impact of disruption of secondary binding site S2 on dopamine transporter function. *Journal of neurochemistry* **138**(5): 694-699.

Zhu J, Reith MEA (2008). Role of dopamine transporter in the action of psychostimulants, nicotine, and other drugs of abuse. *CNS & neurological disorders drug targets* **7**(5): 393-409.

Chapter 4. Mechanistic characterization of tamoxifen analogue, 6c

Abstract

There is growing interest surrounding the creation of selective CNS-permeant protein kinase inhibitors for use as treatments for neurological and psychiatric disorders. Protein kinase C (PKC) inhibitors could be useful to treat amphetamine (AMPH) use disorder and the manic phase of bipolar disorder. Tamoxifen still remains the only available and validated blood-brain barrier permeable PKC inhibitor. However, in addition to being a selective estrogen receptor modulator, it has numerous other targets. In hopes of creating a more selective CNS permeant PKC inhibitor, we revisited the tamoxifen scaffold and generated a brain-permeant tamoxifen analogue, **6c**. We previously showed that **6c** more potently inhibits PKC activity than tamoxifen *in vitro* and reduces AMPH action at the dopamine transporter (DAT). In this study, we expand on the profile of **6c** by investigating the mechanism by which it inhibits PKC, its *in vivo* activity and its selectivity for PKC. Our results indicate that **6c** does not disrupt PKCβ translocation but may instead alter PKCβ conformational changes. Importantly, we next prove that peripheral administration of **6c** inhibits PKC activity *in vivo*. **6c** does not inhibit $Ca^{2+/}$calmodulin-dependent protein kinase II and protein kinase B *in vitro*, enzymes structurally related to PKC. Finally, our data show that synaptosomal preparations are a better system for predicting *in vivo* effects of **6c** at the dopamine transporter as compared to heterologous cell-based assays. This points to the importance

of choosing appropriate models for initial screening studies when evaluating the effects of compounds, such as tamoxifen analogues, on DAT functioning.

Introduction

There is mounting evidence from *in vitro* and *in vivo* animal studies highlighting the therapeutic potential of CNS-permeant PKC inhibitors in treating neurological and psychiatric diseases, including Parkinson's disease and AMPH abuse (Aujla and Beninger, 2003; Burguillos *et al*, 2011; Mochly-Rosen *et al*, 2012; Zestos *et al*, 2016; Zhang *et al*, 2007). In addition to the selective estrogen receptor modulator (SERM), tamoxifen, other PKC inhibitors have been proposed to be CNS permeant. The naturally occurring alkaloid, chelerythrine, has been repeatedly reported as a potent CNS-permeant PKC inhibitor with an IC_{50} of ~660 nM (Herbert *et al*, 1990). However, numerous studies have shown chelerythrine lacks inhibitory effects at PKC in enzyme-purified and cell-based assays, and may even have PKC stimulatory effects (Davies *et al*, 2000; Gould *et al*, 2011; Lee *et al*, 1998). The fungi derived compound, calphostin C, is another known potent PKC inhibitor (IC_{50}; 50 nM (Tamaoki, 1991)),with possible CNS-penetrant properties. For instance, peripheral administration of the compound can affect CNS-related processes, such as reversing tolerance to morphine-induced respiratory depression in mice and reducing morphine withdrawal-induced enhancement of the rat hypothalamus-pituitary-adrenal axis (Cerezo *et al*, 2002; Withey *et al*, 2017). Nonetheless, no thorough investigation documenting the presence and distribution of calphostin C in the brain has been performed.

Tamoxifen therefore remains the only known pharmacokinetically-characterized PKC inhibitor that readily crosses the blood-brain barrier (Lien *et al*, 1991a; Lien *et al*,

1991b). However, tamoxifen is a relatively promiscuous compound, hitting multiple targets such as the estrogen receptor (ER) and calmodulin-dependent enzymes (de Medina *et al*, 2004). In an effort to address this need for selective brain-permeant PKC inhibitors, specifically for treatments for AMPH abuse and addiction, we revisited the tamoxifen scaffold to create a new generation of CNS permeant PKC inhibitors. Through this study we found an attractive drug candidate, **6c**, which possesses significantly improved PKC inhibitory action and shows no appreciable binding at the ER *in vitro* (Carpenter et al, 2016). In this current study, we further investigate the mechanism of action and selectivity of **6c**.

The PKC family of enzymes is divided into three subfamilies based on their mode of activation: the classical or conventional (α, βI, βII, γ) isoforms, the novel (δ, ε, θ, η) isoforms and the atypical (ζ, λ/ι) isoforms (Wu-Zhang and Newton, 2013). Tamoxifen has been shown to inhibit classical PKC isoforms (Bignon *et al*, 1991; O'Brian *et al*, 1985, 1986). Activation of classical PKCs is facilitated by an increase of intracellular calcium and diacylglycerol levels upon cell stimulation. Specifically, cytosolic calcium binds to the C2 domain on PKC and increases the affinity of the enzyme for the negatively-charged membrane lipids (Bazzi and Nelsestuen, 1987). This leads to the translocation of PKC to the membrane. Once at the membrane, PKC interacts with diacylglycerol at its C1 domain, which releases its auto-inhibitory pseudosubstrate domain and exposes the active site of the enzyme (Colón-González and Kazanietz, 2006; Dutil and Newton, 2000).

Many consider PKC translocation to the membrane as the hallmark of PKC activation. However, events such as the accumulation of PKC at a perinuclear site, also

termed the pericentron, have complicated this simplistic model (Becker and Hannun, 2003; Idkowiak-Baldys *et al*, 2006). Additionally, PKCα forms dimers *in vitro* and this may serve as an important step in the regulation of its activation (Swanson *et al*, 2014). Although many PKC inhibitors inhibit PKC translocation, restricting analysis to only this single marker of activation can be misleading. We therefore began our investigation into the direct effects of **6c** on PKC by monitoring its action on both PKCβ translocation and conformational states using fluorescence resonance energy transfer (FRET) experiments.

The addictive properties of AMPH are linked to its ability to significantly increase dopamine release via the dopamine transporter (DAT) in the brain (Di Chiara and Imperato, 1988; Wise and Bozarth, 1985). In addition to PKC, there are other serine/threonine kinases that regulate DAT activity, notably $Ca^{2+/}$calmodulin-dependent protein kinase II (CAMKII) and protein kinase B (AKT). Inhibition of CAMKII and AKT impairs the ability of AMPH to induce dopamine efflux *in vitro* (Speed *et al*, 2011; Steinkellner *et al*, 2014; Steinkellner *et al*, 2012). AKT is a member of the AGC kinase superfamily, to which PKC belongs, and therefore these two enzymes share a high degree of homology (Pearce *et al*, 2010). With this in mind, and in consideration of the fact that tamoxifen inhibits calmodulin-dependent enzymes, we investigated the possibility that the ability of **6c** to reduce AMPH effects *in vivo* could be mediated through AKT and or CAMKII.

Our previous results demonstrated that **6c** could enter the brain, but upon peripheral administration of 6 mg/kg of **6c** only low nM concentrations were measured in the nucleus accumbens (Carpenter *et al*, 2017). We now endeavor to prove that **6c,** even at low concentrations, will inhibit PKC activity *in vivo*. We also hope to revisit the

tamoxifen scaffold to create **6c** analogues with improved CNS permeability. Rapid cell-based assays are usually used to screen compounds. However, this approach may not work in all cases, especially for drugs that are active in the CNS. The data presented in this chapter lead us to conclude that synaptosomal-based *in vitro* assays are more appropriate than cellular assays for future studies evaluating the potential of these tamoxifen analogues to modulate DAT and attenuate AMPH reinforcement.

Materials and methods

Compounds. **6c** (6c•2.5 HCl) was synthesized and provided by the Vahlteich Medicinal Chemistry Core at the University of Michigan (Carpenter *et al*, 2016). Dopamine, ionomycin, 4-hydroxytamoxifen (4-OH) and phorbol-12-myristate-13-acetate (PMA) were purchased from Sigma-Aldrich. Cocaine hydrochloride was provided by NIDA-NIH. [^{3}H]Dopamine was purchased from Perkin Elmer.

Cell culture: Chinese hamster ovary (HEK)-293 cell line. CHO Flp-in cells stably expressing mCerulean (mCer)-PKCβ-mCitrine (mCit)-FLAG were generated and maintained as previously described (Swanson *et al*, 2014). Briefly, cells were cultured in DMEM supplemented with FBS (10%), 4.5 g/liter D-glucose, glutamax (1%), 20 mM HEPES, pH 7.5, and antibiotic-antimycotic (1%) at 37 °C and 5% CO_2. Cells were trypsinized and seeded at 100,000 cells on 35 mm plates (MatTek Corporation) coated with 1 μg fibronectin for at least two hours prior to each experiment.

Live cell imaging experiments. The plate was washed twice with 2 ml of 0.2% dextrose in HEPES-buffered saline followed by the addition of 500 μl of 10 μM **6c**, 10 μM 4-OH or vehicle in this buffer. Cells were incubated at 37 °C for 30 min and then placed on microscope platform for imaging. Imaging was done on a Nikon TiE

microscope fitted with an Evolve 512 x 512 EM-CCD camera (Photometrics), a mercury arc lamp, and the appropriate band pass filters. FRET signal from the mCerulean and mCitrine were acquired at the same time using a Dual-View filter (Photometrics). 1 μM PMA (PKC activator) with 10 μM **6c**, 10 μM 4-OH or vehicle was then added to respective plates and excitation coupled to image acquisition occurred for 200–500 ms every 30 sec for 10 min (600 sec). A subset of plates pretreated with vehicle was treated with buffer to provide a no PMA control. Images were taken from the basolateral membrane and FRET analysis was performed as previously described (Swanson *et al*, 2014) using custom software in Mathlab (Mathworks Incorporated). FRET ratios represent the individual pixel-by-pixel ratio between mCitrine and mCerulean intensities averaged for all pixels in a cell. We observed that when acquiring images focused on the basolateral surface of the cell, PKC membrane recruitment results in an averaging of fluorescent signal throughout the cell. To quantify PKCβ translocation, areas of high contrast were manually chosen (cytosol and nucleus). A line was drawn between these areas and the average of the lowest pixels and the highest pixels were attained for that line for each image and that difference is reported as the translocation ratio.

Animals. Animal use and procedures were approved by the Institutional Animal Care and Use Committee at the University of Michigan and followed the guidelines put forth by the National Institutes of Health. Male Sprague Dawley rats were purchased from Envigo laboratories and were used at 7-12 wks old. All animals were maintained on a 12-h light cycle with lights on at 0700 (or 7 am), with experiments performed during the light phase.

In vivo PKC activity assay. Rats were administered 1 mg/kg of AMPH with 6 mg/kg of **6c** or vehicle *s.c.*, and then sacrificed 10 min or 30 min post-injection. The ventral and dorsal striatum were quickly dissected from each animal on ice and promptly frozen in liquid nitrogen. After at least 5 min in the liquid nitrogen, 250 µl hot 1% SDS was added to the ventral and dorsal striatal samples. All samples were sonicated on a Fisher ultrasonic processor at 50% maximum amplitude with alternating 1 sec on, 1 sec off, for a total of four pulses (Fisher ultrasonic processor, ThermoFisher Scientific, Waltham, MA). The homogenate was centrifuged at 14000 rpm for 10 min and the supernatant was probed for GAP-43 phosphorylation using western blotting.

*Synaptosome preparation***.** Rat striata were dissected on ice and homogenized in 10 volumes of homogenization buffer comprised of 0.32 M sucrose, 1 mM EDTA, and a cocktail of protease inhibitors (Complete Mini, Roche), pH 7.4. Homogenates were centrifuged at 3000 rpm for 10 min and the supernatant saved. The supernatant fractions were then centrifuged at 14000 rpm for 15 min. For the AKT and CAMKII activity experiments, the pellets were resuspended in Kreb's Ringer buffer (KRB) made of 145 mM NaCl, 2.7 mM KCl, 1.2 mM KH_2PO_4, 1.2 mM $CaCl_2$, 1.0 mM $MgCl_2$, 10 mM glucose, 24.9 mM $NaHCO_3$, pH 7.4. For dopamine uptake and suprafusion experiments, the pellets were resuspended in KRB that included 0.05 mM ascorbic acid and 0.05 mM pargyline.

CAMKII activity assay. Rat striatal synaptosomes were incubated in KRB at 37 °C for 15 min followed by a 1 h treatment with 0-3 µM **6c**. The final percentage of DMSO in all samples was 0.01%. CAMKII was activated by adding 2 µM ionomycin to the samples for 5 min and the reaction quenched with 1 ml cold KRB. The samples were

pelleted at 3000 rpm for 3 min. The pellets were washed twice in cold KRB and lysed in solubilization buffer (1% Triton X-100, 50 mM Tris HCl, 150 mM NaCl, pH 7.4). Lysates were rotated at 4 °C for 1 h and centrifuged at 14000 rpm for 15 min to remove debris. Protein assays were conducted using the Biorad DC Protein Assay Kit. Samples were probed for CAMKII phosphorylation using western blotting.

AKT activity assay. Rat striatal synaptosomes were incubated in KRB at 37 °C for 15 min followed by a 1 h treatment with 0-3 μM **6c** and 10 μM enzastaurin (AKT inhibitor, positive control). The final percentage of DMSO in all samples was 0.01%. The reaction was quenched with 1 ml cold KRB and the samples were pelleted at 3000 rpm for 3 min. The pellets were washed twice in cold KRB and lysed in solubilization buffer (1% Triton X-100, 50 mM Tris HCl, 150 mM NaCl, pH 7.4). Lysates were rotated at 4 °C for 1 h and centrifuged at 14000 rpm for 15 min to remove debris. Protein assays were conducted using the Biorad DC Protein Assay Kit. Samples were probed for AKT phosphorylation using western blotting.

Western blotting. Samples (75 μg for PKC assay; 20-25 μg for AKT/CAMKII assay) were resolved on a 12% polyacrylamide gel using SDS-PAGE. The proteins were transferred onto a nitrocellulose membrane at 100 mA for 12-16 h (PKC assay) or 100 V for 90 min (AKT and CAMKII assay) and the membranes were incubated in blocking buffer (5% w/v milk, 150 mM NaCl, 10 mM Tris, 0.05% Tween 20). The antibodies used for protein detection are as follows:

In vivo PKC activity assay. Membranes were probed with anti-phospho-ser[41]-GAP43 (1:500, catalogue # sc-135697, Santa Cruz Biotechnology, Inc., Santa Cruz, CA) and anti-GAP-43 (1:1000, catalogue # sc7457, Santa Cruz Biotechnology, Inc., Santa

Cruz, CA) antibodies for 24 h at 4 °C. Primary phospho-GAP-43 antibody was detected using goat-anti rabbit antibody (1:2000, catalogue # sc-2054, Santa Cruz Biotechnology, Inc., Santa Cruz, CA) for 1 h at room temperature and Chemiluminescent Western Substrate (catalogue # WBKLS0500, EMD Millipore, Darmstadt, Germany).

AKT activity assay. Membranes were probed with anti-AKT (1:1000, catalogue # 9272, Cell Signaling Inc, Danvers, MA) and anti-phospho-ser473-AKT (1:1000, catalogue # 4060S, Cell Signaling Inc, Danvers, MA) antibodies for 24 h at 4 °C. Primary AKT and phospho-AKT were detected using goat-anti rabbit antibody (1:2000, catalogue # sc-2054, Santa Cruz Biotechnology, Inc., Santa Cruz, CA) for 1 h at room temperature followed by ECL Western Blotting Substrate and Chemiluminescent Western Substrate respectively.

CAMKII activity assay. Membranes were probed with anti-pan-CAMKII (1:1000, catalogue # 4436S, Cell Signaling Inc, Danvers, MA) and anti-phospho-thr286-CAMKII (1:1000, catalogue # 12716S, Cell Signaling Inc, Danvers, MA) antibodies for 24 h at 4 °C. Primary CAMKII and phospho-CAMKII were detected using goat-anti rabbit antibody (1:2000, catalogue # sc-2054, Santa Cruz Biotechnology, Inc., Santa Cruz, CA) for 1 h at room temperature followed by ECL Western Blotting Substrate and Chemiluminescent Western Substrate respectively. Band densities were quantified using Image J software.

Cell culture: human embryonic kidney (HEK)-293 cell line. HEK cells stably expressing rat DAT (HEK rDAT) were cultured in high glucose Dulbecco's modified Eagle's medium supplemented with fetal bovine serum (10%), penicillin (1%) at 37 °C and 5% CO_2. Cells were trypsinized one day prior to experiments and seeded on 24-well

plates at 125,000 cells per well to achieve 80-90% confluence the next day (experiment day).

[^{3}H]Dopamine uptake in cells. HEK rDAT were treated with 0-10 μM **6c** in Kreb's Ringer Hepes buffer (25 mM HEPES, 125 mM NaCl, 4.8 mM KCl, 1.2 mM KH_2PO_4, 1.3 mM $CaCl_2$, 1.2 mM $MgSO_4$, 5.6 mM glucose, 50 μM pargyline, and 50 μM ascorbic acid, pH 7.4) at 25 °C for 1 h. [^{3}H]Dopamine (PerkinElmer Life Sciences) was added for 3 min and uptake was terminated by aspirating the hot solution followed by three quick washes with approximately 2 ml cold KRH. Cells were lysed in 1% triton X solution and samples were counted in a Beckman LS 5801 liquid scintillation counter. Non-specific uptake was determined using 100 μM cocaine.

[^{3}H]Dopamine efflux in cells. Cells were plated on a 24-well plate at 100,000 cells/well 24 h prior to the experiments. Following three washes with KRH, [^{3}H]dopamine was added to each well and incubated at 37 °C for 20 min. Cells were again washed three times with KRH followed by the addition of vehicle or 0-3 μM **6c** in KRH and incubation for 1 h at 37 °C. A steady basal efflux was achieved by removing and replacing these solutions every 10 min for a total of 50 min. The counts from the final fraction was set as the baseline. Ten micromolar AMPH was added to each well and three fractions were obtained by collecting and replacing the solution in the wells every 10 min. 1% SDS was added to each well to lyse the cells and the lysate counted to quantify total remaining [^{3}H]dopamine. Dopamine efflux was calculated by normalizing the amount of dopamine released during the efflux fractions to the total dopamine content in the cells.

Statistics. The results were analyzed using GraphPad Prism 6 software (San Diego, CA) and are plotted as mean ± SEM. Statistical significance was determined using 2-way repeated measures ANOVA or a 2-tailed Students *t* test.

Results

***6c** modulates conformational states of PKCβ but not its translocation*. Although PKC translocation is considered the hallmark for PKC activation, inhibition of PKC can be achieved *via* other mechanisms. In a study performed by Gundimeda and colleagues (Gundimeda *et al*, 1996), incubation with tamoxifen and 4-hydroxytamoxifen initially induced PKC translocation but ultimately downregulated the enzyme. To get a more holistic picture of the direct effects of **6c** on PKC, we monitored the effect of the compound on both PKC translocation and conformational changes. Using a mammalian cell line stably expressing PKCβ containing an N-terminal mCerulean and C-terminal mCitrine, we concomitantly monitored subcellular localization as well as FRET between the fluorophores fused to PKCβ. In this cell line FRET is an indicator of both conformational and oligomeric states of PKCβ. By monitoring FRET we can assess if compounds directly influence PKCβ structurally, although we cannot assess the nature of those structural changes. A 30 min pretreatment of CHO cells with 10 μM **6c** did not alter PMA-stimulated PKCβ translocation but did elicit significantly lower FRET levels (FRET: In 2-way RM ANOVA, $F_{(120, 4200)}$ =3.85, $p<0.0001$ for time; $F_{(1, 35)}$=8.64, $p<0.01$ for drug; and $F_{(120, 4200)}$ =3.45, $p<0.0001$ for interaction of time and drug, Figure 1B). The change in FRET levels indicates that compound **6c** is directly influencing PKCβ function. 4-hydroxytamoxifen was employed as a positive control and inhibited both PMA-induced PKCβ translocation and FRET increases.

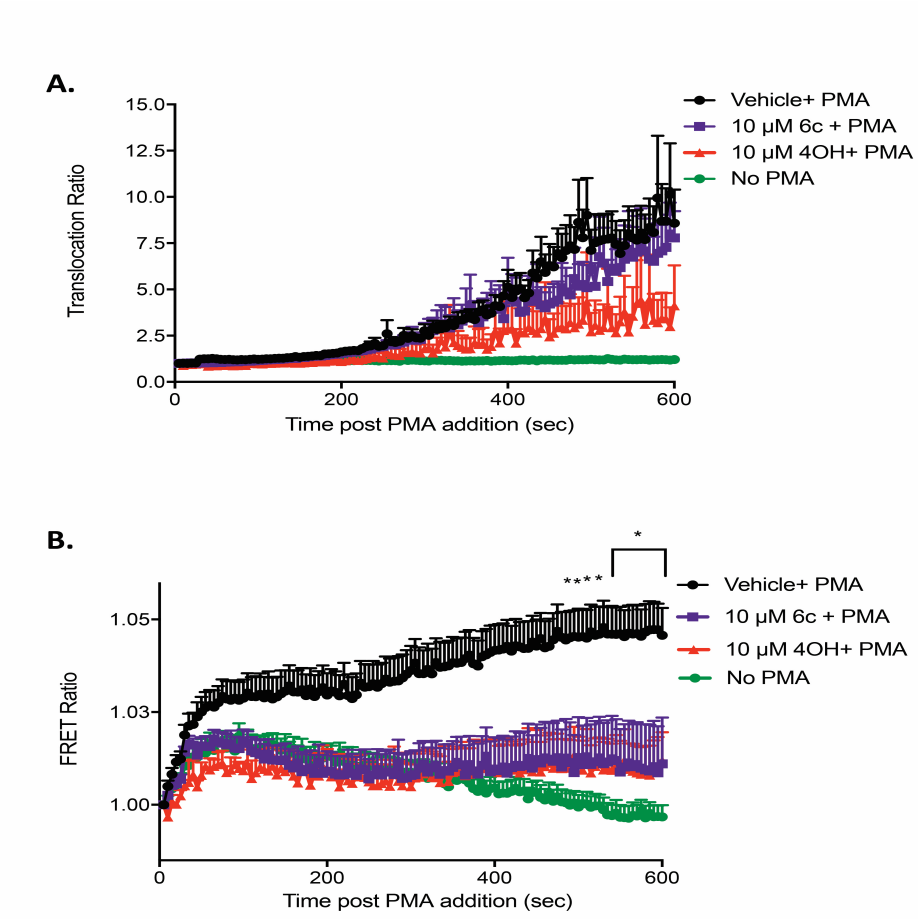

Figure 4.1. 6c does not inhibit PKCβ translocation but prevents the increase in FRET elicited by PMA. Cells were preteated for 30 min at 37°C with 10 µM **6c**, 10 µM 4-OH (positive control) or vehicle. PKC activity was stimulated with 1 µM PMA and frames were taken over 10 min. Control: n=19; 10 µM 6c n=18; 10 µM 4OH: n=11; No PMA, n=15. *Post hoc* Sidak's multiple comparison test, *p<0.05.

***6c** reduces striatal PKC activity in vivo*. We recently showed that **6c** inhibits *in vitro* PKC-induced phosphorylation of growth associated protein-43, GAP-43, a protein enriched in nerve terminals (Gispen *et al*, 1985; Van Lookeren Campagne *et al*, 1990), and myristoylated alanine rich C kinase substrate, MARCKS, which is widely expressed throughout the brain (Brudvig and Weimer, 2015; Carpenter *et al*, 2017; Ouimet *et al*, 1990). We also demonstrated that peripheral administration of 6 mg/kg of **6c** will reduce efflux through DAT at extracellular concentrations in the nucleus accumbens of ≤ 20 nM (Carpenter *et al*, 2017). Because we are postulating that the effects of **6c** on DAT

function may involve PKC, we investigated whether peripherally-administered **6c** would inhibit PKC *in vivo* in the ventral striatum. The ventral striatum contains dopaminergic terminals in the nucleus accumbens and plays an important role in reinforcement and reward (Kravitz and Kreitzer, 2012). AMPH increases PKC activity *in vivo* (Giambalvo, 1992; Gnegy *et al*, 1993), therefore we co-administered 6 mg/kg of **6c** with 1 mg/kg of AMPH and probed the effect of **6c** 10 min and 30 min post-injection. In experiments where the rats were sacrificed 10-min post injection, we found that **6c** significantly reduced PKC activity in the ventral striatum, however had no effect in the dorsal striatum (Figure 4.2A-B). At 30 min however, we see no effect of **6c** within the dorsal or ventral striatum (Figure 4.2C-D).

***6c** does not inhibit AKT and CAMKII*. In addition to PKC, there are other structurally similar kinases that modulate DAT, such as AKT and CAMKII. With the knowledge that tamoxifen is a promiscuous drug (de Medina *et al*, 2004), we investigated whether **6c**'s effect on DAT could also be due its blockade of AKT and CAMKII activity. We found that unlike its effect on PKC, **6c** does not affect the auto-phosphorylation of CAMKII or AKT, which serves as a marker of the respective enzyme activities (Figure 4.3).

***6c** does not alter [^{3}H] dopamine uptake or efflux in HEKrDAT cells*. **6c** is a member of our first, small library of tamoxifen analogues that were designed to be more selective PKC inhibitors when compared with tamoxifen (Carpenter *et al*, 2016). **6c** exhibits limited CNS permeability and we hope to expand this library by using **6c** as a scaffold to create another generation of tamoxifen analogues with improved CNS penetrability. In doing this we evaluated whether a cellular model would be more

efficient for initially screening the action of these compounds on DAT. In contrast to its effectiveness in synaptosomes, pretreatment with 3 μM **6c** had no effect on [^{3}H]dopamine uptake or efflux in our cellular, HEKrDAT, model (Figure 4.4).

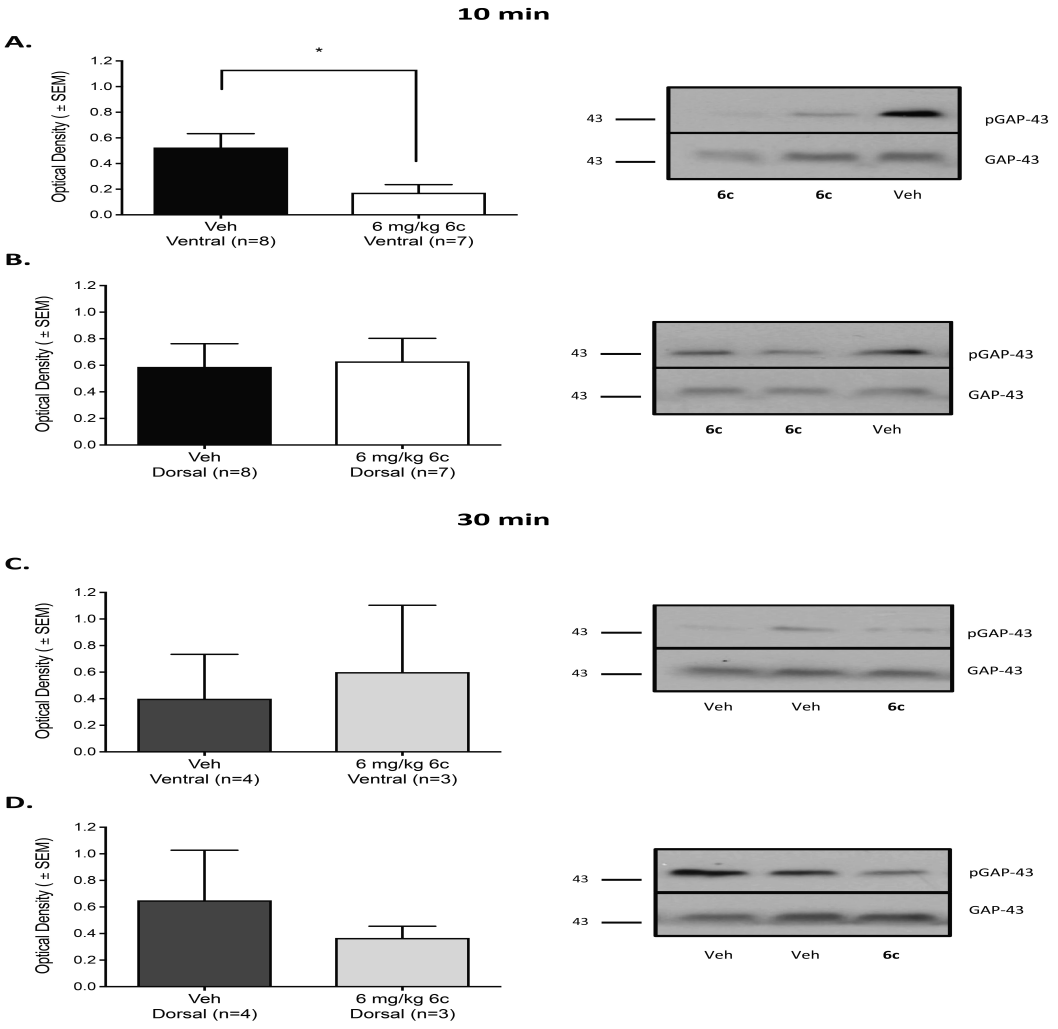

Figure 4.2. 6c reduces PKC activity in the ventral striatum.
Rats were given 6 mg/kg of **6c** or saline (Veh) with 1 mg/kg of AMPH *s.c.*, sacrificed 10 min (**A-B**) or 30 min (**C-D**) post-injection and levels of GAP-43 phosphorylation probed in ventral and dorsal striatal sections. **A.** Data from ventral striatal samples (10 min) shown as mean ± SEM and representative blots. Two-tailed Students *t* test, *p<0.05. **B.** Data from dorsal striatal samples (10 min) shown as mean ± SEM and representative blots. **C-D.** Data from ventral and dorsal striatal samples (30 min) shown as mean ± SEM and representative blots.

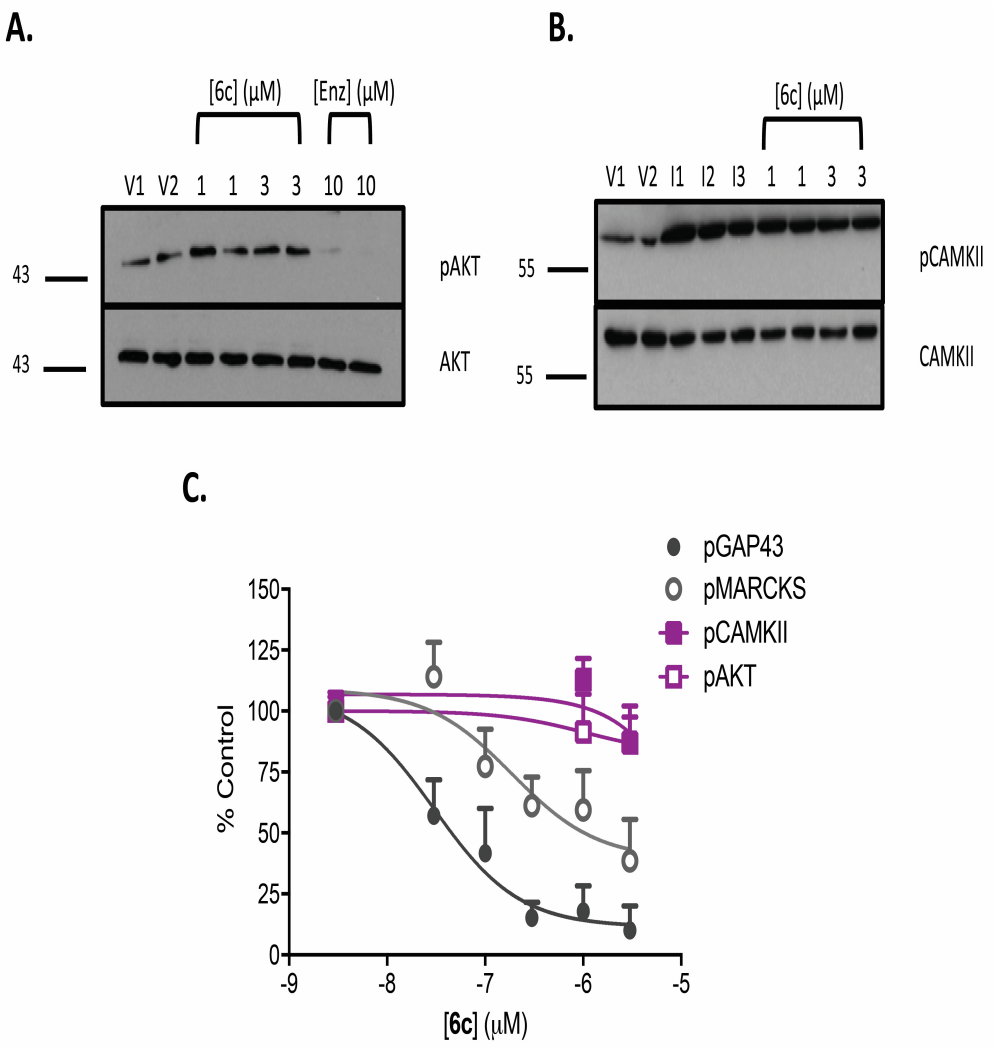

Figure 4.3. 6c does not inhibit AKT or CAMKII activity.

A. Representative blots for AKT assay**:** Rat striatal synaptosomes were incubated in the presence or absence of **6c** for 1 h at 37 °C, lysed and then probed for total AKT and phospho-ser^{473}-AKT. V1, V2: vehicle; Enz: enzastaurin (positive control; AKT inhibitor). **B.** Representative blots for CAMKII assay: Rat striatal synaptosomes were incubated in the presence or absence of **6c** for 1 h at 37 °C. Ionomycin (2 μM) was added for 5 min to stimulate CAMKII activity and the samples were lysed and probed for pan-CAMKII and phospho-thr^{286}-CAMKII. V1, V2: vehicle; I1, I2, I3: Ionomycin. **C.** The effect of **6c** on CAMKII (n=3) and AKT (n=4) phosphorylation overlayed on curves showing the inhibition of MARCKS (n=5) and GAP-43 (n=4) phosphorylation, Figure 2.1, Chapter 3. pGAP-43 and pMARCKS (normalized to GAPDH): percent phorbol 12-myristate 13-acetate (PMA) control; pCAMKII (normalized to CAMKII): percent ionomycin control; pAKT (normalized to AKT): percent vehicle control. All points are mean ± SEM.

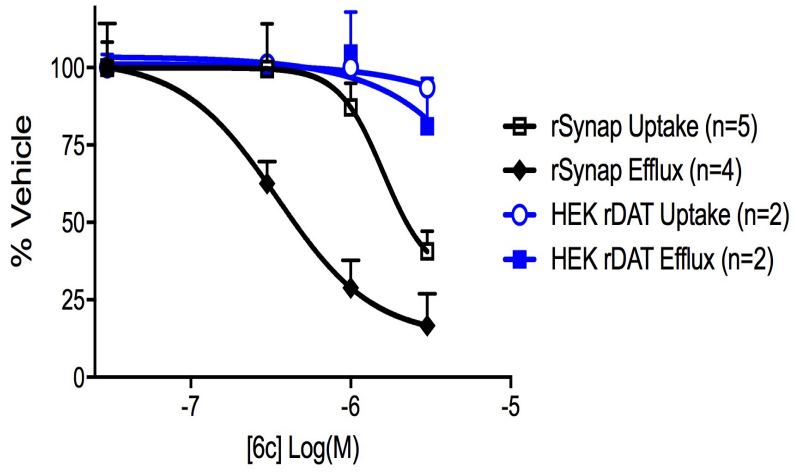

Figure 4.4. 6c modulation of DAT uptake and efflux processes in HEKrDAT cells.
HEKrDAT cells were incubated with vehicle or **6c** for 1 h at 25 °C and [^{3}H]dopamine uptake was quantified (n=2, ± SD). HEKrDAT cells were incubated in the presence or absence of **6c** for 1 h at 37 °C, efflux was stimulated with 10 μM AMPH (n=2, ± SD). Overlayed on plot of the modulation of DAT uptake and efflux processes by **6c** in rat striatal synaptosomes, Figure 3.2, Chapter 3.

Discussion

*Direct effects of **6c** on PKC*

Our investigations of **6c** so far at PKC have entailed looking at down-stream substrates of the enzyme. Nevertheless, we wanted to take a step back to investigate the direct mechanistic effects of **6c** on PKC. Our group has shown PKCβ is the likely isoform mediating the modulation of AMPH-stimulated dopamine efflux by PKC. LY379196, a selective inhibitor of PKCβ, reduces AMPH-stimulated dopamine release *in vitro* (Johnson *et al*, 2005). Furthermore, pharmacological and genetic silencing of PKCβ *in vivo* also reduces AMPH-stimulated dopamine release and behavioral effects in both mouse and rat models (Chen *et al*, 2009; Zestos *et al*, 2016). Importantly, DAT colocalizes with PKCβ (Hadlock *et al*, 2011; Johnson *et al*, 2005). Our group demonstrated that **6c** effectively attenuates AMPH-stimulated dopamine release and

behaviors related to AMPH reinforcement (Carpenter *et al*, 2017). The current study aims to elucidate the direct effects of **6c** at PKC, particularly at the PKCβ isoform.

We utilized a version of a previously reported unimolecular construct (mCer-PKC-mCit-FLAG) of PKCβ to monitor the effect of **6c** on PMA-stimulated translocation and changes in FRET (Swanson *et al*, 2014). Employing a bimolecular FRET reporter system (mCer-PKC-FLAG and PKC-mCit-FLAG), it was shown that PMA-stimulated increases in levels of FRET from the unimolecular PKC construct are likely due to intermolecular interactions between different PKC molecules and the investigation provided a novel mechanism of PKC regulation through dimerization (Swanson *et al*, 2014). It is therefore intriguing that though **6c** does not affect PKCβ translocation, it significantly reduces the PMA-induced FRET increases. Our data suggest that **6c** could be inhibiting PKC activity by interfering with conformational changes and dimerization of the enzyme. We utilized 4-hydroxytamoxifen, an active metabolite of tamoxifen, as our positive control (PKC inhibitor) for these experiments. Similar to many other PKC inhibitors, 4-hydroxytamoxifen inhibits PMA-induced translocation of PKC; we found it also blocked increases in PMA-stimulated FRET. Thus, although **6c** is an analogue of tamoxifen, its mechanism of interaction with PKC may differ from the parent molecule. We hope to employ this methodology to investigate the effect of **6c** on other PKC isoforms as a way to gain insight into isoform specificity.

*Differential effects of PKC inhibition by **6c** between striatal sub-regions*

Our data demonstrate that the systemic administration of the novel tamoxifen analogue, **6c**, causes a significant decrease in PKC activity in the striatum. The striatum is a subcortical region of the forebrain and receives dopaminergic inputs from the

midbrain. It is divided into the ventral (nucleus accumbens, olfactory tubercle) and dorsal striatum (caudate and putamen), with both regions implicated in the mediation of motivation and the reinforcement of natural rewards and drugs of abuse (Voorn *et al*, 2004). Much early attention was focused on the ventral striatum because drugs of abuse more strikingly increase dopamine in the ventral as compared with the dorsal striatum (Di Chiara *et al*, 1988). Rats will self-administer d-AMPH when delivered directly to the nucleus accumbens (Hoebel *et al*, 1983) and destroying dopaminergic terminals in the nucleus accumbens extinguishes AMPH self-administration (Lyness *et al*, 1979). However, there is growing evidence that compulsivity of drug addiction is driven through dorsal pathways (Everitt and Robbins, 2005, 2013). Therefore in determining the *in vivo* effects of **6c** on PKC, we investigated whether or not it had differential effects on the ventral and dorsal striatum.

Compared to vehicle treated rats, we found that co-administration of 6 mg/kg of **6c** with 1 mg/kg of AMPH significantly reduced GAP-43 phosphorylation in the ventral striatum but not the dorsal striatum 10 min post-injection. Coupling and regulation of signaling molecules can differ between the ventral and dorsal striatum. For example, dopamine D1-receptor induced extracellular signal-regulated protein kinases 1 or 2 activation is dependent on the dopamine- and cAMP-regulated phosphoprotein of 32 kDa (DARPP-32) in the ventral but not dorsal striatum (Gerfen *et al*, 2008). Furthermore there are innervation and protein expression differences between the two regions. There is an apparent gradient in DAT expression and uptake rates, with increased levels observed dorsally (Coulter *et al*, 1996; South and Huang, 2008). It is therefore feasible to envision how differences in the regulation or levels of PKC and its substrates between the

ventral and dorsal striatum could lead to differences in the PKC inhibitory potency of **6c** within the two areas. Following a dose of 6 mg/kg, levels of **6c** reaches ~20 nM in the nucleus accumbens (Carpenter *et al*, 2017). We have not yet measured **6c** levels in the dorsal striatum. If the levels are lower than in the nucleus accumbens, we may need to increase the dosage of **6c** or perform repeated administration to see a notable decrease of dorsal PKC activity. The effect of **6c** on PKC activity in the ventral striatum is transient and is lost by 30 min post-injection. It is therefore possible that an early, transient inhibition of PKC in the ventral striatum leads to more sustained reductions in AMPH-induced changes, such as increased dopamine release and locomotion (Carpenter *et al*, 2017).

***6c**'s modulation of DAT is likely independent AKT and CAMKII*

Two other important protein kinase mediators of dopamine uptake and efflux through DAT and potential targets for **6c** are CAMKII and AKT. DAT directly interacts with CAMKII at the last 11 amino acids on the C-terminus domain (Fog *et al*, 2006). On the other hand, it has yet to be shown that DAT directly interacts with AKT and there are no AKT consensus sequences on the transporter. However, through an indirect pathway, inhibition of AKT downregulates surface DAT levels and function (Garcia *et al*, 2005; Speed *et al*, 2010). Using the same synaptosomal preparations utilized for our PKC activity assay, we found that 3 μM **6c** causes a roughly 13% and 22% decrease in AKT and CAMKII activity. Since we only achieve much lower concentrations of **6c** in the brain during our *in vivo* experiments, these proteins likely do not mediate **6c**'s effect on AMPH-stimulated dopamine release or -reinforcement. Tamoxifen also displayed no significant effects on AKT or CAMKII activity (data not shown).

Optimal model systems

Our first round of tamoxifen analogues proved successful but we hope to use the information gained from our small SAR study (Carpenter *et al*, 2016) to guide the creation of new tamoxifen analogues with improved physicochemical properties for CNS penetrance. In anticipation of future screening studies we wanted to evaluate whether the effects of **6c** on dopamine uptake and effux through DAT could be replicated in cellular models. This would improve the efficiency and scalability of the current screening process. We employed HEK cells stably expressing DAT to avoid problems with transiently transfected systems, such as low protein levels and inconsistent transfection efficiencies (Gibson *et al*, 2013). Unfortunately, we found that **6c** had no effect on uptake or efflux in the HEK-rDAT cells.

This lack of effect of **6c** in these cells could be due to multiple reasons. It is possible that the ratio of DAT to PKC for **6c** to modulate transporter function is not optimal in this cellular overexpression system. The inhibition of PKC by tamoxifen is competitive with phospholipids (Su *et al*, 1985), therefore differences in the lipid environment or even the presence of different neuronal factors in synaptosomes *versus* cells may also account for this discrepancy. There are many compounds that affect DAT function in a consistent manner when cellular models with cloned DAT and synaptosomal preparations are compared. Nevertheless, the opposite is also true. Both dopamine and AMPH are much more potent in synaptosomal preparations than in heterologous cells (Giros and Caron, 1993). Therefore, careful considerations should be made in choosing appropriate models for effectively screening compounds for DAT function. Albeit more labor intensive, these data support the use of a synaptosomal-based

assay for initial screening of future generations of tamoxifen analogues with respect to evaluating their action at DAT.

Conclusion

Through this investigation, we have extended our mechanistic view of **6c**. We provide evidence suggesting **6c** may inhibit PKC activity by interrupting its intermolecular interactions and possible dimerization with other PKC molecules. We have proven that systemic administration of **6c** leads to inhibition of PKC in the ventral striatum. Furthermore, we propose that the ability of **6c** to reduce AMPH-induced dopamine release and AMPH reinforcement-related behavior is independent of CAMKII and AKT. In refining our SAR for the creation of new tamoxifen analogues, our data support the use of synaptosomal or possibly neuronal-based preparations for optimizing the *in vivo* translatability of screening results.

References

Aujla H, Beninger RJ (2003). Intra-accumbens protein kinase C inhibitor NPC 15437 blocks amphetamine-produced conditioned place preference in rats. *Behavioural Brain Research* **147**(1–2): 41-48.

Bazzi MD, Nelsestuen GL (1987). Association of protein kinase C with phospholipid vesicles. *Biochemistry* **26**(1): 115-122.

Becker KP, Hannun YA (2003). cPKC-dependent sequestration of membrane-recycling components in a subset of recycling endosomes. *Journal of Biological Chemistry* **278**(52): 52747-52754.

Bignon E, Pons M, Dore JC, Gilbert J, Ojasoo T, Miquel JF, Raynaud JP, Crastes de Paulet A (1991). Influence of di- and tri-phenylethylene estrogen/antiestrogen structure on the mechanisms of protein kinase C inhibition and activation as revealed by a multivariate analysis. *Biochemical pharmacology* **42**(7): 1373-1383.

Brudvig JJ, Weimer JM (2015). X MARCKS the spot: myristoylated alanine-rich C kinase substrate in neuronal function and disease. *Frontiers in Cellular Neuroscience* **9**: 407.

Burguillos MA, Deierborg T, Kavanagh E, Persson A, Hajji N, Garcia-Quintanilla A, Cano J, Brundin P, Englund E, Venero JL, Joseph B (2011). Caspase signalling controls microglia activation and neurotoxicity. *Nature* **472**(7343): 319-324.

Carpenter C, Sorenson RJ, Jin Y, Klossowski S, Cierpicki T, Gnegy M, Showalter HD (2016). Design and synthesis of triarylacrylonitrile analogues of tamoxifen with improved binding selectivity to protein kinase C. *Bioorganic & medicinal chemistry* **24**(21): 5495-5504.

Carpenter C, Zestos AG, Altshuler R, Sorenson RJ, Guptaroy B, Showalter HD, Kennedy RT, Jutkiewicz E, Gnegy ME (2017). Direct and systemic administration of a CNS-permeant tamoxifen analog reduces amphetamine-induced dopamine release and reinforcing effects. *Neuropsychopharmacology : official publication of the American College of Neuropsychopharmacology*.

Cerezo M, Laorden ML, Milanés MV (2002). Inhibition of protein kinase C but not protein kinase A attenuates morphine withdrawal excitation of rat hypothalamus–pituitary–adrenal axis. *European journal of pharmacology* **452**(1): 57-66.

Chen R, Furman CA, Zhang M, Kim MN, Gereau RW, Leitges M, Gnegy ME (2009). Protein kinase Cβ is a critical regulator of dopamine transporter. *The Journal of pharmacology and experimental therapeutics* **328**(3): 912-920.

Colón-González F, Kazanietz MG (2006). C1 domains exposed: from diacylglycerol binding to protein–protein interactions. *Biochimica et Biophysica Acta (BBA)-Molecular and Cell Biology of Lipids* **1761**(8): 827-837.

Coulter CL, Happe HK, Murrin LC (1996). Postnatal development of the dopamine transporter: a quantitative autoradiographic study. *Developmental Brain Research* **92**(2): 172-181.

Davies SP, Reddy H, Caivano M, Cohen P (2000). Specificity and mechanism of action of some commonly used protein kinase inhibitors. *Biochemical Journal* **351**(1): 95-105.

de Medina P, Favre G, Poirot M (2004). Multiple targeting by the antitumor drug tamoxifen: a structure-activity study. *Current medicinal chemistry Anti-cancer agents* **4**(6): 491-508.

Di Chiara G, Imperato A (1988). Drugs abused by humans preferentially increase synaptic dopamine concentrations in the mesolimbic system of freely moving rats. *Proceedings of the National Academy of Sciences of the United States of America* **85**(14): 5274-5278.

Dutil EM, Newton AC (2000). Dual role of pseudosubstrate in the coordinated regulation of protein kinase C by phosphorylation and diacylglycerol. *Journal of Biological Chemistry* **275**(14): 10697-10701.

Everitt BJ, Robbins TW (2005). Neural systems of reinforcement for drug addiction: from actions to habits to compulsion. *Nature neuroscience* **8**(11): 1481-1489.

Everitt BJ, Robbins TW (2013). From the ventral to the dorsal striatum: devolving views of their roles in drug addiction. *Neuroscience & Biobehavioral Reviews* **37**(9): 1946-1954.

Fog JU, Khoshbouei H, Holy M, Owens WA, Vaegter CB, Sen N, Nikandrova Y, Bowton E, McMahon DG, Colbran RJ, Daws LC, Sitte HH, Javitch JA, Galli A, Gether U (2006). Calmodulin kinase II interacts with the dopamine transporter C terminus to regulate amphetamine-induced reverse transport. *Neuron* **51**(4): 417-429.

Garcia B, Wei Y, Moron J, Lin R, Javitch J, Galli A (2005). Akt is essential for insulin modulation of amphetamine-induced human dopamine transporter cell-surface redistribution. *Molecular pharmacology* **68**(1): 102-109.

Gerfen CR, Paletzki R, Worley P (2008). Differences between dorsal and ventral striatum in drd1a-dopamine receptor coupling of DARPP-32 to activation of extracellular receptor kinase (ERK1/2). *The Journal of neuroscience : the official journal of the Society for Neuroscience* **28**(28): 7113-7120.

Giambalvo CT (1992). Protein kinase C and dopamine transport--1. Effects of amphetamine in vivo. *Neuropharmacology* **31**(12): 1201-1210.

Gibson TJ, Seiler M, Veitia RA (2013). The transience of transient overexpression. *Nature methods* **10**(8): 715-721.

Giros B, Caron MG (1993). Molecular characterization of the dopamine transporter. *Trends in pharmacological sciences* **14**(2): 43-49.

Gispen W, Leunissen J, Oestreicher A, Verkleij A, Zwiers H (1985). Presynaptic localization of B-50 phosphoprotein: the (ACTH)-sensitive protein kinase substrate involved in rat brain polyphosphoinositide metabolism. *Brain research* **328**(2): 381-385.

Gnegy ME, Hong P, Ferrell ST (1993). Phosphorylation of neuromodulin in rat striatum after acute and repeated, intermittent amphetamine. *Brain research Molecular brain research* **20**(4): 289-298.

Gould CM, Antal CE, Reyes G, Kunkel MT, Adams RA, Ziyar A, Riveros T, Newton AC (2011). Active site inhibitors protect protein kinase C from dephosphorylation and stabilize its mature form. *Journal of Biological Chemistry* **286**(33): 28922-28930.

Gundimeda U, Chen ZH, Gopalakrishna R (1996). Tamoxifen modulates protein kinase C via oxidative stress in estrogen receptor-negative breast cancer cells. *The Journal of biological chemistry* **271**(23): 13504-13514.

Hadlock GC, Nelson CC, Baucum AJ, Hanson GR, Fleckenstein AE (2011). Ex vivo identification of protein-protein interactions involving the dopamine transporter. *Journal of neuroscience methods* **196**(2): 303-307.

Herbert J, Augereau J, Gleye J, Maffrand J (1990). Chelerythrine is a potent and specific inhibitor of protein kinase C. *Biochemical and biophysical research communications* **172**(3): 993-999.

Hoebel BG, Monaco AP, Hernandez L, Aulisi EF, Stanley BG, Lenard L (1983). Self-injection of amphetamine directly into the brain. *Psychopharmacology* **81**(2): 158-163.

Idkowiak-Baldys J, Becker KP, Kitatani K, Hannun YA (2006). Dynamic sequestration of the recycling compartment by classical protein kinase C. *Journal of Biological Chemistry* **281**(31): 22321-22331.

Johnson LA, Guptaroy B, Lund D, Shamban S, Gnegy ME (2005). Regulation of amphetamine-stimulated dopamine efflux by protein kinase C beta. *The Journal of biological chemistry* **280**(12): 10914-10919.

Kravitz AV, Kreitzer AC (2012). Striatal mechanisms underlying movement, reinforcement, and punishment. *Physiology (Bethesda, Md)* **27**(3): 10.1152/physiol.00004.02012.

Lee SK, Qing WG, Mar W, Luyengi L, Mehta RG, Kawanishi K, Fong HH, Beecher CW, Kinghorn AD, Pezzuto JM (1998). Angoline and chelerythrine, benzophenanthridine alkaloids that do not inhibit protein kinase C. *Journal of Biological Chemistry* **273**(31): 19829-19833.

Lien EA, Solheim E, Ueland PM (1991a). Distribution of tamoxifen and its metabolites in rat and human tissues during steady-state treatment. *Cancer research* **51**(18): 4837-4844.

Lien EA, Wester K, Lønning PE, Solheim E, Ueland PM (1991b). Distribution of tamoxifen and metabolites into brain tissue and brain metastases in breast cancer patients. *British Journal of Cancer* **63**(4): 641-645.

Lyness WH, Friedle NM, Moore KE (1979). Destruction of dopaminergic nerve terminals in nucleus accumbens: effect on d-amphetamine self-administration. *Pharmacology, biochemistry, and behavior* **11**(5): 553-556.

Mochly-Rosen D, Das K, Grimes KV (2012). Protein kinase C, an elusive therapeutic target? *Nature reviews Drug discovery* **11**(12): 937-957.

O'Brian CA, Liskamp RM, Solomon DH, Weinstein IB (1985). Inhibition of protein kinase C by tamoxifen. *Cancer research* **45**(6): 2462-2465.

O'Brian CA, Liskamp RM, Solomon DH, Weinstein IB (1986). Triphenylethylenes: a new class of protein kinase C inhibitors. *Journal of the National Cancer Institute* **76**(6): 1243-1246.

Ouimet CC, Wang JK, Walaas SI, Albert KA, Greengard P (1990). Localization of the MARCKS (87 kDa) protein, a major specific substrate for protein kinase C, in rat brain. *The Journal of neuroscience : the official journal of the Society for Neuroscience* **10**(5): 1683-1698.

Pearce LR, Komander D, Alessi DR (2010). The nuts and bolts of AGC protein kinases. *Nature reviews Molecular cell biology* **11**(1): 9-22.

South T, Huang X-F (2008). High-fat diet exposure increases dopamine D2 receptor and decreases dopamine transporter receptor binding density in the nucleus accumbens and caudate putamen of mice. *Neurochemical research* **33**(3): 598-605.

Speed N, Saunders C, Davis AR, Owens WA, Matthies HJ, Saadat S, Kennedy JP, Vaughan RA, Neve RL, Lindsley CW (2011). Impaired striatal Akt signaling disrupts dopamine homeostasis and increases feeding. *PloS one* **6**(9): e25169.

Speed NK, Matthies HJG, Kennedy JP, Vaughan RA, Javitch JA, Russo SJ, Lindsley CW, Niswender K, Galli A (2010). Akt-dependent and isoform-specific regulation of dopamine transporter cell surface expression. *ACS Chemical Neuroscience* **1**(7): 476-481.

Steinkellner T, Mus L, Eisenrauch B, Constantinescu A, Leo D, Konrad L, Rickhag M, Sørensen G, Efimova EV, Kong E (2014). In vivo amphetamine action is contingent on αCaMKII. *Neuropsychopharmacology : official publication of the American College of Neuropsychopharmacology* **39**(11): 2681-2693.

Steinkellner T, Yang J-W, Montgomery TR, Chen W-Q, Winkler M-T, Sucic S, Lubec G, Freissmuth M, Elgersma Y, Sitte HH (2012). Ca2+/Calmodulin-dependent protein kinase IIα (αCaMKII) controls the activity of the dopamine transporter implications for Angelman syndrome. *Journal of Biological Chemistry* **287**(35): 29627-29635.

Su HD, Mazzei GJ, Vogler WR, Kuo JF (1985). Effect of tamoxifen, a nonsteroidal antiestrogen, on phospholipid/calcium-dependent protein kinase and phosphorylation of its endogenous substrate proteins from the rat brain and ovary. *Biochemical pharmacology* **34**(20): 3649-3653.

Swanson CJ, Ritt M, Wang W, Lang MJ, Narayan A, Tesmer JJ, Westfall M, Sivaramakrishnan S (2014). Conserved modular domains team up to latch-open active protein kinase Calpha. *The Journal of biological chemistry* **289**(25): 17812-17829.

Tamaoki T (1991). [28] Use and specificity of staurosporine, UCN-O1, and calphostin C as protein kinase inhibitors. *Methods in enzymology* **201**: 340-347.

Van Lookeren Campagne M, Oestreicher A, Van Bergen En Henegouwen P, Gispen W (1990). Ultrastructural double localization of B-50/GAP43 and synaptophysin (p38) in the neonatal and adult rat hippocampus. *Journal of neurocytology* **19**(6): 948-961.

Voorn P, Vanderschuren LJ, Groenewegen HJ, Robbins TW, Pennartz CM (2004). Putting a spin on the dorsal–ventral divide of the striatum. *Trends in neurosciences* **27**(8): 468-474.

Wise RA, Bozarth MA (1985). Brain mechanisms of drug reward and euphoria. *Psychiatric medicine* **3**(4): 445-460.

Withey SL, Hill R, Lyndon A, Dewey WL, Kelly E, Henderson G (2017). Effect of tamoxifen and brain penetrant PKC and JNK inhibitors on tolerance to opioid-induced respiratory depression in mice. *Journal of Pharmacology and Experimental Therapeutics* **361**(1): 51-59.

Wu-Zhang AX, Newton AC (2013). Protein kinase C pharmacology: refining the toolbox. *The Biochemical journal* **452**(2): 195-209.

Zestos AG, Mikelman SR, Kennedy RT, Gnegy ME (2016). PKCβ inhibitors attenuate amphetamine-stimulated dopamine efflux. *ACS Chemical Neuroscience* **7**(6): 757-766.

Zhang D, Anantharam V, Kanthasamy A, Kanthasamy AG (2007). Neuroprotective effect of protein kinase C delta inhibitor rottlerin in cell culture and animal models of Parkinson's disease. *The Journal of pharmacology and experimental therapeutics* **322**(3): 913-922.

Chapter 5. Discussion

Amphetamine (AMPH) abuse is a global burden and unfortunately, attempts at creating therapeutics to combat this problem have been unfruitful. Work by our group has centered on understanding the mechanism of action of AMPH in hopes of elucidating novel targets for drug development. *Our central hypothesis* is that protein kinase C (PKC) is a fundamental mediator of AMPH action at the dopaminergic synapse and that PKC inhibitors will reduce the reinforcing effects of AMPH, hence providing a suitable pharmacological treatment for AMPH abuse and addiction. In pursuit of a CNS permeant PKC inhibitor, we identified tamoxifen, a drug commonly used to prevent breast cancer recurrence, as a promising candidate (Osborne 1998). In addition to PKC, tamoxifen has other *in vivo* targets. However, the numerous reported structure-activity relationship (SAR) studies conducted with tamoxifen afforded us the opportunity to create a new generation of more selective CNS-permeant PKC inhibitors. My thesis highlights the creation of a small library of novel tamoxifen analogues and my work evaluates their *in vitro* and *in vivo* actions on the dopaminergic system.

Scaffold repositioning

In Chapter 2, I provide the rationale by which we designed the tamoxifen analogues. The substitution of a cyano group for the ethyl group and changes to the α and α' ring (refer to Figure 1.7) generated compounds that trended towards improved PKC inhibitory activity and/or loss of estrogen receptorα (ERα) affinity compared with

tamoxifen. The lead compound, **6c**, which was by far the most soluble compound, was 250 times more potent at inhibiting PKC than tamoxifen. Solubility issues may have accounted for the lower PKC inhibitory effects exhibited by some of the other tamoxifen analogues. We synthesized most of the compounds as hydrochloride salts in hopes of preventing these issues. However, future efforts should take a more systematic approach in making structural modifications that can improve the solubility of tamoxifen analogues in future SAR studies. One way to do this is by adding moieties, such as solubilizing appendages, that can increase polarity and hence lower the calculated logP (Walker, 2013). Notably, the three tamoxifen analogues from our library with the most improved clogP (6b, **6c** and 12) were also the compounds which exhibited the most favorable profiles: improved PKC inhibition and decreased affinity to ERα as compared to tamoxifen.

We believe that repurposing the scaffold of a drug already on the market, such as tamoxifen, can expedite the drug development process since the parent drug provides hints of the pharmacokinetic and pharmacodynamic properties of future analogues. Of course, the ideal situation would be to repurpose tamoxifen itself since its pharmacology and toxicology have been studied in great detail. There are countless reports of drug repositioning successes, even for the treatment of neuropsychiatric disorders. Galantamine, an acetylcholinsterase inhibitor, is used in the treatment of individuals with mild-to-moderate Alzheimer's disease (Corbett *et al*, 2012). Recently, the nicotinic receptor modulator, dexmecamylamine showed promising results for the treatment of major depressive disorder (Moller *et al*, 2015; Vieta *et al*, 2014). Also, as previously discussed, tamoxifen reduces the manic symptoms in patients suffering from bipolar

mania (Bebchuk *et al*, 2000; Fallah *et al*, 2016; Yildiz *et al*, 2008; Zarate *et al*, 2007). Although tamoxifen had no serious complications in these short studies, we are aware of its side effects (such as ER-mediated hot flashes) that lead to compliance issues with longer usage. Therefore we thought it would be more useful to use the tamoxifen scaffold to create more targeted tamoxifen analogues for the context of AMPH abuse and addiction treatment.

There is encouraging work done in the area of repurposing drug scaffolds as well. This is especially true in cancer drug discovery and drug development. For example, analogues of the 90 kDa heat shock protein (Hsp90) inhibitor, novobiocin, and the selective estrogen receptor modulator, raloxifene, show superior target selectivity or display improved pharmacology when compared to their parent drug in preclinical studies. In addition to our work centered on using the tamoxifen scaffold to make CNS-permeant PKC inhibitors, others have revisited the structure to create tamoxifen analogues that are immune to cytochrome P450 2D6 metabolism (Ahmed *et al*, 2016). Therefore we are excited by the prospect that the work from this thesis will further support drug scaffold repositioning, especially in a field such as addiction, where it is not commonly seen.

We know that AMPH (A) can activate PKC (**1**) and cause the reverse transport of dopamine through DAT (**2**). In chapter 3, we show that **6c** crosses the blood-brain barrier, inhibits PKC activity (**3**) and blocks the dopamine efflux (**4**), Figure 5.1. Unlike classical PKC inhibitors, such as enzastaurin and ruboxistaurin, **6c** significantly decreases uptake in the μM range in our rat synaptosomal preparations (Carpenter *et al*,

2017; Zestos *et al*, 2016). The effect of **6c** on dopamine uptake and efflux is asymmetrical because the compound more potently affects the latter process.

Our model

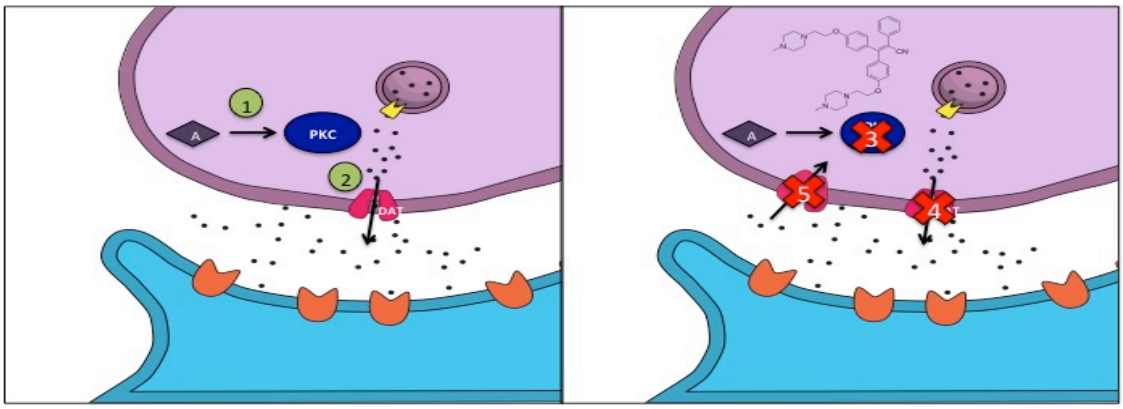

Figure 5.1. Proposed action of 6c at the dopaminergic terminal *in vivo*.

Through our binding studies using the cocaine analogue [^{3}H]WIN35,428, we have ruled out an interaction of **6c** with the cocaine site that overlaps the substrate binding site. This may seem odd as compounds that block dopamine uptake tend to alter [^{3}H]WIN35,428 binding. However, work by Kitayama and colleagues demonstrate that the cocaine and substrate site on DAT can be uncoupled, providing evidence that one can alter one site without affecting the function of the other. Specifically, mutations of the only aspartic acid residue (Asp79) in the first hydrophobic transmembrane domain of DAT will significantly affect dopamine transport without altering the binding of [^{3}H]WIN35,428 (Kitayama *et al*, 1992). Moreover, mutating the serines at positions 356 and 359 in the seventh transmembrane domain to alanine and glycine leads to a preferential effect on dopamine uptake compared to binding of the cocaine analogue (Kitayama *et al*, 1992). It is possible that binding of **6c** to an allosteric site on the transporter could lead to conformational changes that disrupt the optimal orientation at

Asp79, Ser356 or Ser359 while preserving optimal contacts at the cocaine site, ultimately causing an effect on dopamine uptake and not [^{3}H]WIN35,428 binding.

Another point to consider is that **6c** may not alter the initial binding of dopamine to the substrate site but instead may affect the rate or efficiency by which the transporter transitions through its open-occluded-closed conformations to release dopamine on the cytosolic face of the transporter. In future studies, we must therefore attain the kinetic parameters, such as the K_m (Michaelis constant) and V_{max} (maximal velocity) of dopamine uptake, in the presence or absence of **6c** to examine this possibility. Although we believe the *in vivo* effects of **6c** on the neurochemical and behavioral effects of AMPH are largely due to a reduction of dopamine efflux, we cannot rule out the possibility the compound is blocking the uptake of both dopamine and AMPH (**5**), Figure 5.1.

A decade ago, the effect of **6c** on dopamine uptake would be considered a red flag for further development of the compound. The notion was that by blocking the normal uptake functioning at the transporter, DAT inhibitors would increase extracellular dopamine levels and hence act as primary reinforcers. However this assumption has been repeatedly challenged by compounds, called atypical DAT inhibitors, which inhibit dopamine uptake but exhibit no or low stimulant and/or reinforcing properties (Schmitt *et al*, 2013). Furthermore, these compounds can block the effects of other stimulants. For example, the benztropine analogue, JWH007, is a potent DAT inhibitor that antagonizes the *in vivo* effects of cocaine (Desai *et al*, 2005; Velazquez-Sanchez *et al*, 2010). Work from our group recently showed that tamoxifen binds to DAT and likely inhibits dopamine uptake *via* an uncompetitive or mixed mechanism at the transporter (Mikelman

et al, 2017). Tamoxifen does not exhibit stimulant or reinforcing effects in humans or laboratory animals but it does inhibit AMPH-stimulated locomotion in laboratory animals *in vivo* (Einat et al, 2007). Therefore tamoxifen may also be classified as atypical DAT inhibitor. In the case of **6c**, the one caveat is that although it presents as a functional dopamine uptake inhibitor, we cannot truly classify it as an atypical DAT inhibitor without confirming its direct interaction with the transporter. This further supports the need for future molecular docking studies that can investigate the binding of **6c** to the allosteric sites on DAT.

Atypical inhibitors have expanded our understanding of DAT modulation. Simply envisioning the transporter as a gate is now insufficient; we now realize that different ligands binding to DAT can elicit different responses. More specifically, the protein exhibits dual transporter-receptor functioning. Initially it was thought that atypical DAT inhibitors functioned by stabilizing the inward-facing conformation of the transporter while typical inhibitors stabilized the outward-facing orientation (Loland *et al*, 2008; Reith *et al*, 2015). By 2016, this theory was debunked (Hiranita, 2016). Differences in kinetics between atypical and typical inhibitors were also postulated as the likely basis for their different downstream effects. Studies correlated the rate of onset with reinforcing efficacy of various compounds at DAT, where compounds with slower rates of onset were weaker reinforcers (Desai *et al*, 2005; Lile *et al*, 2002; Tanda *et al*, 2005; Woolverton *et al*, 2002). However, it was later revealed that a group of benztropine-based atypical DAT inhibitors possessed relatively fast rates of onset at DAT, yet were not stimulant-like or did not produce conditioned place preference when administered alone (Li *et al*, 2011).

Poly-pharmacology may be at the root of the mechanism of atypical DAT inhibitors. Apart from DAT, there are a few common targets shared by many of the atypical inhibitors, including binding to non-opioid σ receptors (Reith *et al*, 2015). Sigma receptors are expressed widely in the brain (Jansen *et al*, 1991a; Jansen *et al*, 1991b; Kitaichi *et al*, 2000) and can be divided into two subtypes: σ1 and σ2 receptor. The σ1 receptor is a small protein possibly containing one or two transmembrane domain and likely resides in the endoplasmic reticulum membrane (Aydar *et al*, 2002; Hanner *et al*, 1996; Hayashi and Su, 2005). The gene responsible for coding the σ2 receptor remained a mystery until recently, when it was revealed that the σ2 receptor is the cloned endoplasmic reticulum-transmembrane protein, TMEM97 (Alon *et al*, 2017). Although much remains unknown about the molecular coupling of σ receptors in the cell, subtype-selective ligands exist for the receptors (Narayanan *et al*, 2011).

Interestingly, the administration of σ antagonists with DAT inhibitors that are behaviorally inactive on their own, reduces methamphetamine self-administration in combination (Hiranita *et al*, 2011). Moreover, the σ1 receptor agonist, (+)-pentazocine, enhances AMPH-stimulated dopamine release and this effect is blocked by PKC inhibition (Derbez *et al*, 2002). Through the National Institute of Mental Health psychoactive drug screening program at the University of North Carolina Chapel Hill, we found **6c** and tamoxifen both potently bind to the σ1 receptor (K_d's of 261 nM and 203 nM respectively) and the σ2 receptor (K_d's of 5.6 nM and 31 nM respectively). Therefore, the effect of **6c** on the dopaminergic system may indeed be mediated by its action on the σ receptor. One of the next steps will be to establish whether **6c** is an agonist or antagonist at the σ receptor. With little information available on the σ receptor,

there is no standard means to distinguish between compounds that are agonists or antagonists at the receptor. One of the more trusted methods is to monitor the dissociation of the σ receptor from the molecular chaperone, binding immunoglobulin protein (BiP). The principle here is that agonist binding at the σ receptor leads to its separation from BiP and subsequent translocation from the endoplasmic reticulum to other regions in the cell. Sigma antagonists block this process (Hayashi and Su, 2007). Nonetheless, the creation of the σ1 receptor knockout mice (Langa *et al*, 2003) and the availability of σ receptor ligands gives us an opportunity to begin tackling questions of whether there is a σ component of **6c**'s action on dopamine uptake and AMPH-stimulated dopamine efflux.

Isoform specificity

It is obvious that much more needs to be done to evaluate the potential PKC-independent mechanisms through which **6c** is working to attenuate AMPH activity. Nevertheless, we are still left with many questions regarding **6c**'s action at PKC, especially with respect to PKC isoform specificity. We showed earlier that **6c** inhibits phorbol 12-myristate 13-acetate (PMA)-stimulated increases in PKC activity in both in cells and striatal synaptosomes. By acting as a diacylglerol mimic, PMA can activate both classical and novel PKC isoforms. However, with the knowledge that **6c** is a tamoxifen analogue and that tamoxifen is an inhibitor of classical PKCs, we hypothesized that the action of **6c** on PKC and ultimately AMPH, is mediated via PKC α, β or γ. Interestingly, **6c** inhibits phosphorylation of GAP-43 more potently than that of MARCKS, and GAP-43 displays more sensitivity for phosphorylation by PKCβ as compared to the other classical isoforms (Sheu *et al*, 1990). Considering all the lines of evidence that strongly point to PKCβ as the prominent PKC isoform mediating AMPH

action at DAT (Chen *et al*, 2009; Johnson *et al*, 2005; Zestos *et al*, 2016), it is likely that **6c** is at least partly working through PKCβ to block the effects of AMPH reported in this thesis.

Rapid screening assays used to identify kinase inhibitors or activators generally rely on a purified enzyme system. A major advantage is speed and knowing that the readouts are a reflection of individual kinase activity. Tamoxifen, however, exhibits greater PKC inhibitory potency in cellular versus purified enzyme systems (Gundimeda *et al*, 1996; Horgan *et al*, 1986; Huai-De *et al*, 1985; O'Brian *et al*, 1985). This was our rationale for creating a cell-based PKC assay, which quantified PKC activity *via* substrate phosphorylation. However, even though substrates can display isoform preference, there are no known isoform-specific substrates. Therefore no conclusions on specificity can be made from these types of experiments and this question is best addressed using assays such as the FRET-based experiment described in Chapter 4, which directly monitors PKC subtypes. Another option would be to monitor the effect of **6c** on MARCKS and GAP-43 phosphorylation in cells with a kinase-dead or genetically-silenced PKC isoform. The idea would be that changes in the potency of the PKC inhibitor would signify the importance of specific isoforms to these downstream actions. Along these lines, we could use PKC isoform-specific global or conditional knockout animal models to identify the isoform associated with **6c**'s effects on AMPH-stimulated dopamine release and reinforcement-related behaviors.

Animal models

In choosing an animal model, we focused on rats versus mice in evaluating the *in vitro* and *in vivo* effects of **6c** for two main reasons:

1) The pharmacokinetics and metabolism of tamoxifen in humans more resembles that observed in rats than in mice (Kisanga *et al*, 2003; Lien *et al*, 1991; Lim *et al*, 1994).

2) There are practical disadvantages in using mice in behavioral models, especially for self-administration studies (Ellenbroek and Youn, 2016). Therefore we wanted to be consistent with our choice of animal models for our initial studies.

However, we have begun studies investigating the actions of **6c** on AMPH-related processes in mice. As shown below, systemic administration of **6c** decreases AMPH-stimulated locomotion (in 2-way RM ANOVA, $F_{(25, 725)}=74.58$, $p<0.0001$ for time; $F_{(1, 29)}=22.49$, $p<0.0001$ for drug; and $F_{(25, 725)}=10.43$, $p<0.0001$ for interaction of time and drug) and does not induce locomotion on its own, Figure 5.2. Interestingly, unlike in rats,

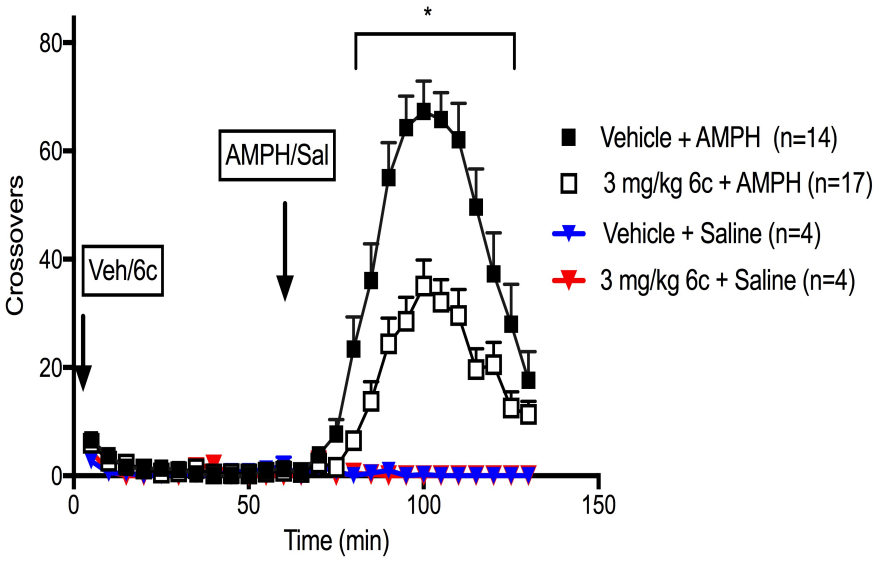

Figure 5.2. Effect of 3 mg/kg of 6c on locomotion induced by 3 mg/kg of AMPH in C57BL/6 wild type mice. Mice were allowed to habituate to experimental boxes for two days (two hours daily) and given two saline injections to mimic treatment on the experiment day. On test day, mice were given either vehicle (5% tween) or 3 mg/kg of 6c *i.p.* and one hour later given 3 mg/kg of AMPH or saline. Locomotion activity was recorded as chamber crossovers, i.e., the number of times breaking one photocell beam at one end of the chamber was followed by breaking the other photocell beam at the other end of the chamber. Data represented as ± SEM. *Post hoc* Sidak's multiple comparison test, *$p<0.05$.

we find that the inhibition of dopamine uptake by **6c** directly correlates with its inhibition of AMPH-stimulated dopamine efflux. This would suggest, at least with respect to mice, that these processes are coupled. We have yet to investigate PKC inhibition by **6c** in mouse striatal synaptosomes and it would also be beneficial to investigate whether the blockade of AMPH-stimulated dopamine release and locomotor behavior also translates into a reduction of AMPH reinforcement-like behaviors. Ultimately, it is possible that **6c** modulates DAT through a different mechanism in mice as compared to rats.

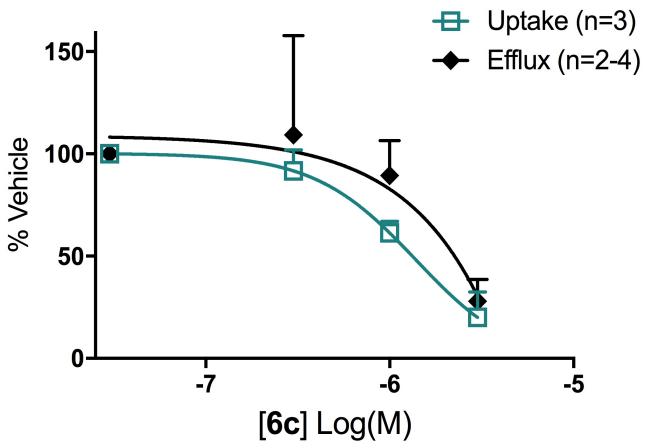

Figure 5.3. 6c modulation of dopamine efflux and uptake through DAT in mice.
A. Mouse striatal synaptosomes were incubated in the presence or absence of **6c** for 1 h at 37 °C. Dopamine efflux was stimulated with 10 µM AMPH (n=4 for all points but 0.3 µM, n=2)**.** Synaptosomes were incubated with vehicle or **6c** for 1 h at 37 °C and [^{3}H]dopamine uptake was quantified (n=3). **C.** Efflux and uptake results represented as % vehicle. All points are mean ± SEM.

Final remarks

The work highlighted in this thesis focuses on the action of **6c** at DAT and shows that we successfully designed a tamoxifen analogue that can attenuate the neurochemical and behavioral effects of AMPH. Nonetheless, the dopamine D2 autoreceptor (D2R) represents another major regulator of extracellular dopamine at the dopaminergic terminal. Work from our group shows PKC inhibition potentiates D2R function

(Luderman *et al*, 2015). In moving forward, it is therefore important to investigate if **6c** potentiates D2R activity as a mechanism of modulating dopaminergic signaling. Additionally, work must be done to better understand the pharmacokinetic and pharmacodynamic profile of **6c**, as this will provide useful information for further SAR studies using the tamoxifen scaffold. In summary, this work gives us hope for the future of drug development for AMPH addiction treatment and provides a new use for the tamoxifen scaffold.

References

Ahmed NS, Elghazawy NH, ElHady AK, Engel M, Hartmann RW, Abadi AH (2016). Design and synthesis of novel tamoxifen analogues that avoid CYP2D6 metabolism. *European journal of medicinal chemistry* **112**: 171-179.

Alon A, Schmidt HR, Wood MD, Sahn JJ, Martin SF, Kruse AC (2017). Identification of the gene that codes for the sigma2 receptor. *Proceedings of the National Academy of Sciences of the United States of America*.

Aydar E, Palmer CP, Klyachko VA, Jackson MB (2002). The sigma receptor as a ligand-regulated auxiliary potassium channel subunit. *Neuron* **34**(3): 399-410.

Bebchuk JM, Arfken CL, Dolan-Manji S, Murphy J, Hasanat K, Manji HK (2000). A preliminary investigation of a protein kinase C inhibitor in the treatment of acute mania. *Archives of general psychiatry* **57**(1): 95-97.

Carpenter C, Zestos AG, Altshuler R, Sorenson RJ, Guptaroy B, Showalter HD, Kennedy RT, Jutkiewicz E, Gnegy ME (2017). Direct and systemic administration of a CNS-permeant tamoxifen analog reduces amphetamine-induced dopamine release and reinforcing effects. *Neuropsychopharmacology : official publication of the American College of Neuropsychopharmacology*.

Chen R, Furman CA, Zhang M, Kim MN, Gereau RW, Leitges M, Gnegy ME (2009). Protein kinase Cβ is a critical regulator of dopamine transporter. *The Journal of pharmacology and experimental therapeutics* **328**(3): 912-920.

Corbett A, Smith J, Ballard C (2012). New and emerging treatments for Alzheimer's disease. *Expert Rev Neurother* **12**(5): 535-543.

Derbez AE, Mody RM, Werling LL (2002). Sigma(2)-receptor regulation of dopamine transporter via activation of protein kinase C. *The Journal of pharmacology and experimental therapeutics* **301**(1): 306-314.

Desai RI, Kopajtic TA, Koffarnus M, Newman AH, Katz JL (2005). Identification of a dopamine transporter ligand that blocks the stimulant effects of cocaine. *Journal of Neuroscience* **25**(8): 1889-1893.

Einat H, Yuan P, Szabo ST, Dogra S, Manji HK (2007). Protein kinase C inhibition by tamoxifen antagonizes manic-like behavior in rats: implications for the development of novel therapeutics for bipolar disorder. *Neuropsychobiology* **55**(3-4): 123-131.

Ellenbroek B, Youn J (2016). Rodent models in neuroscience research: is it a rat race? *Disease Models & Mechanisms* **9**(10): 1079-1087.

Fallah E, Arman S, Najafi M, Shayegh B (2016). Effect of tamoxifen and lithium on treatment of acute mania symptoms in children and adolescents. *Iranian journal of child neurology* **10**(2): 16.

Gundimeda U, Chen ZH, Gopalakrishna R (1996). Tamoxifen modulates protein kinase C via oxidative stress in estrogen receptor-negative breast cancer cells. *The Journal of biological chemistry* **271**(23): 13504-13514.

Hanner M, Moebius FF, Flandorfer A, Knaus HG, Striessnig J, Kempner E, Glossmann H (1996). Purification, molecular cloning, and expression of the mammalian sigma1-binding site. *Proceedings of the National Academy of Sciences of the United States of America* **93**(15): 8072-8077.

Hayashi T, Su T-P (2007). Sigma-1 receptor chaperones at the ER-mitochondrion interface regulate Ca 2+ signaling and cell survival. *Cell* **131**(3): 596-610.

Hayashi T, Su TP (2005). The sigma receptor: evolution of the concept in neuropsychopharmacology. *Current Neuropharmacology* **3**(4): 267-280.

Hiranita T (2016). DAT conformation does not predict the ability of atypical dopamine uptake inhibitors to substitute for cocaine. *Journal of alcoholism and drug dependence* **4**(4).

Hiranita T, Soto PL, Kohut SJ, Kopajtic T, Cao J, Newman AH, Tanda G, Katz JL (2011). Decreases in cocaine self-administration with dual inhibition of the dopamine transporter and sigma receptors. *The Journal of pharmacology and experimental therapeutics* **339**(2): 662-677.

Horgan K, Cooke E, Hallett MB, Mansel RE (1986). Inhibition of protein kinase C mediated signal transduction by tamoxifen. *Biochemical pharmacology* **35**(24): 4463-4465.

Huai-De S, Mazzei GJ, Vogler WR (1985). Effect of tamoxifen, a nonsteroidal antiestrogen, on phospholipid/calcium-dependent protein kinase and phosphorylation of its endogenous substrate proteins from the rat brain and ovary. *Biochemical pharmacology* **34**(20): 3649-3653.

Jansen K, Faull R, Dragunow M, Leslie R (1991a). Autoradiographic distribution of sigma receptors in human neocortex, hippocampus, basal ganglia, cerebellum, pineal and pituitary glands. *Brain research* **559**(1): 172-177.

Jansen KL, Dragunow M, Faull RL, Leslie RA (1991b). Autoradiographic visualisation of [3 H] DTG binding to σ receptors,[3 H] TCP binding sites, and l-[3 H] glutamate binding to NMDA receptors in human cerebellum. *Neuroscience letters* **125**(2): 143-146.

Johnson LA, Guptaroy B, Lund D, Shamban S, Gnegy ME (2005). Regulation of amphetamine-stimulated dopamine efflux by protein kinase C beta. *The Journal of biological chemistry* **280**(12): 10914-10919.

Kisanga ER, Gjerde J, Schjott J, Mellgren G, Lien EA (2003). Tamoxifen administration and metabolism in nude mice and nude rats. *The Journal of steroid biochemistry and molecular biology* **84**(2-3): 361-367.

Kitaichi K, Chabot J-G, Moebius FF, Flandorfer A, Glossmann H, Quirion R (2000). Expression of the purported sigma 1 (σ 1) receptor in the mammalian brain and its possible relevance in deficits induced by antagonism of the NMDA receptor complex as revealed using an antisense strategy. *Journal of chemical neuroanatomy* **20**(3): 375-387.

Kitayama S, Shimada S, Xu H, Markham L, Donovan DM, Uhl GR (1992). Dopamine transporter site-directed mutations differentially alter substrate transport and cocaine binding. *Proceedings of the National Academy of Sciences* **89**(16): 7782-7785.

Langa F, Codony X, Tovar V, Lavado A, Gimenez E, Cozar P, Cantero M, Dordal A, Hernandez E, Perez R, Monroy X, Zamanillo D, Guitart X, Montoliu L (2003). Generation and phenotypic analysis of sigma receptor type I (sigma 1) knockout mice. *The European journal of neuroscience* **18**(8): 2188-2196.

Li SM, Kopajtic TA, O'Callaghan MJ, Agoston GE, Cao J, Newman AH, Katz JL (2011). N-substituted benztropine analogs: selective dopamine transporter ligands with a fast onset of action and minimal cocaine-like behavioral effects. *The Journal of pharmacology and experimental therapeutics* **336**(2): 575-585.

Lien EA, Solheim E, Ueland PM (1991). Distribution of tamoxifen and its metabolites in rat and human tissues during steady-state treatment. *Cancer research* **51**(18): 4837-4844.

Lile JA, Morgan D, Birmingham AM, Wang Z, Woolverton WL, Davies HM, Nader MA (2002). The reinforcing efficacy of the dopamine reuptake inhibitor 2beta-propanoyl-3beta-(4-tolyl)-tropane (PTT) as measured by a progressive-ratio schedule and a choice procedure in rhesus monkeys. *The Journal of pharmacology and experimental therapeutics* **303**(2): 640-648.

Lim CK, Yuan Z-X, Lamb JH, White IN, De Matteis F, Smith LL (1994). A comparative study of tamoxifen metabolism in female rat, mouse and human liver microsomes. *Carcinogenesis* **15**(4): 589-593.

Loland CJ, Desai RI, Zou MF, Cao J, Grundt P, Gerstbrein K, Sitte HH, Newman AH, Katz JL, Gether U (2008). Relationship between conformational changes in the dopamine transporter and cocaine-like subjective effects of uptake inhibitors. *Molecular pharmacology* **73**(3): 813-823.

Luderman KD, Chen R, Ferris MJ, Jones SR, Gnegy ME (2015). Protein kinase C beta regulates the D(2)-like dopamine autoreceptor. *Neuropharmacology* **89**: 335-341.

Mikelman SR, Guptaroy B, Gnegy ME (2017). Tamoxifen and its active metabolites inhibit dopamine transporter function independently of the estrogen receptors. *Journal of neurochemistry* **141**(1): 31-36.

Moller HJ, Demyttenaere K, Olausson B, Szamosi J, Wilson E, Hosford D, Dunbar G, Tummala R, Eriksson H (2015). Two Phase III randomised double-blind studies of fixed-dose TC-5214 (dexmecamylamine) adjunct to ongoing antidepressant therapy in patients with major depressive disorder and an inadequate response to prior antidepressant therapy. *The world journal of biological psychiatry : the official journal of the World Federation of Societies of Biological Psychiatry* **16**(7): 483-501.

Narayanan S, Bhat R, Mesangeau C, Poupaert JH, McCurdy CR (2011). Early development of sigma-receptor ligands. *Future medicinal chemistry* **3**(1): 79-94.

O'Brian CA, Liskamp RM, Solomon DH, Weinstein IB (1985). Inhibition of protein kinase C by tamoxifen. *Cancer research* **45**(6): 2462-2465.

Reith ME, Blough BE, Hong WC, Jones KT, Schmitt KC, Baumann MH, Partilla JS, Rothman RB, Katz JL (2015). Behavioral, biological, and chemical perspectives on atypical agents targeting the dopamine transporter. *Drug and alcohol dependence* **147**: 1-19.

Schmitt KC, Rothman RB, Reith ME (2013). Nonclassical pharmacology of the dopamine transporter: atypical inhibitors, allosteric modulators, and partial substrates. *The Journal of pharmacology and experimental therapeutics* **346**(1): 2-10.

Sheu F-S, Marais RM, Parker PJ, Bazan NG, Routtenberg A (1990). Neuron-specific protein F1GAP-43 shows substrate specificity for the beta subtype of protein kinase C. *Biochemical and biophysical research communications* **171**(3): 1236-1243.

Tanda G, Ebbs A, Newman AH, Katz JL (2005). Effects of 4'-chloro-3 alpha-(diphenylmethoxy)-tropane on mesostriatal, mesocortical, and mesolimbic dopamine transmission: comparison with effects of cocaine. *The Journal of pharmacology and experimental therapeutics* **313**(2): 613-620.

Velazquez-Sanchez C, Ferragud A, Murga J, Carda M, Canales JJ (2010). The high affinity dopamine uptake inhibitor, JHW 007, blocks cocaine-induced reward, locomotor stimulation and sensitization. *European neuropsychopharmacology : the journal of the European College of Neuropsychopharmacology* **20**(7): 501-508.

Vieta E, Thase ME, Naber D, D'Souza B, Rancans E, Lepola U, Olausson B, Szamosi J, Wilson E, Hosford D, Dunbar G, Tummala R, Eriksson H (2014). Efficacy and tolerability of flexibly-dosed adjunct TC-5214 (dexmecamylamine) in patients with

major depressive disorder and inadequate response to prior antidepressant. *European neuropsychopharmacology : the journal of the European College of Neuropsychopharmacology* **24**(4): 564-574.

Walker MA (2013). Improving solubility via structural modification. *Tactics in Contemporary Drug Design*. Springer, pp 69-106.

Woolverton W, Ranaldi R, Wang Z, Ordway G, Paul I, Petukhov P, Kozikowski A (2002). Reinforcing strength of a novel dopamine transporter ligand: pharmacodynamic and pharmacokinetic mechanisms. *Journal of Pharmacology and Experimental Therapeutics* **303**(1): 211-217.

Yildiz A, Guleryuz S, Ankerst DP, Ongur D, Renshaw PF (2008). Protein kinase C inhibition in the treatment of mania: a double-blind, placebo-controlled trial of tamoxifen. *Archives of general psychiatry* **65**(3): 255-263.

Zarate CA, Jr., Singh JB, Carlson PJ, Quiroz J, Jolkovsky L, Luckenbaugh DA, Manji HK (2007). Efficacy of a protein kinase C inhibitor (tamoxifen) in the treatment of acute mania: a pilot study. *Bipolar disorders* **9**(6): 561-570.

Zestos AG, Mikelman SR, Kennedy RT, Gnegy ME (2016). PKCβ inhibitors attenuate amphetamine-stimulated dopamine efflux. *ACS Chemical Neuroscience* **7**(6): 757-766.